Interruption of small inductive currents in A.C. circuits

INTERRUPTION OF SMALL INDUCTIVE CURRENTS IN A.C. CIRCUITS

W.M.C. VAN DEN HEUVEL

INTERRUPTION OF SMALL INDUCTIVE CURRENTS IN A.C. CIRCUITS

PROEFSCHRIFT

TER VERKRIJGING VAN DE GRAAD VAN DOCTOR IN DE TECHNISCHE WETENSCHAPPEN AAN DE TECHNISCHE HOGESCHOOL TE EINDHOVEN OP GEZAG VAN DE RECTOR MAGNIFICUS DR. K. POSTHUMUS, HOOGLERAAR IN DE AFDELING DER SCHEIKUNDIGE TECHNOLOGIE, VOOR EEN COMMISSIE UIT DE SENAAT TE VERDEDIGEN OP DINSDAG 14 JUNI 1966 TE 16.00 UUR

DOOR

WILHELM MARIA CORNELIS VAN DEN HEUVEL

ELEKTROTECHNISCH INGENIEUR

GEBOREN TE EINDHOVEN

GREVE OFFSET EINDHOVEN

DIT PROEFSCHRIFT IS GOEDGEKEURD DOOR DE PROMOTOR
PROF. DR. D. Th. J. TER HORST

aan mijn ouders
aan Emellie

CONTENTS

ACKNOWLEDGEMENTS

This work was carried out in the Laboratory for High Voltages and High Currents of the Technological University, Eindhoven. The author desires to express his sincere gratitude to Professor Dr. D. Th. J. ter Horst, head of this laboratory, for his continuous encouragement and many valuable suggestions. He is furthermore greatly indebted to Mr. W. F. J. Kersten who expertly carried out the measurements and prepared the figures and oscillograms.
The author also wishes to express his thanks to his colleagues for their interest and appreciated discussions. This thank is particularly due to Mr. H. M. Pflanz who moreover greatly participated in the translation of the manuscript. In this field valuable cooperation was also rendered by Mrs. M. L. S. van den Heuvel-Kerkhofs. Further assistance in the preparation of the manuscript was gratefully received from Miss H. C. G. Smolenaars and some of her colleagues.
A part of the applied high voltage equipment was unselfishly placed at the author's disposal by some public utility companies and industries. Therefore the author is greatly indepted to Mr. E. Hustinx, director of G. E. B., Eindhoven and his co-worker Mr. G. H. Michels, to Mr. M. A. Deurvorst, director of N. V. P. L. E. M., Maastricht, to Mr. J. J. Richters, chief engineer with N. V. Hazemeyer, Hengelo and to Mr. P. Bloch, chief engineer with L'Electricité Industrielle Belge S. A., Verviers, Belgium.

LIST OF SYMBOLS

(only symbols used in more than one section are listed in detail)

A	coefficient in expressions for restriking current.
B	coefficient in expressions for restriking current.
B	indication for "breaker under test".
C	capacitance.
C'	substitute capacitance $C' = C_s + C_t$.
C''	substitute capacitance $C'' = C_s C_t/(C_s + C_t)$.
C_p	equivalent capacitance of the parallel circuit in the direct vicinity of the breaker.
C'_p	added capacitance parallel to the breaker.
C_s	equivalent capacitance of the source side.
C_t	equivalent capacitance of the load circuit.
e	base of natural logarithm.
e	electronic charge.
E	voltage gradient.
f	frequency.
f_i	frequency of instability-oscillation.
f_n	industrial frequency.
f_{p1}	frequency of first parallel-oscillation.
f_{p2}	frequency of second parallel-oscillation.
f_s	frequency of feeder-circuit L_s, C_s.
f_{st}	frequency of main-circuit-oscillation.
f_t	frequency of load-circuit L_t, C_t
G	electrical conductance.
G_b	electrical conductance of a discharge.
G_{b1}	instantaneous electrical conductance of high conductivity discharge.
G_{b2}	instantaneous electrical conductance of residual discharge.
G_s	steady electrical conductance after a disturbance of the discharge.
G_1	electrical conductance, initial value of high conductivity discharge.
G_2	electrical conductance, initial value of residual discharge.
H	enthalpy.
i	disturbance in current through discharge.
I	current to be interrupted.
I_b	current through a gas-discharge.
I_B	current through a breaker and its parallelcircuit C_p, L_p

I_c	current through C_p
I'_c	current through C'_p
$I_{c'}$	current through C' (after a reignition)
I_{Cs}	current through C_s
I_{Ct}	current through C_t
I_d	instantaneous value of I_b at the instant of a residual-current reignition.
I_n	amplitude of current to be interrupted.
I_s	current through source and L_s.
I_{st}	current of main-circuit-oscillation, portion of I_B
I_{stat}	steady-state portion of restriking current I_B
I_t	current through L_t.
I_o	chopping level of current I_b
J	current density.
k	Boltzmann constant
k	thermal diffusivity.
K	constant of (quasi-)static gas-discharge characteristic.
l	contact - distance
L	self-inductance.
L'	substitute for $L_s L_t/(L_s + L_t)$
L''	substitute for $L'_s + L'_t + L_g$
L_a	self-inductance in equivalent circuit for a gasdischarge by Rizk.
L_g	self-inductance of return-connection from load to source.
L_p	self-inductance of the first parallel-circuit (in the direct vicinity of the breaker)
L_s	equivalent self-inductance of the feeder circuit.
L'_s	ancillary self-inductance of the feeder circuit.
L_t	equivalent self-inductance of the load.
L'_t	ancillary self-inductance of the load.
N	number of reignitions.
Osc	indication for "oscilloscope"
P	power.
r	conduction radius of a gas-discharge.
R	resistance.
R_b	resistance of a gas-discharge.
R_d	dynamic resistance of a gas-discharge.
R_g	equivalent resistance for a glow-discharge.
R_i	negative resistance in equivalent circuit for a gas-discharge by Rizk.
R_s	equivalent resistance for feeder-circuit.
R_t	equivalent resistance for load-circuit.

R_o	resistance of the discharge at the chopping level $I_b = I_o$
S	auxiliary heat function.
S_h	indication for "shunt".
t	time.
t_d	time-interval between two reignitions.
t_r	rise-time of restriking voltage before reignition.
T	temperature.
T_1	indication for "transformer in feeder-circuit".
T_2	indication for "transformer in load-circuit".
U	main-voltage, instantaneous value.
U_b	voltage across a gas-discharge.
U_B	voltage across breaker B.
$U_{C'}$	voltage across $C' = C_s + C_t$ after a reignition.
U_d	breakdown voltage (dielectric or residual-current reignition).
U_{max}	peak value of restriking voltage.
U_{max1}	first or suppression peak of restriking voltage.
U_{max2}	second or recovery peak of restriking voltage.
U_n	amplitude of main voltage U.
U_s	source-side voltage (across C_s).
U_t	load-side voltage (across C_t).
$U_{t\,max\,1}$	instantaneous voltage U_t when $U_B = U_{max1}$
$U_{t\,max\,2}$	instantaneous value U_t when $U_B = U_{max2}$
U_o	instantaneous value U_B at natural or forced current-zero.
V.D.	indication for "voltage-divider".
W	energy content.
y	admittance.
Z	impedance.
α	exponent of current I_b in (quasi-)static discharge characteristic.
ϑ	time-constant of main-circuit during glow-discharge.
Θ	time-constant of a gas-discharge.
Θ_C	time-constant according Cassie.
Θ_M	time-constant according Mayr.
Θ_R	time-constant according Rizk.
Θ_1	time-constant for high-conductivity discharge.
Θ_2	time-constant for residual discharge.
κ	coefficient of thermal conductivity.
ρ	density
σ	coefficient of electrical conductivity.

τ''	time-constant of the second parallel-circuit.
τ_1	time-constant of the load circuit.
φ	phase angle in expressions for restriking current.
ψ	phase angle.
ω	angular frequency.
ω_i	angular frequency of instability-oscillation.
ω_n	angular industrial frequency.
ω_{p1}	angular frequency of first parallel-oscillation.
ω_{p2}	angular frequency of second parallel-oscillation.
ω_s	angular frequency of feeder-circuit L_s, C_s
ω_{st}	angular frequency of main-circuit-oscillation.
ω_t	angular frequency of load-circuit L_t, C_t.

CHAPTER 1 INTRODUCTION

1.1. Problem.

High-voltage circuit-breakers for alternating-current systems are nearly as old as the electrical power supply. While in the first three-phase power transmission over a longer distance in 1891 the switching was performed exclusively at the low voltage side, were round 1900 the air circuit-breaker, the oil circuit-breaker and the air-blast circuit-breaker already known [1].
The basic principle of performance of the breakers has not been changed during all the years they exist: with help of mechanical separable conductors a firm connection with low contact impedance in closed position and an infinitely high resistance in open position is obtained. During the transition time the conductivity is maintained by an electrical gas-discharge, which interrupts during the passage through zero of the current to be switched off.

The designers of circuit-breakers have always succeeded in keeping the development of their apparatus more or less in step with the steadily increasing short-circuit power of the systems. Nowadays they are already faced with system-voltages up to 750 kV and prospective currents up to about 100 kA.

It could be surprising that - notwithstanding the apparently simple principle of interruption and the many successful designs - the way in which the interruption of current occurs is not yet fully understood.
The main reason is that the success or failure of interruption is mostly determined in some tens of microseconds. During this time the behaviour of the circuit-breaker will be influenced by the characteristics of the gas-discharge between the contacts together with the transient voltages across the contacts. The dynamical pattern of the discharge under the complicated circumstances which appear near the current zero values is not yet fully known.
The high-voltage circuits in which the circuit-breakers are installed consist of a large amount of elements with distributed self-inductances, capacitances and resistances, which are partly dependent on frequency

and voltage. Therefore, it is difficult to get a clear insight into the character of the restriking voltage.

On interruption of small inductive currents (such as no-load currents of transformers) the restriking voltage can rise rapidly to high values as a result of "current-chopping". Current-chopping is the sudden collapse of the current prior to its natural zero value. The electromagnetic power which is built up in the self-inductances of the circuit at the moment of current-chopping, becomes free suddenly. Consequently the capacitances in parallel or in series with these inductances are charged. With small valued capacitances voltage-oscillations with high rate of rise and amplitude can occur.

These overvoltages can introduce a dielectric breakdown or flashover in the disconnected circuit. However, they can also be the cause of reignitions in the breaker itself and hence of an interruption failure. The investigation therefore should be directed to:

a) the mechanism of current-chopping,
b) the restriking voltage,
c) the mechanism of the reignitions,
d) the restriking current.

The instantaneous behaviour of the gas-discharge has to be seen always in connection with the influence of the circuit.

1.2. Purpose of the investigation

The time between the instant of contact separation and the instant at which the restriking voltage is practically damped out, we shall call interruption-time. All phenomena which appear in the voltage and in the current within the interruption-time form together the interruption-cycle.

During the breaking of small currents this interruption-cycle shows, overall as well as detailed a very complicated pattern. This pattern is dependent on the type of breaker, the amplitude (and the frequency) of the current to be interrupted, the system-voltage, the elements from which the circuit is set-up and the way of earthing. With accurate measurements oscillations can be established showing frequencies between 50 c/s (industrial frequency) and 10 Mc/s, voltages with initial rate of rise to 10 000 V/μsec and currents with initial rate of rise to 10 000 A/μsec.

In this thesis an effort is made to give a survey and an explanation of the many phenomena which occur during the interruption of small inductive currents (varying between amperes and some tens of amperes RMS).

1.3. The breakers investigated.

The research mainly concentrated on a bulk oil-breaker and a small-oil-volume breaker in a single-phase circuit at a voltage of 10 kV. The results were compared with those obtained with an air-blast circuit-breaker and a load-break switch in a similar circuit. A small-oil-volume circuit-breaker with oil-injection was also investigated.

The main data of the breakers investigated are:

No.	Type	Rated voltage	Rated current	Symm. 3 phase short circuit power	Remarks
1.	bulk-oil	10 kV	600 A	230 MVA	with double-interruption
2.	small-oil-volume	10 kV	630 A	250 MVA	with axial- and radial-blast
3.	air-blast	24 kV	400 A	500 MVA	working air-pressure 14.5×10^5 n/m^2
4.	load-break switch	10 kV	350 A	-	with synthetic arc-control-chamber
5.	small-oil-volume	10 kV	400 A	250 MVA	with oil-injection

During the experiments with oil-circuit-breakers no. 1 and no. 2 no large differences were observed in the behaviour at small currents. Therefore these breakers will not be explicitely distinguished during the discussion, they will be referred to as "oil-circuit-breakers" or "oil-breakers". The load-break switch has its fixed contact in a chamber of insulation material. With larger currents gas is developed from the walls of the extinction-chamber which stimulates the interruption. The above switch is thus of the "hardgas" type. At the currents investigated (up to 60 A R.M.S.) it was found that the material of the extinction chamber had no noticeable effect on the interruption. Clearly during interruption of these small currents negligible amounts of gas are developed. The interruption seems thus to be similar as in an air-break switch. This switch will therefore be treated as an air-break switch.

CHAPTER 2 THE CIRCUITS

2.1. The test-circuits.

In electric generation and transmission generally three-phase circuits are used. They may be presented in their most simple form by fig. 2.1.1. The source side S consists of the whole transmission-network including the last transformer at the feeder-side of circuit-breaker B.

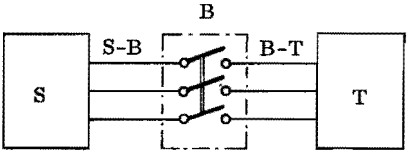

Fig. 2.1.1. Block diagram of the inductive circuits.

The inductive load T is mostly constituted of an unloaded or inductively loaded transformer. The conductors between the feeder-transformer and B is here represented by S-B, the conductors between the circuit-breaker and T by B-T. S-B and B-T may be composed of cables, overhead-lines and/or busbar systems. Very often the circuit-breaker is placed in the direct vicinity of the feeding- or the load-side transformer.

In circuit-breaker testing laboratories S consists often of a short-circuit alternator and a transformer. In this case the required inductive load is obtained from air-cored reactor-coils. Here the connections S-B and B-T are generally relatively short.

For a fundamental study of the interruption phenomena the three-phase circuit is not quite convenient. It requires complicated measuring techniques because prior and during interruption all terminals of the breaker come on high potential (see section 3.2). Furthermore, by inductive and capacitive coupling, disturbances in the current and voltage of each phase occur due to the interruption phenomena in both other phases. These disturbances do not contribute to the interruption of the other phases, because their current zeroes are normally shifted 60^{o} with respect to each other. However, they may seriously interfere with the interpretation of the oscillograms. On the other side the variety of circuits prevailing in practice

is so large, that the results obtained from a certain three-phase circuit would be fully equivalent in some special cases only.
For all these reasons the investigation was mainly carried out in single-phase circuits. The connections S-B and B-T were very short. One pole of the circuit breaker was used for interruption.
Depending on the location of earthing, in principle three different circuits can be investigated. They will be indicated by diagram 1 (fig. 2.1.2), diagram 2 (fig. 2.1.3) and diagram 3 (fig. 2.1.4).

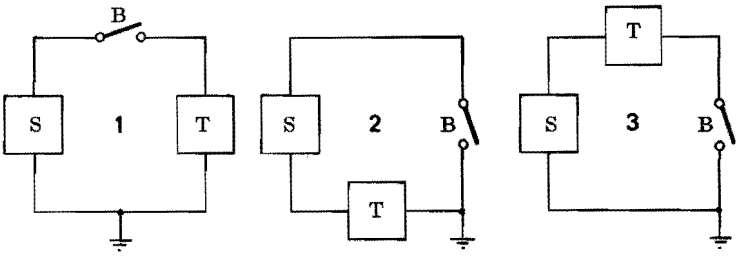

Principles of grounding.

Fig. 2.1.2. Grounding of the return conductor. Diagram 1.
Fig. 2.1.3. Grounding between circuit-breaker and load. Diagram 2.
Fig. 2.1.4. Grounding between circuit-breaker and source. Diagram 3.

Diagram 1 agrees best with one phase of a three-phase circuit. However, it presents the same difficulties: both terminals of the breaker are on high potential during interruption.
In section 7.5 it will be shown that diagram 2 fundamentally does not differ from diagram 1. This does not apply to diagram 3. In the latter the "main-circuit-oscillation" (section 7.3 to 7.5) cannot occur. Therefore the greater part of the experiments was carried out in circuits according to diagram 2. Diagrams 1 and 3 were mainly used for checking the results.
The system-voltage was always 10 kV(RMS). This voltage was obtained from a 380V/10kV transformer fed by the low voltage cable-network of the municipal power supply. The load was a second 10 kV/380 V transformer. At the low voltage side of this transformer a number of air-cored reactor-coils was connected to obtain the required currents. The complete diagram is given in fig. 2.1.5.
Moreover a great number of measurements was carried out with a small-oil-volume circuit-breaker in a three-phase circuit. In this case the circuit-breaker was directly connected to the municipal 10 kV cable-network (symmetrical short-circuit power about 180 MVA). For B-T short connexions were used as well as a three-phase cable with earthed lead-sheath of about 80 m length. The cross-section per phase was 95 mm^2. The total

capacitance per phase came to 3 x 10^4 pF. The load-side transformer was connected in star with earthed neutral.

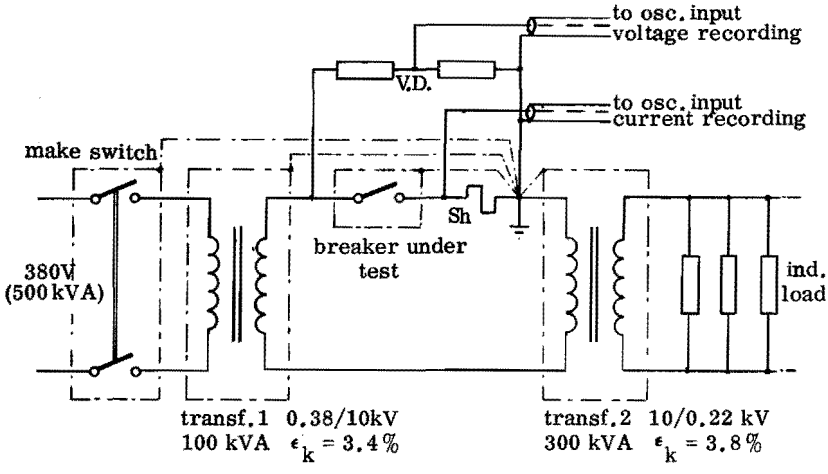

Fig. 2.1.5. Single phase test circuit.
V.D. = voltage divider
Sh = shunt
ϵ_k = relative impedance voltage

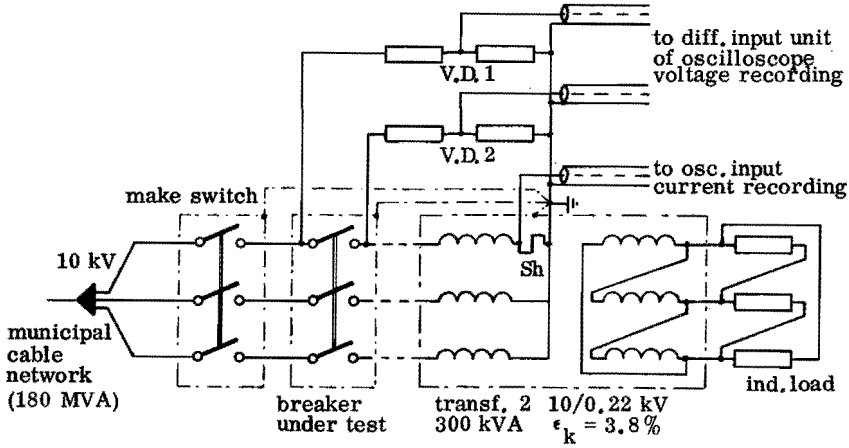

Fig. 2.1.6. Three phase test circuit.
V.D.1, V.D.2 = voltage dividers
Sh = shunt
ϵ_k = relative impedance voltage

Fig. 2.1.6. gives the complete circuit. However, the current measured in this circuit by the shunt Sh is not the same as the current I_b through the breaker. Only a very small part of the high-frequency components of the breaker-current can penetrate as far as the location of the shunt. The results obtained in the three-phase circuits showed no fundamental differences to those of the single-phase circuits. Except the earlier mentioned disturbances produced by the other phases in the phase under investigation, the modified circuitry showed differences in frequency and amplitude of the appearing oscillations only. These differences were largest in those cases where for B-T the lead-sheath cable was used. With a short connection for B-T all measurable phenomena were of the same order as in the single-phase circuits.

Therefore the experimental results and the conclusions given in chapters 8, 9 and 10 are not necessarily applicable to all three-phase circuits occurring in practice. The conclusions are particularly useful under conditions where the circuit-breaker is installed in the direct vicinity of the load-side transformer or inductive-load, while the load is connected in star with grounded neutral.

2.2. The equivalent diagrams of the test-circuits.

The elements from which the circuits are assembled consist of complicated networks of self-inductances and capacitances. In order to treat the circuits analytically, these networks should be simplified as much as possible by replacing the distributed elements by lumped ones.

Several authors have done theoretical work in this field [2 to 5] .

For the investigation dealt with in this thesis only the action of the circuit noticeable by the breaker is of importance for the mechanism of interruption. (The voltage distribution across the circuit-elements will not be considered). Therefore it should turn out from the details of the interruption-cycle to what extent such a simplification is allowed. In first approximation the source-side as well as the load-side circuit of one phase of a three phase-system may be considered a parallel circuit of a self-inductance and a capacitance (fig. 2.2.1). The latter is a substitute for all distributed ground capacitances of the self-inductances. The self-inductance of the source side L_s can be derived from the short-circuit-impedance. The self-inductance of the load L_t from the load-current at rated voltage. The active ground-capacitance C_s and C_t then follow from ω_s and ω_t, the oscil-

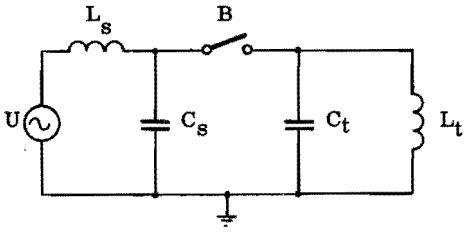

Fig. 2.2.1. Equivalent circuit for interruption of inductive currents. First approximation.

lation frequencies of the circuits after current-chopping. Fig. 2.2.1. is not fully representative for an explanation of the high initial rate of rise of the restriking voltage after current-chopping nor for the oscillations of the restriking current after a reignition in the circuit-breaker.
After a reignition the differences between the charge voltages of C_s and C_t will not be equalized infinitely fast. From the "second parallel-oscillation" then arising (section 7.2), the value of an active self-inductance L" can be deduced. In fact L" is divided in a section L'_s in front of the breaker, L'_t after the breaker and L_g in the earthed connection, compare fig. 2.2.2. Moreover it will turn out that the small equivalent capacitance of the direct vicinity of the circuit-breaker is of essential importance for current-chopping (chapter 4), the initial rise of the transient recovery voltage (section 6.2) and the "first parallel-oscillation" after a quickly arising reignition (section 7.1). This capacitance is composed of the inherent parallel-capacitance of the circuit-breaker, the earth-capacitance of both terminals of the breaker and the connected conductors in the direct vicinity. Together they form the high-frequency equivalent capacitance C_p parallel to the circuit-breaker. During measurement also the capacitance of the voltage-divider is to be included in C_p.

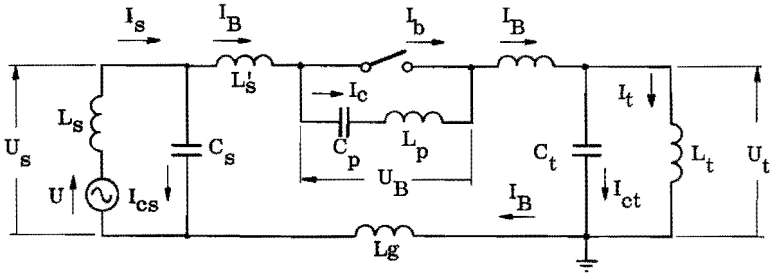

Fig. 2.2.2. High frequency equivalent circuit for interruption of inductive currents.

The small self-inductance of the circuit-breaker and its direct vicinity L_p should be taken in account as well.

Therefore the equivalent diagram of fig. 2.2.2 is required for a comprehensive explanation of all details of the interruption-cycle. In this diagram the resistances of the self-inductances and the discharge are not inserted. In section 7.5 it will be shown that this equivalent-circuit can also be used for diagram 2 (fig. 2.1.3). The equivalent-circuit for diagram 3 (fig. 2.1.4) will be considered in section 7.5 as well. In fig. 2.2.2. the notations for the currents and the voltages which will be used in this thesis are likewise indicated.

CHAPTER 3 THE EXPERIMENTAL TECHNIQUES

In order to investigate all phenomena of the interruption cycle careful attention was paid to frequency-independent measuring circuits covering a range from 50 c/s to 10 Mc/s. Since the measuring-circuits should not influence the interruption, demands were made for very high impedance for the voltage-recording and very low impedance for the current-recording equipment. In order to be able to investigate each detail of the interruption-cycle, an accurate timing was required for the making-switch, beginning of the contact-separation and triggering of the oscilloscope. Much attention was paid to a central earthing of the circuits to be investigated, the measuring-circuits and the metal-cladding of the transformers and the circuit-breaker under test.

3.1. Voltage recording.

For voltage measurement, voltage-dividers were developed which may be applied capacitively or mixed (capacitively-resistively) as desired. Fig. 3.1.1. shows the design. In fig. 3.1.2. the diagram is given. The high-voltage side of the divider is built-up from one or more series-connected vacuum capacitors (50 pF) and a break-down voltage of 32 kV (peak) each. The low-voltage side is composed of a parallel circuit consisting of 8 capacitors with a total capacitance C_2 of 10^4 pF. The resistor Z equal to the surge-impedance of the cable serves to damp waves reflected at the oscilloscope. The 8 capacitors are grouped concentric around the load resistor. In this way minimum self-inductance is obtained. The resistance of the oscilloscope input is 1 MΩ. For very low-frequency phenomena a resistor $R_1 = R_2C_2/C_1$ should therefore be installed parallel to the high-voltage side of the divider. R_1 consists of a column of series connected carbon-resistors. The divider can easily be equipped with this column. Fig. 3.1.3 gives the frequency characteristics for the voltage measuring circuits with and without R_1 (400 MΩ), with C_2 = 25 pF, Z = 50 Ω and a 2 m coaxial cable.

A more detailed description of these and other high-impedance voltage dividers will be published elsewhere.

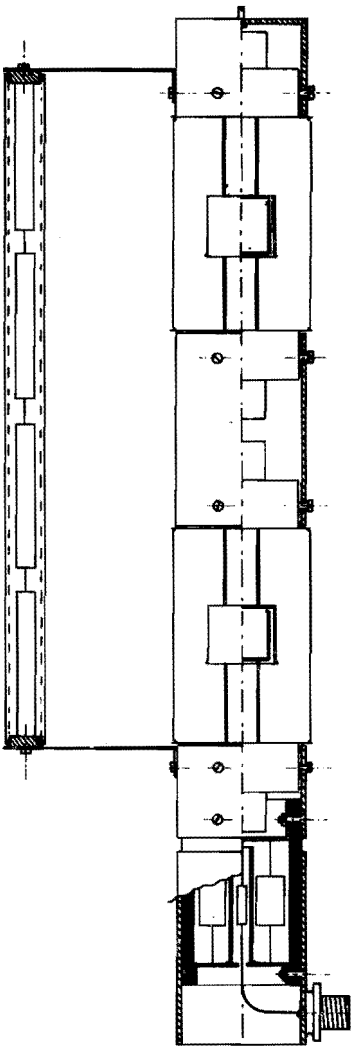

Fig. 3.1.1. Design of the voltage divider.

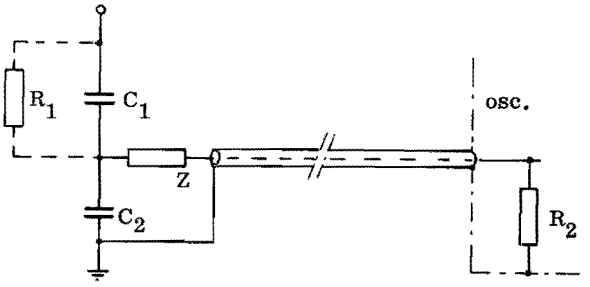

Fig. 3.1.2. Diagram of the voltage measuring circuit.

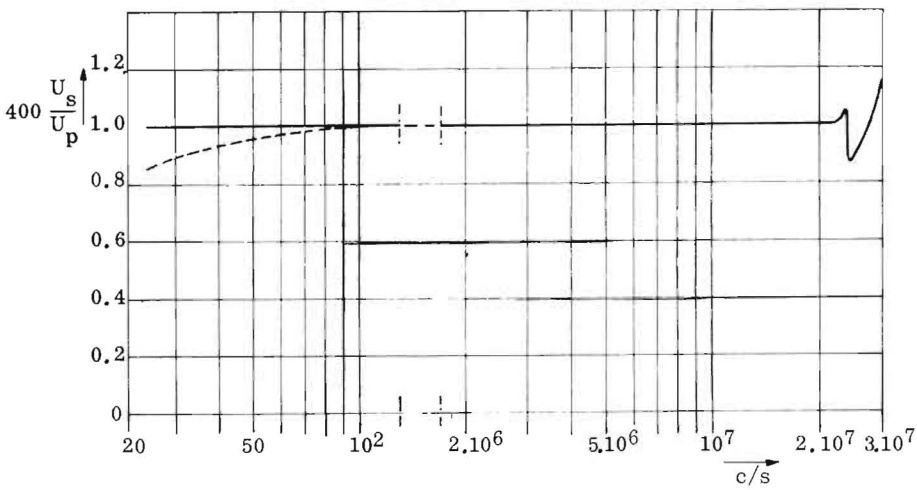

Fig. 3.1.3. Frequency response of the voltage measuring circuit.
Solid line : voltage divider with R_1 = 400 M Ω
Dashed line : voltage divider without R_1.

3.2. Current recording.

The current through the breaker was measured with coaxial shielded shunts (resistance 1.412 Ω or 0.5722 Ω). These shunts (made by Emil Haefely, Basel) have a very low self-inductance, so that the results are reliable over a very large frequency-range (d.c. to > 10 Mc/s).
Fig. 3.2.1. shows the response of the current measuring circuit to an unit-step current with a rise time of about 0.03 μs.

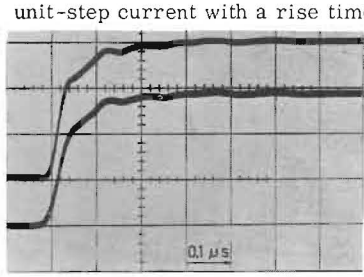

Fig. 3.2.1. Response of the current measuring circuit.
Upper line : applied current pulse (appr. 4 A)
Lower line: voltage on the oscilloscope
Time base : 0,1 μs per division.
Shunt resistance: 0.572 Ω.

A disadvantage of using shunts involves earthing of the circuit at the location of the shunt. Neglecting this could bring the oscilloscope on high potential. Quite apart from the need for extended safety measures, it is objectionable since a complicated circuit with unknown self-inductances and large ground capacitances is added to the test-circuit at the location of the shunt. Consequently, unwanted disturbances in the high-frequency phenomena as well as measuring errors as a result of varying potentials in the oscilloscope may occur. In order to measure the discharge-current

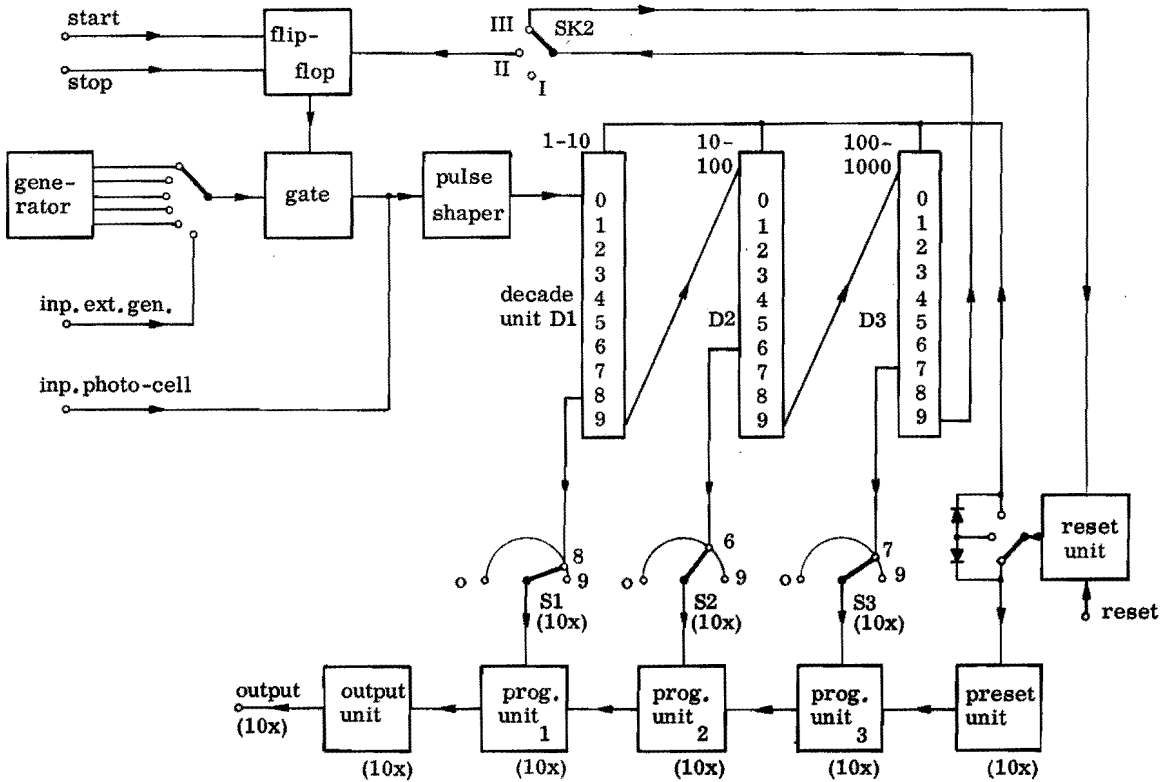

Fig. 3.4.1. Block diogram of the timing device.

I_b the shunt was always connected directly to the breaker. At the other terminal of the shunt the test circuit was earthed. At this location also the earthing of the measuring circuits, the metal cladding of the transformers and the breaker-frame were terminated (fig. 2.1.5).

3.3. Recording of the oscillograms.

Records were obtained using a Tektronix cathode-ray oscilloscope type 555 with a Polaroid Land-camera or a Robot Star-camera. This oscilloscope has a frequency range from dc to 30 Mc/s. It is provided with 2 separate inputs each with its own time base unit. Plug-in units type K, L, CA or 1A1 could be applied. The following films were used: type 47 (speed 3000 ASA) or type 410 (speed 10000 ASA) in the Polaroid camera and Agfa Record (speed 1250 ASA) in the Robot camera.

3.4. The timing-device.

For exact timing of the test cycles a timing device with 10 independently variable output channels was developed. In this apparatus 3 digital counting units are applied, so that 1000 counting pulses are available for a full measuring cycle. *)

Fig. 3.4.1. shows the block diagram. The counting pulses may be generated by multiplying the industrial frequency. Thus normal industrial frequency variations do not disturb the timing. The minimum puls-repetition-time is 500 μs. For a more detailed adjustment of the oscilloscope-trigger, an additional delay-line was used.

*) Compare W. F. J. Kersten to be published shortly.

CHAPTER 4 INSTABILITY AND CURRENT-CHOPPING

The nature of the gas-discharge during the interruption of small a.c. currents by high-voltage breakers is extremely complicated. In most cases one can speak of an arc-discharge. However, a glow-discharge may occur for very small currents even at a pressure of about one atmosphere. Whenever such a discharge suddenly ceases prior to the natural zero of the current of industrial frequency one speaks of current-chopping.

Current-chopping can be produced by a variety of causes:

a. Under the influence of motion of an interrupting medium the discharge can be lengthened considerably until it ceases.

b. The electrical characteristics of the discharge together with those of the circuit in which the breaker is placed may give rise to an unstable condition at a definite value of the current.
Then, superimposed on the current of industrial frequency a high-frequency current-oscillation with increasing amplitude (instability-oscillation, ω_i) is observed. As a result of this oscillation the instantaneous value of I_b can become zero, and the discharge is chopped (see fig. 4.1).

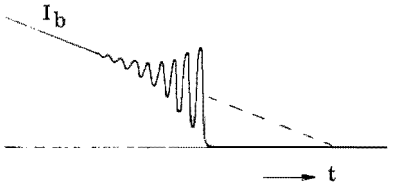

Fig. 4.1. Instability oscillation leads to current-chopping.

c. By stepwise variations of the impedance of the discharge an oscillation may be produced in the circuit to be interrupted (main-circuit-oscillation, ω_{st}). This oscillation is also superimposed on the current of industrial frequency and can result in a forced current zero.

d. In oil-circuit-breakers at currents of about 1.5 A the arc-discharge transfers into a glow-discharge. The latter requires a considerably higher voltage. Because such a sudden voltage increase is prevented by the circuit, the discharge ceases.

In this chapter the reasons for the cases a, b and d mentioned will be trea-

ed. Current-chopping due to main-circuit-oscillation will be discussed in chapter 7.

4.1. The variations of the gas-discharge in oil-circuit-breakers.

In oil-circuit-breakers the interrupting medium is produced by the discharge itself. Due to the high temperature the oil is decomposed. A gas-mixture results, which consists mainly of hydrogen (appr. 70%). Other major components are acethylene (C_2H_2), ethylene (C_2H_4) and methane (CH_4) [6] . Pressure and volume of this mixture are determined by the discharge-current and the contact-distance. In case the current does not exceed tens of amperes the average pressure of the gas is still of the order of one atmosphere (absolute).

The gas expands and mixes with the oil. This effect and the rapid contact separation results in a violent motion of the oil.

In oil-circuit-breakers equipped with arc-control-devices fresh oil is introduced into the chambers during the interruption process either by axial- and/or cross-blast or by oil-injection usually through one of the contacts. As a result the gas-discharge is continuously kept in motion and undergoes in rapid sequence elongations and transitions to shorter paths. This can be shown on oscillographic records of interruption-cycles. The discharge-voltage U_B increases to a high value and drops suddenly to lower values. These voltage variations occur more pronounced and frequently for larger contact-distances. Theyare particular violent in breakers with oil-injection and are observed immediately after contact separation (fig.4.1.1.). In other types of oil-breakers these voltage variations are usually not observed for small contact-gaps.

The record of the discharge-voltage of bulk-oil-breakers (without arc control-devices) shows the least disturbance. These voltage variations are completely arbitrary and not reproducible. Under identical test-conditions with respect to circuit and timing entirely different records are observed on successive interruptions (compare fig. 4.1.2. to 4.1.4. incl.). However, these motions of the discharge never result in perceptable current-chopping. Even for most violent voltage drops hardly any variation is found in the recording of the current (fig.4.1.1. to 4.1.4. incl.).

With exact timing of the contact separation the reproducibility of test-records with breakers without oil-injection was extremely good (disregarding the sudden voltage variations). In particular the instant at which current-chopping was initiated appeared to be not or hardly dependent on the

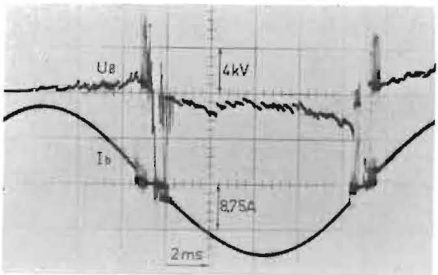

Fig. 4.1.1. Variations of the discharge-voltage in a small-oil-volume breaker with oil-injection. I =10.8 A (R.M.S.)

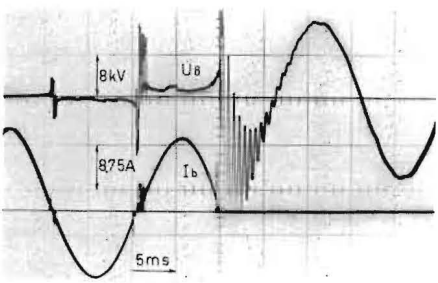

Fig. 4.1.2. Variations of the discharge voltage in a bulk-oil breaker. I =10.8 A (R.M.S.) Copper contacts.

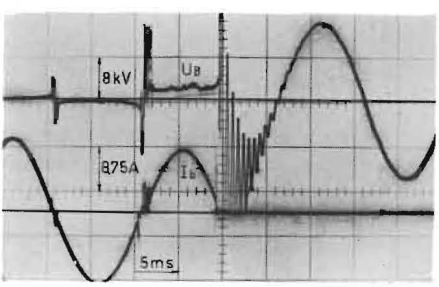

Fig. 4.1.3. Some conditions as fig. 4.1.2.

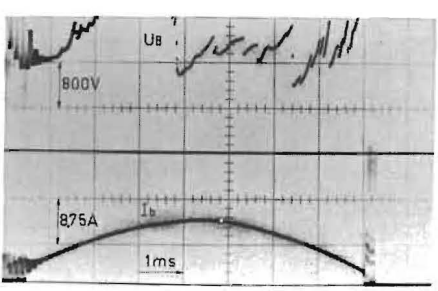

Fig. 4.1.4. Same conditions as fig. 4.1.2.

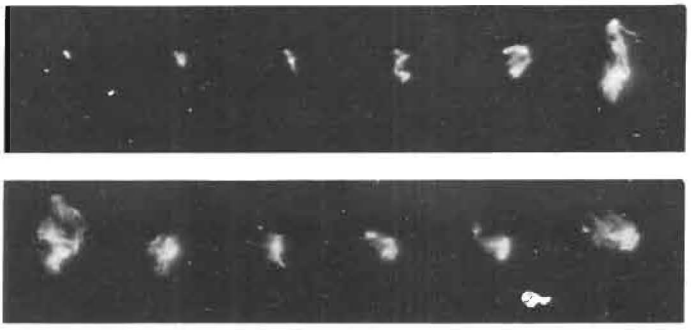

Fig. 4.2.1. Selected frames from high speed film showing movement of the discharge in an air-blast breaker. I =18 A (R.M.S.)

4.2.1.a : Instantaneous value I ≈ 12 to 4 A.
4.2.1.b : Instantaneous value I ≈ 3 to 6 A.

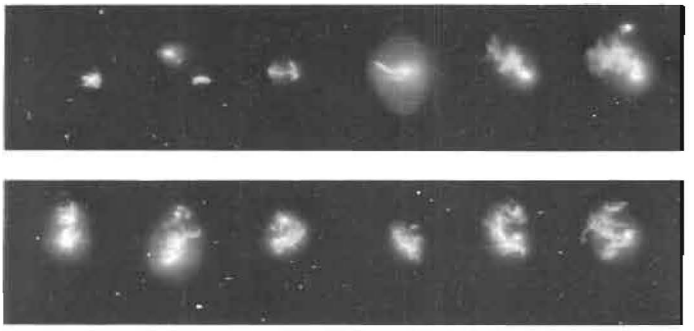

Fig. 4.2.2. Movement of the discharge in an air-blast breaker.
I =55 A (R.M.S.) Instantaneous value I ≈ 25 to 56 A for both strips.

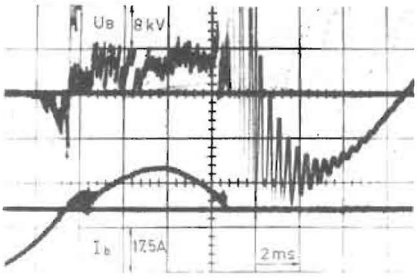

Fig. 4.2.3. Oscillogram to fig. 4.2.1.

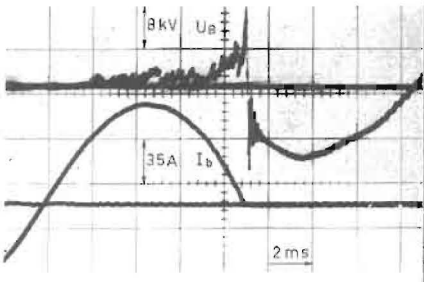

Fig. 4.2.4. Oscillogram to fig. 4.2.2.

motion of the discharge but on the instantaneous value of the current (section 4.8).

Oscillograms of an interruption-cycle of a breaker with oil-injection are much less reproducible. Current-chopping following instability-oscillation sets in at higher but less defined values. Frequently an instability-oscillation is excited by a sudden change of the impedance of the discharge.

4.2. The variations of the gas-discharge in air-blast breakers.

In an air-blast breaker the discharge is cooled by a forced air stream. It causes curls and elongations in the gas-discharge. Fig. 4.2.1. and 4.2.2. show a number of frames of high speed movies (7000 frames per second) of the gas-discharge in an air-blast breaker. Fig. 4.2.3. and 4.2.4. are corresponding oscillograms of current and voltage. Fig. 4.2.5. shows the test set-up.

The discharge is cooled by the air stream between the fixed contact (a) and the separating ring-shaped contact (b). It is blown throught the nozzle and observed via a small mirror (c) and a window (d) in the exhaust tube. In this way approximately 90% of the moving contact was visible. The movies were taken with a Fairchild camera, type HS-101. The exposure time per frame was approx. 50 μs.

The air-blast breaker was originally equipped with a resistor which was removed when the movies were taken. Comparison of oscillograms of interruption cycles of these small currents taken with and without this resistor did not produce noticeable gross or detail differences.

The erratic behaviour of the discharge is clearly seen from these frames. Rotation, elongation and curving (fig. 4.2.6.) can be distinguished when

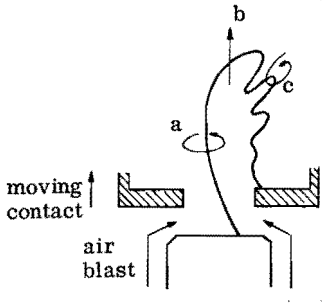

Fig. 4.2.6. Movement of the gas-discharge in an air-blast breaker.
a. rotations
b. elongations
c. curles.

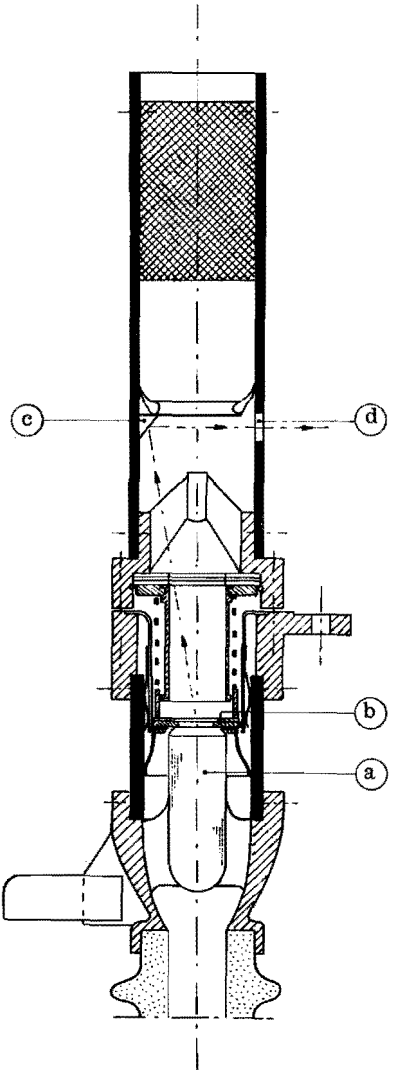

Fig. 4.2.5. Test set-up for high speed movies.

the films are projected. The elongations can be found back in the repeating phenomena of rising and rapidly decaying voltages (fig. 4.2.3 and 4.2.4). In principle two different mechanisms may occur:

a. By elongation the discharge voltage rises above the breakdown voltage of the fixed and moving contact. The current is then taken over without interruption by a new discharge path.
b. The loop of the discharge is interrupted and reignited over a shorter distance. The current is interrupted for a short time and in this case one may speak of current-chopping.

As a result of the high voltage prior to the transition to the new discharge a new breakdown follows rapidly also in the second case. Because of the parallel capacitance of the breaker (see section 6.2) it is impossible to determine from oscillograms which of the two mechanisms is active. Most likely for small or large contact gaps the first or the second mechanism respectively is predominant. The curls in the discharge channel show up on detailed oscillograms as an erratic pattern (see section 9.2).
In addition it is concluded from all stability theories that a large value of the derivative of the arc voltage with respect to the current, dU_b/dI_b, leads to instability (sections 4.4 and 4.5). This instability causes high-frequency oscillation. Curls and electrical instability can occur simultaneously, in particular for highly elongated discharges and most of all for small values of the current to be interrupted. The picture is further complicated by the two parallel-oscillations and the main-circuit-oscillation (chapter 7).
The reproducibility of interruption cycles particularly for small currents is minute due to these phenomena.

In the circuits investigated current-chopping due to elongation of the discharge never resulted in extreme overvoltages because it was always rapidly followed up by a new low-impedance breakdown.

Generally "electrical instability" was clearly recognizeable by increasing instability-oscillation. Frequently the instability starts after sudden drops in de discharge-voltage.

4.3. Stability criteria for gas-discharges.

The static characteristic of a gas-discharge $U_b = f(I_b)$ relates burning voltage U_b and d.c. discharge current I_b under steady-state condition. For the currents considered here this characteristic has a negative slope (fig. 4.3.1) and may be approximated by the expression [7, 8, 9]

$$U_b I_b^{\alpha} = K \qquad (4.3.-1)$$

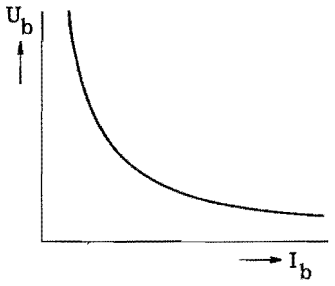

Fig. 4.3.1. Static characteristic of a gas-discharge.

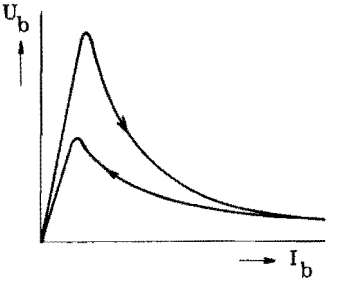

Fig. 4.3.2. Dynamic characteristic of a gas-discharge.

Here α and K are constants, dependent on the length of the discharge and the manner in which the electric input is balanced by power-dissipation. Yoon and Spindle [8] found for stationary discharges $0,3 \leq \alpha \leq 1$.

As far back as 1905 Simon [10] pointed out that a.c. discharges do not follow the static characteristics. He termed the relation $U_b = f(I_b)$ in case of a.c. the dynamic characteristic (fig. 4.3.2). The difference between the two characteristics is caused by thermal lag over the varying electric input. Simon introduced for this phenomenon the term "arc hysteresis". Later other investigators [11, 12] derived from energy considerations of arc discharges, that thermal adjustment of the arc column follows an exponential law and introduced a time-constant Θ. For further details see section 4.5 and equation (4.5.-4). In chapter 5 a brief review of these theories is given, including a more thorough discussion fo the time-constant.

Whenever the current through the discharge undergoes slow variations the voltage follows in first approximation the static characteristic and one may speak of a quasi-static characteristic. Because the time-constants of discharges in circuit-breakers are usually small, ($\approx 1\,\mu s$) no differentiation is made in this thesis between static and quasi-static charac-

teristics whenever the discharge current is varying with industrial frequency.

The combined system consisting of electric circuit and gas-discharge is stable as long as a small disturbance of the current or the voltage has such a damped transient response that after some time the same conditions prevail as prior to the disturbance. Already in 1900 Kaufman [13] utilized this criterion to determine stability-conditions of a discharge which was fed via a series resistor from a d.c. source

$$\frac{dU_b}{dI_b} + R > 0 \qquad (4.3.-2)$$

A number of investigators paid since attention to stability-criteria of gas-discharges in various circuits. Nöske [14] and Rizk [9] give extensive literature references. Some of these theories try to explain current-chopping in high-voltage breakers. One can distinguish theories which consider exclusively the static discharge characteristic, and theories which include in addition the influence of the time constant on the stability. The first kind, referred to as "static stability theory" will be discussed in section 4.4, the second kind referred to as "dynamic stability theory",most extensively studied by Rizk [9], in section 4.5.

4.4. Static stability theories.

In the simplest and still broadly accepted explanation of current-chopping the static characteristic and the parallel capacitance C_p are considered exclusively.

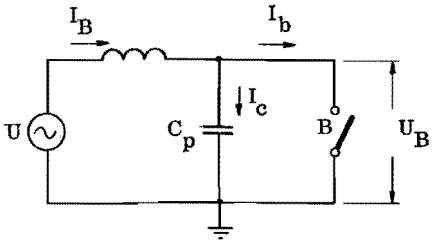

Fig. 4.4.1. Equivalent circuit for current-chopping on short circuit interruption.

The fundamental concept is the equivalent circuit shown in fig. 4.4.1. As the current I_b decays to zero the voltage across C_p rises as a result of the negative slope of the discharge-characteristic, causing the charging current I_c to increase. Since the relatively large self-inductance L does not permit a rapid variation of I an increase of I_c must result in a de-

crease of I_b. Consequently U_B increases further involving an even faster rise of I_c, with a corresponding accelerated decay of I_b towards zero.

This train of thought is not new. It was already published in 1935 by van Sickle [15], however to explain the advancement of the current-zero on interruption of short-circuit currents. Puppikofer [16] expanded it further in 1939 and gave the well known illustration fig. 4.2.2. Besides he stipulated that the influence of the parallel-capacitance should be very much more pronounced on interruption of unloaded transformers because there the currents are of so much lower magnitude. This explanation of current-chopping was accepted since by many authors, for example by Young [17]. However the latter shows in support of the theory an oscillogram on which occurs not a monotonic approach to zero of I_b (fig. 4.4.2) but a current-chop after an instability oscillation (fig. 4.1).

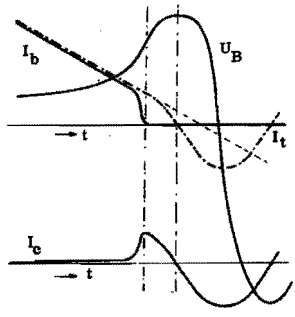

Fig. 4.4.2. Illustration of current-chopping by Puppikofer.
I_b = current through the discharge.
I_c = current through the parallel capacitance.
$I_B = I_b + I_c$
U_B = voltage across the breaker.

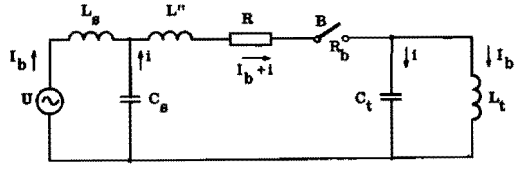

Fig. 4.4.3. Equivalent circuit used by Baltensperger.

The equivalent circuit fig. (4.4.1) can only be applied to short-circuits near the terminal of the breaker. Then C_p represents the capacitance of the feeding line and can have a sizeable value. The current limiting self-inductance L is the equivalent of the short-circuit reactance of the feeding source and network or of the short-circuit test-station. Diagram fig. 4.4.1. is acceptable only for the evaluation of the short-circuit interrupting ability of circuit-breakers. However circuits in which small inductive currents are observed have entirely different characteristics (fig. 2.1.6

and 2.2.2). These circuits imply a small value of the parallel capacitance C_p (of the order of 100 pF). Hence an explanation of current-chopping by the above given mechanism is an over-simplification as will be shown later in this section. Current-chopping after a monotonic decreasing current as in fig. 4.4.2. was never observed in our test-circuits.

In 1950 Baltensperger [18] showed that instability-oscillation with increasing amplitude can arise as a result of the negative $U_b - I_b$-characteristic. He used the equivalent circuit of fig. 4.4.3. C_s and C_t are the lumped capacitances of the source and load respectively. L'' is the self-inductance of the circuit between source and load in which the breaker is located. The self-inductances L_s (source) and L_t (load) are so large that they have no influence in first approximation on high-frequency oscillation. The rather large capacitances C_s and C_t act in that respect like a short-circuit. Baltensperger approximated the static characteristic by the equation $U_b = a - b\, I_b$, with $a > 0$ and $b > 0$, and expressed the frequency of the instability-oscillation by

$$\omega_i = \frac{1}{\sqrt{L'' C''}} \qquad (4.4.-1)$$

and the stability criterion by

$$b < R \qquad (4.4.-2)$$

A somewhat more exact result is obtained for the same circuit by assuming a discharge characteristic according equation (4.4.-1): $U_b I_b^{\alpha} = K$. Considering the decreasing current I_b constant over a short interval and assuming a disturbance of magnitude i on the discharge, where $i \ll I_b$, then the circuit equation becomes

$$L'' \frac{d(I_b + i)}{dt} + (R + R_b)\ (I_b + i) + \int \frac{i}{C''}\, dt + U_o = 0 \qquad (4.4.-3)$$

where

$$C'' = \frac{C_s C_t}{C_s + C_t} \qquad U_o = (U_s)_o + (U_t)_o \qquad R_b = \frac{U_b}{I_b}$$

$(U_s)_o$, $(U_t)_o$ = initial voltages across C_s and C_t at t = 0.

The solution of this equation has the form

$$i(t) = i\, e^{-\beta t} \cos \omega_i t \qquad (4.4.-4)$$

where

$$\beta = \frac{R - \alpha R_b}{2 L''} \qquad (4.4.-5)$$

$$\omega_i = \sqrt{\frac{1}{L''C''} - \left(\frac{\alpha R_b - R}{2\,L''}\right)^2} \qquad (4.4.-6)$$

The system is unstable, when $\beta < 0$, or

$$R_b > \frac{R}{\alpha} \qquad (4.4.-7)$$

At the stability limit ($\beta = 0$) the frequency ω_i is

$$\omega_i = \frac{1}{\sqrt{L''C''}} \qquad (4.4.-8)$$

Besides it is the maximum possible value.

From equation (4.4-6) it is concluded that transient oscillations occur when

$$R_b < \frac{1}{\alpha}\,(R + 2\sqrt{L''/C''}) \qquad (4.4.-9)$$

The region within which unstable oscillations are possible is bounded by

$$\frac{R}{\alpha} < R_b < \frac{R + 2\sqrt{L''/C''}}{\alpha} \qquad (4.4.-10)$$

(see fig. 4.4.4).

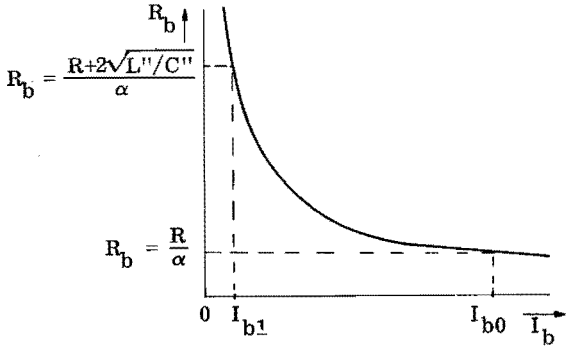

Fig. 4.4.4. Results of static stability theory.

$I_{b_1} < I_b < I_{b_0}$ range for current-chopping after high frequency oscillation.

$0 < I_b < I_{b_1}$ range for current-chopping with monotonic decaying current.

The system remains unstable for

$$R_b > \frac{R + 2\sqrt{L''/C''}}{\alpha} \qquad (4.4.-11)$$

but the current chops without oscillation.

In practical circuits

$$2\sqrt{L''/C''} \gg R \qquad (4.4.-12)$$

Therefore in agreement with this consideration a zero approaching current pass through a large region over which current-chopping after an instability-oscillation can occur, before current-chopping with a monotonic decrease is possible. This shows that the Puppikofer theory fails for circuits with small inductive currents. However, there are also objections against this static-stability concept.

a) Often instability-oscillations are observed with frequencies higher than given by equation (4.4.-8)

b) The resistance R is very small. In an extension to this theory Baltensperger [19] suggested in 1955 resistance values of $R \approx 0.05\,\Omega$ for low frequencies ($< 10^3$ c/s) and $R \approx 1\,\Omega$ for high frequency oscillation ($\approx 10^5$ c/s). Since α is of the order of 1, the stability limit should be exceeded according to equation (4.4.-10) for decreasing currents when $R_b \approx 1\Omega$, i.e. relatively large currents. In fact the discharge is chopped at currents of a few amperes for which the arc resistance is hundreds or a few thousands of ohms.

From paragraph a) above it is concluded, that the instability oscillation is not (exclusively) determined by the self-inductances and capacitances of the circuit of fig. 4.4.3. The parallel-capacitance C_p and the self-inductance L_p turn out to be important (see section 4.7). This cannot explain why the discharge still remains stable long after the (static) stability limit has been exceeded. However the dynamic considerations will produce criteria which are in better agreement with experimental results.

4.5. Dynamic stability theories.

The most extensive study of the dynamic stability of discharges in circuit-breakers may be found in the thesis of Rizk [9] who has expanded on the theories of Mayr [12] and Nöske [14].

The starting point is the response of a stationary discharge (I_b, U_b) to a small unit-step disturbance i at t = 0, according fig. 4.5.1.
Since for an abrupt change the discharge behaves like a resistor, the voltage U(t) at first drops by iR_b such that:

$$U(t)_o = U_b - iR_b \qquad (4.5.-1)$$

Thereafter U(t) approaches the value

$$U(t)_\infty = U_b - i\left(\frac{dU}{dI}\right)_{I=I_b} = U_b + iR_d \qquad (4.5.-2)$$

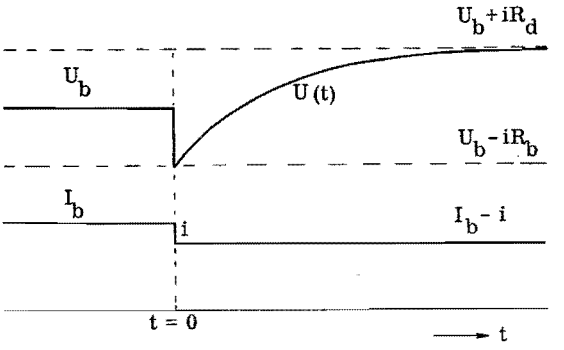

Fig. 4.5.1. Response of a static arc to a unit-step current according Rizk.

where

$$R_d = -\left(\frac{dU}{dI}\right)_{I = I_b} \qquad (4.5.-3)$$

R_d represents the dynamic or transient resistance of the discharge. Experimentally it is shown [8, 9] that in first approximation the new stationary condition is approached exponentially. This may be expressed as:

$$u(t) = U(t) - U_b = i R_d - (R_d + R_b)\, i\, e^{-t/\Theta} \qquad (4.5.-4)$$

Here u(t) is the difference between the discharge-voltage U(t) at time t and the initial steady-state voltage. Rizk calls Θ the time-constant of the discharge. (His time-constant is exclusively based on the electric performance of the discharge and is not derived from theoretical considerations). Since conversely a current i is the response to a voltage variation u(t) across the discharge an effective admittance can be determined from (4.5.-4).

Laplace transformation of u(t) yields

$$u(p) = \frac{iR_d}{p} - \frac{i\,(R_d + R_b)}{p + 1/\Theta} \qquad (4.5.-5)$$

The admittance in operational form is:

$$y(p) = \frac{i(p)}{u(p)} = \frac{1}{R_b} + \frac{1}{R_i + pL_a} \qquad (4.5.-6)$$

with

$$R_i = -\frac{R_b R_d}{R_b + R_d} \qquad (4.5.-7)$$

and

$$L_a = \frac{R_b^2\, \Theta}{R_b + R_d} \qquad (4.5.-8)$$

Assuming a discharge characteristic $U_b I_b^{\alpha} = K$ and hence $R_d = \alpha R_b$ there follows for R_i and L_a

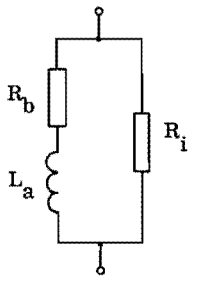

$$R_i = - \frac{\alpha R_b}{1+\alpha} \qquad (4.5.-9)$$

$$L_a = \frac{\Theta R_b}{1+\alpha} \qquad (4.5.-10)$$

Fig. 4.5.2. Equivalent circuit for a single time-constant arc for a small deviation from static conditions according Rizk.

A number of equivalent circuits can be synthesized which satisfy the expression for y (p). Rizk substitutes in the Baltensperger circuit (fig. 4.4.3) the equivalent of the discharge according fig. 4.5.2. He too assumes that L_s and L_t have such high values that they may be neglected in an equivalent high frequency circuit.

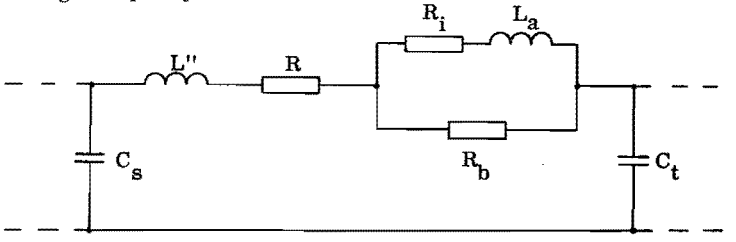

Fig. 4.5.3. Equivalent circuit used by Rizk.

The remainder is the circuit of fig. 4.5.3. for which he derives the differential equation

$$\frac{d^3 I}{dt^3} + a_2 \frac{d^2 I}{dt^2} + a_1 \frac{dI}{dt} + a_o I = 0 \qquad (4.5.-11)$$

with the characteristic equation

$$p^3 + a_2 p^2 + a_1 p + a_o = 0 \qquad (4.5.-12)$$

where

$$a_2 = \frac{R_i}{L_a} + \frac{R_b}{L_a} + \frac{R_b}{L''} + \frac{R}{L''} \qquad (4.5.-13)$$

$$a_1 = \frac{1}{L''C''} + \frac{RR_i}{L''L_a} + \frac{RR_b}{L''La} + \frac{R_i R_b}{L'' L_a} \qquad (4.5.-14)$$

$$a_o = \frac{R_i + R_b}{L'' L_a C''} \qquad (4.5.-15)$$

$$C'' = \frac{C_s C_t}{C_s + C_t} \qquad (4.5.-16)$$

Hurwitz criteria require for stable solutions of (4.5.-11)

$$\frac{R_b}{C''} - \frac{L'' R_d}{\Theta^2} - \frac{R_b R_d}{\Theta} = 0 \qquad (4.5.-17)$$

assuming $R \ll R_b$ and $R \ll R_d$ in agreement with experimental results.

At the stability limit a set of roots of (4.5.-12) becomes imaginary.
As a result this equation can be resolved into factors

$$(p + \beta)(p^2 + \omega_i^2) = 0 \qquad (4.5.-18)$$

or

$$p^3 + \beta p^2 + \omega_i^2 p + \beta \omega_i^2 = 0 \qquad (4.5.-19)$$

and one finds $a_1 = \omega_i^2$.

Hence there results an oscillation of frequency

$$\omega_i = \frac{1}{\sqrt{C''(L'' + \Theta R_b)}} \qquad (4.5.-20$$

Assuming again a characteristic $U_b I_b^{\alpha} = K$, equation (4.5.-17) becomes

$$\frac{1}{C''} - \frac{\alpha L''}{\Theta^2} - \frac{\alpha R_b}{\Theta} > 0 \qquad (4.5.-21)$$

At the stability limit (4.5.-21) becomes identical zero.
As a result (4.5.-20) changes to

$$\omega_i = \frac{\sqrt{\alpha}}{\Theta} \qquad (4.5.-22)$$

This same relation was obtained by Mayr earlier but in a more elaborate way (equation 49 in [12])

Mayr also determined the stability criterion for the special case $\alpha = 1$ (hence $R_d = R_b$), $L_s + L_t \to \infty$ and $L'' = 0$ (fig. 4.5.4).

$$\Theta > R_b C_p \qquad (4.5.-23)$$

But here C_p is an arbitrary capacitance parallel to the discharge. With the same simplifications expression (4.5.-23) can also be obtained following Rizk's method.

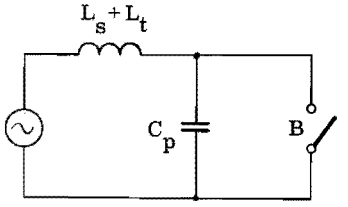

Fig. 4.5.4. Circuit used by Mayr.

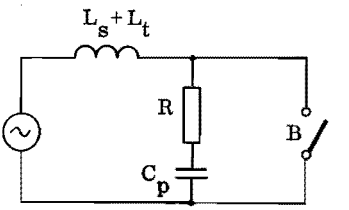

Fig. 4.5.5. Circuit used by Kopplin.

Nöske's [14] circuit consists of a source, a circuit-breaker and a transformer. He substituted a simple parallel connection of a breaker and a transformer capacitance C_t and derived the stability criterion

$$\Theta > R_d C_t \qquad (4.5.-24)$$

At the stability limit the frequency equals $\omega_i = \frac{1}{\sqrt{\Theta R_b C_t}}$ (4.5.-25)

The same result is obtained from equations (4.5.-16) and (4.5.-17) when $L'' = 0$ and $R_d = \alpha R_b$.

Kopplin [20] enlarged Mayr's criterion (4.5.-19) by assuming an arbitrary characteristic and placing a resistance R in series with capacitance C_p (fig. 4.5.5). He obtained thus the stability criterion

$$\Theta > - C_p \left\{ \frac{dU_b}{dI_b} + R \left(1 + \frac{\Theta R_b}{L}\right)\right\} \qquad (4.5.-26)$$

where $L = L_s + L_t$

Under normal circumstances is $\frac{\Theta R_b}{L} \ll 1$, then with $\frac{dU_b}{dI_b} = \alpha R_b$,

Kopplin's stability criterion becomes

$$\Theta > C_p (\alpha R_b - R) \qquad (4.5.-27)$$

Setting $L'' = 0$, $R = 0$ and $C_p = C''$ this turns out to be a special case of Rizk's criterion (equation 4.5.-17).

4.6. Check of the stability criteria.

Checking the preceding stability criteria in the usual circuits is rather difficult. Since according sections 4.1 and 4.2 the intensity of cooling and the length of the discharge are subject to continued variation also the values α and K in the expression $U_b I_b^{\alpha} = K$ assumed initially constant are variable.

Moreover it is not simple to determine exact values of active capacitances and self-inductances.

In 1955 Mayr [21] published a method to derive the time constant from the oscillation (ω_i) of an unstable arc. He utilized an arc in air between horizontal electrodes carrying an a.c. current of I = 2 A (R.M.S.). This arc was elongated by means of a vertical airblast resulting in a repetitive cycle of chopping and reignition (as discussed in section 4.2).

Assuming $\alpha = 1$ he derived Θ from the oscillations prior to the chopping of the discharge according equation (4.5.-22), i.e. $\omega_i \Theta = 1$. Thus a mean value of $\Theta = 22\ \mu s$ was found which showed to be more or less independent of the velocity of the air stream (12.5 m/s to 100 m/s) and of the capacitance parallel to the discharge (0.002 μF to 0.1 μF). Mayr considered this result to be in good agreement with his theory. He reported further that the condition $\Theta = R_b C_p$ (4.5.-23) was satisfied or in other words that the discharge supposedly followed a characteristic given by $U_b I_b = K$.

This last statement disagrees with out measurements.

The approximation of the discharge characteristic by $U_b I_b^{\alpha} = K$ with fixed values α and K can be applied only to elongating arcs for very short time intervals. A large number of such approximations with continually varying α and K would be necessary to describe an entire interruption cycle. Because even for an increasing current the voltage can rise as a result of increasing arc path also negative values of α would be possible.

Also the results of Yoon and Browne [22] are not in agreement with those of Mayr. They investigated time-constants in vertical axially blasted arcs and found a large dependence of Θ on the air-velocity (see fig. 5.4.1 and 5.4.2).

Damstra [23] performed a (very limited) check on the theory of Mayr in an entirely different manner. He investigated with an oil-breaker model (plain break) the influence of the parallel capacitance C_p on the chopping level I_o. Starting with Mayr's characteristic $U_b I_b = K$ and the stability

conditions $\Theta = R_o C_p$ and $\omega_i \Theta = 1$ it can be shown that

$$I_o = \sqrt{\omega_i C_p K} \qquad (4.6.-1)$$

If one assumes the time-constant to be independent of the instantaneous value of the current I_b then ω_i may be considered constant as well. This leads to

$$I_o \sim \sqrt{C_p} \qquad (4.6.-2)$$

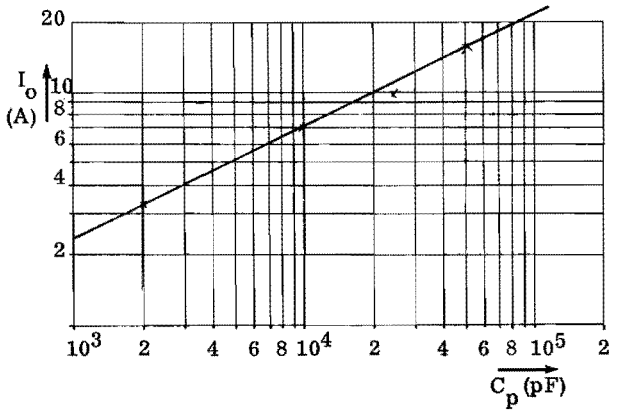

Fig. 4.6.1. Relation between chopping level I_0 and parallel capacitance C_p according Damstra.

Fig. 4.6.1. shows the chopping level I_o as a function of the parallel capacitor C_p as given by Damstra. It may be seen that I_o indeed increases with the square root of the capacitance. Also our measurements on a bulk-oil breaker proved that the characteristic $U_b I_b = K$ is an aceeptable approximation (for decreasing currents).
See fig. 4.8.1 to 4.8.4 inclusive.

However from Damstra's experiments it turned out that the arc length has a very limited influence on the chopping level. This is not in agreement with theory. When the characteristic $U_b I_b = K$ is introduced into equation (4.6.-1) there follows

$$I_o = U_o \omega_i C_p \qquad (4.6.-3)$$

and with $\omega_i \Theta = 1$

$$I_o = \frac{U_o C_p}{\Theta} \qquad (4.6.-4)$$

For the arcs under consideration the arc voltage is nearly proportional to the arc length (fig. 4.8.1 to 4.8.4). The time-constant on the other hand is

is according to the theory of Mayr independent of the length of discharge. This is confirmed by Rizk [9] while Yoon and Spindle [8] found only a very small dependence.
Therefore from (4.6.-4) it follows that the chopping level I_o should increase proportional with arc length.

Rizk [9] attempted to prove his theory experimentally using a circuit according fig. 4.6.2. L is a lumped self-inductance representing the distributed self-inductance L'' while C is a capacitor substituted for the distributed capacitances C_s and C_t. He assumed that the inherent parallel capacitance of the breaker C_p is negligible.
With the aid of equation (4.5.-18): $\omega_i \Theta = \sqrt{\alpha}$, Θ was determined from the frequency of the instability oscillation ω_i.

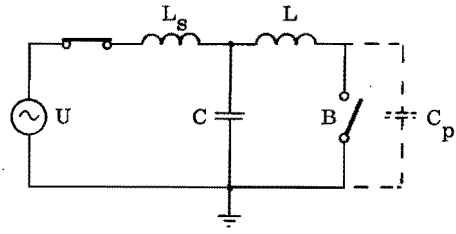

Fig. 4.6.2. Circuit used by Rizk for experimental checking of stability criteria.

The exponent α was determined from a U_b-I_b-characteristic obtained by measuring arc-voltages at the peak value of sinusoidal currents of different amplitude. In this way α showed to be $\alpha \approx 0.4$.
The arc-resistance R_b was determined from current and voltage at the instant of noticeable onset of the oscillation. With these data the left-hand side of equation (4.5.-21) was computed and its difference from zero evaluated

$$\frac{1}{C} - \frac{\alpha L}{\Theta^2} - \frac{\alpha R_b}{\Theta} \equiv \Delta \qquad (4.6.-5)$$

Rizk related Δ to $^1/C$, the positive portion of the above expression only and obtained for $\frac{\Delta}{1/C} \cdot 100\%$ values between 1.6% and 30.8%.

Since Rizk assumes L, C and α to be constant and Θ hardly varies, R_b is the only variable which determines the instant of current-chopping. Therefore a check on the theory should consist of a comparison of R_b with the theoretical value R_o, valid at the stability limit $\Delta = 0$.

Following this path one finds from the measurements which Rizk (p.p. 95, 96, 97 in [9]) assembled in three tables:

Table I $\frac{R_b - R_o}{R_o}$ =	- 3.9	0.11	- 2.46	26	4.13
Table II $\frac{R_b - R_o}{R_o}$ =	6.2	7.2	- 0.5	0.59	0.82
Table III $\frac{R_b - R_o}{R_o}$ =	- 0.20	0.36	- 0.10	0.27	

The deviations in the first two tables are so large that at best contrary conclusions are justified. On the other hand in these measurements $L/\Theta \approx 5\, R_b$. Therefore the arc resistance has a minute influence while small errors in the measurement of α and ω_i have a significant effect on R_o.

The results of table III are in better agreement with theory. For this series on purpose values of L and C were chosen such that ω_i deviates considerably from the natural frequency of the LC-circuit.
In this case is according equation (4.5.-20) $R_b \Theta \gg L$ and therefore the second term of equation (4.6.-5) has hardly any influence on the stability limit.

4.7. The influence of the parallel-capacitance and the self-inductance of the circuit-breaker on stability.

In the preceding it was shown that a quantitative check on the stability criteria even in simple circuits is compli cated and till now has produced little results. This becomes even worse when the circuit-breaker is located in a circuit with distributed capacitances and self-inductances. Following Baltensperger [18], Rizk is of the opinion that the stability is determined by the discharge together with the feeding- and load-circuit. Then the active capacitance C'' of equation (4.5.-21) consists of the series connection of the equivalent capacitances of the station (C_s) and of the transformer (C_t), see fig. 2.2.2, 4.4.3 and 4.5.3

$$C'' = \frac{C_s C_t}{C_s + C_t} \qquad (4.7.-1)$$

The active self-inductance L'' is considered to consist of the series connection of the equivalent inductances of the lines between the station and

the circuit-breaker and between the transformer and the outgoing side of the breaker (fig. 2.2.2)

$$L'' = L'_s + L'_t + L_g \qquad (4.7.-2)$$

Rizk also paid attention to the influence of the parallel-capacitance C_p. He concluded that this capacitance always tends to disturb the stability at a higher level of the discharge current.

On the other hand the influence of C_p should be negligible provided $\alpha R_b C_p \ll \Theta$.

However, when stability conditions are set up considering also C_p then in principal the self-inductance L_p must be accounted for too.

L_p consists mainly of the inherent inductance of the circuit-breaker. Because the combinations L'', C'' and L_p, C_p must now be considered simultaneously the equivalent circuit of fig. 4.7.1 is more satisfactory than that of fig. 2.2.2.

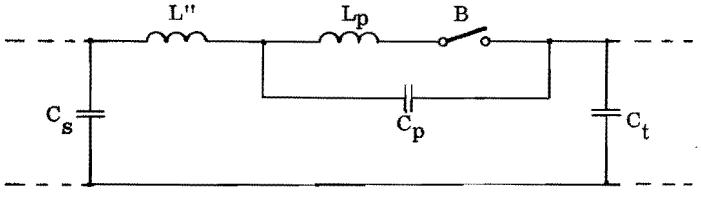

Fig. 4.7.1. Equivalent circuit, C_p and L_p included.

Substituting again fig. 4.5.2 for the breaker B the complete circuit fig. 4.7.2 is obtained. The differential equation of this circuit is of the fifth order and has as characteristic equation

$$a_5 p^5 + a_4 p^4 + a_3 p^3 + a_2 p^2 + a_1 p + a_o = 0 \qquad (4.7.-3)$$

with coefficients

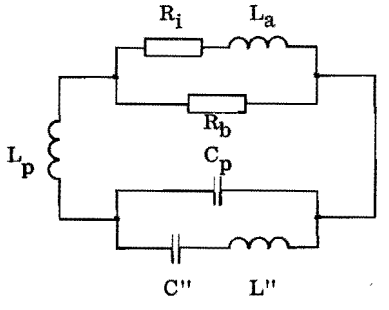

Fig. 4.7.2. Complete equivalent circuit for stability investigation, C_p, L_p and substitute for gas-discharge included.

$$a_0 = \frac{R_i + R_b}{L_a L'' C'' L_p C_p} \tag{4.7.-4}$$

$$a_1 = \frac{R_i R_b}{L'' L_p L_a} \left(\frac{1}{C_p} + \frac{1}{C''} \right) + \frac{1}{L_p C_p L'' C''} \tag{4.7.-5}$$

$$a_2 = \frac{R_i + R_b}{L_a} \left(\frac{1}{L_p C_p} + \frac{1}{L'' C_p} + \frac{1}{L'' C''} \right) + \frac{R_b}{L_p L'' C''} + \frac{R_b}{L'' L_p C_p} \tag{4.7.-6}$$

$$a_3 = \frac{R_i R_b}{L_p L_a} + \frac{1}{L_p C_p} + \frac{1}{L'' C_p} + \frac{1}{L'' C''} \tag{4.7.-7}$$

$$a_4 = \frac{R_b}{L_p} + \frac{R_i + R_b}{La} \tag{4.7.-8}$$

$$a_5 = 1 \tag{4.7.-9}$$

Introducing as before equations (4.5-8) and (4.5-9)

$$R_i = -\frac{\alpha R_b}{1 + \alpha} \tag{4.7.-10}$$

and

$$L_a = \frac{\Theta R_b}{1 + \alpha} \tag{4.7.-11}$$

and putting further

$$\omega_{p1}^2 = \frac{1}{L_p C_p} \tag{4.7.-12}$$

$$\omega_{p2}^2 = \frac{1}{L'' C''} \tag{4.7.-13}$$

$$\omega_{p3}^2 = \frac{C'' + C_p}{C_p} \omega_{p2}^2 \tag{4.7.-14}$$

then the coefficients a_0 to a_5 become

$$a_0 = \frac{\omega_{p1}^2 \omega_{p2}^2}{\Theta} \tag{4.7.-15}$$

$$a_1 = \omega_{p1}^2 \omega_{p2}^2 - \frac{\alpha R_b}{\Theta L_p} \omega_{p3}^2 \tag{4.7.-16}$$

$$a_2 = \frac{\omega_{p1}^2}{\Theta} + \omega_{p3}^2 \left(\frac{1}{\Theta} + \frac{R_b}{L_p} \right) \tag{4.7.-17}$$

$$a_3 = \omega_{p1}^2 + \omega_{p3}^2 - \frac{\alpha R_b}{\Theta L_p} \qquad (4.7.-18)$$

$$a_4 = \frac{1}{\Theta} + \frac{R_b}{L_p} \qquad (4.7.-19)$$

$$a_5 = 1 \qquad (4.7.-20)$$

At the limit of oscillatory instability the real part of the impedance of the circuit (fig. 4.7.2) can be set equal to zero

$$\frac{R_i (R_i + R_b) + \omega_i^2 L_a}{(R_i + R_b)^2 + \omega_i^2 L_a} = 0 \qquad (4.7.-21)$$

Introducing (4.7.-10) and (4.7.-11) the instability-oscillation ω_i is obtained

$$\omega_i = \frac{\sqrt{\alpha}}{\Theta} \qquad (4.7.-22)$$

which is obviously in agreement with the previously derived result (4.5.-22).

Equation (4.7.-3) describes a stable system when a_0 to a_5 incl. are all positive and further Hurwitz' criteria are satisfied

$$a_1 a_2 - a_0 a_3 > 0 \qquad (4.7.-23)$$

$$a_3(a_1 a_2 - a_0 a_3) - a_1(a_1 a_4 - a_0 a_5) > 0 \qquad (4.7.-24)$$

$$(a_3 a_4 - a_2 a_5)(a_1 a_2 - a_0 a_3) - (a_1 a_4 - a_0 a_5)^2 > 0 \qquad (4.7.-25)$$

With $\omega_i^2 = \alpha/\Theta^2$ the following conditions result therefrom

$a_1 > 0$ requires $\qquad R_b < \frac{\Theta}{\alpha (C_p + C'')}$ $\qquad (4.7.-26)$

$a_3 > 0$ requires $\qquad R_b < \frac{\Theta}{\alpha C_p} \left(1 + \frac{L_p}{L''} \cdot \frac{C_p + C''}{C''}\right)$ $\qquad (4.7.-27)$

Requirement (4.7.-23) results in

$$R_b < \frac{\Theta}{\alpha (C'' + C_p)} - \frac{L''}{\Theta} \left(\frac{C''}{C'' + C_p}\right) - \frac{L_p}{\Theta} \qquad (4.7.-28)$$

and (4.7.-25) in

$$R_b < \frac{\frac{\Theta}{\alpha C''} - \frac{L''}{\Theta}}{1 - \frac{\alpha}{\Theta^2} \cdot \frac{L'' C'' C_p}{C'' + C_p}} - \frac{L_p}{\Theta} \qquad (4.7.-29)$$

The condition following from (4.7.-24) can be given in a condensed expression only if one assumes $C'' \gg C_p$, $L'' \gg L_p$ and neglects all second

order terms

$$R_b < \frac{\frac{\Theta}{\alpha C''} - \frac{L''}{\Theta}}{1 - \frac{\alpha}{\Theta^2} \cdot \frac{L''C''C_p}{C'' + C_p}} \qquad (4.7.-30)$$

Condition (4.7.-30) is in close agreement with (4.7.-29). It is easy to see that conditions (4.7.-26) and (4.7.-27) permit a larger R_b than (4.7.-28) or (4.7.-29). Which of these two requires the smallest value of R_b and hence determines the stability limit for decreasing current cannot be said with certainty without further study. Determining factors are α, Θ, L'', C'' and C_p and to a smaller extent L_p. Writing (4.7.-29) in the form

$$R_b < \frac{\Theta}{\alpha C''} \cdot \frac{1 - \frac{\omega_i^2}{\omega_{p_2}^2}}{1 - \frac{\omega_i^2}{\omega_{p_2}^2} \cdot \frac{C_p}{C_p + C''}} - \frac{L_p}{\Theta} \qquad (4.7.-31$$

it may even be seen that for $\omega_i > \omega_{p2}$ a stable discharge is possible if the additional condition

$$\omega_i^2 \frac{C_p}{C_p + C''} > \omega_{p2}^2 \qquad (4.7.-32)$$

is satisfied.

(Here $\omega_i = \alpha/\Theta^2$ and $\omega_{p2}^2 = 1/L''C''$ are exclusively determined by the discharge and the circuit respectively).

Letting $C_p = 0$ and $L_p = 0$ equation (4.7.-28) as well as (4.7.-29) becomes Rizk's criterion (4.5.-21).

The foregoing considerations show, particularly for small time-constants (oil-breakers) and large values of α (rapidly elongating discharges of air-blast breakers), that already a small C_p influences the stability in a considerable way.

This results in the fact that in this case an experimental check of the stability criteria is very difficult.

4.8. Current-chopping in oil-breakers due to transition from arc to glow-discharge

The interruption cycle of oil-breakers without oil-injection shows a more regular and more reproducible pattern than air-blast breakers (compare sections 8.1 and 9.1). In our circuits current-chopping occured always at instantaneous values between 1.3 and 2 A. Also Damstra [23] reports $I_o = 1.3$ A as the lowest attainable value. The values of R_b and $R_d = \alpha R_b$ at the chopping level show a sizeable spread, see e.g. fig. 4.8.1. The discharge characteristics shown in fig. 4.8.1 to 4.8.4 inclusive are obtained from x - y - oscillograms of sections of the interruption cycle. The chopping level (for somewhat larger contact gaps) shows to be independent of the contact material as follows from comparison of fig. 4.8.2, 4.8.3 and 4.8.4. The same can be said of the frequency ω_i of the instability-oscillation. Also the main circuit has no noticeable effect. Even on interruption of resistive currents chopping occurs in the same current region after an instability-oscillation (see e.g. fig. 8.2.1). (The frequency ω_i however, can vary considerably although current, circuit and timing of the measurement are kept constant, see section 8.2). This suggests that here current-chopping is not caused by the previously treated instabilities but by the nature of the discharge itself.

If one records the $U_b - I_b$ - characteristic of a discharge of a few centimeters length in hydrogen of appr. 1 atmosphere (abs) a sudden jump of the voltage near a critical current of $I_t \approx 1.5$ A is observed, see fig. 4.8.5 . (See also Suits [24] and Edels [25]). Edels studied arcs of different lengths at pressures from 0.5 to 2 atmospheres (abs) and always found these transitions at a maximum of 1.5 A. He stated that an arc-discharge

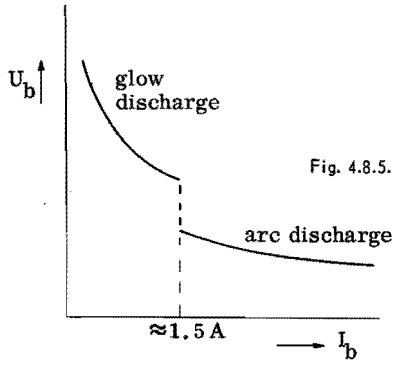

Fig. 4.8.5. Transition from arc- to glow-discharge in hydrogen.

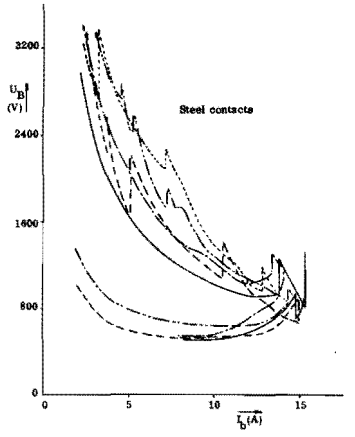

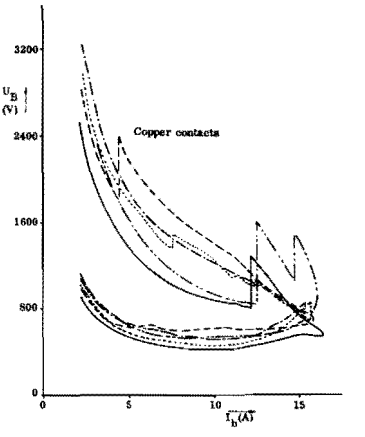

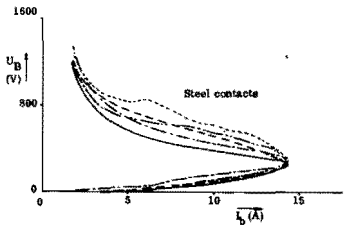

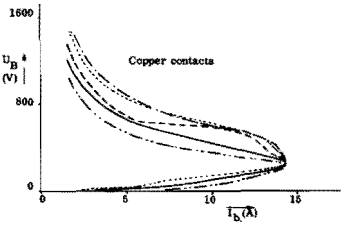

Fig. 4.8.2. U_B - I_b - characteristics of first and second
Fig. 4.8.3. loop of the interruption cycle
Fig. 4.8.4. bulk-oil breaker. I =10.5 A (R.M.S.).

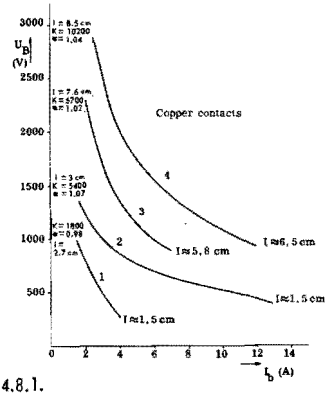

Fig. 4.8.1.
U_B - I_b characteristics, bulk-oil breaker, copper contacts. Each curve is the average of 6 x-y-oscillograms recorded at decreasing current.
1 : I = 1.7 A (peak), first loop of the interruption-cycle
2 : I = 14.5 A (peak), first loop of the interruption-cycle
3 : I = 7.5 A (peak), second loop of the interruption-cycle
4 : I = 15.5 A (peak), second loop of the interruption-cycle.

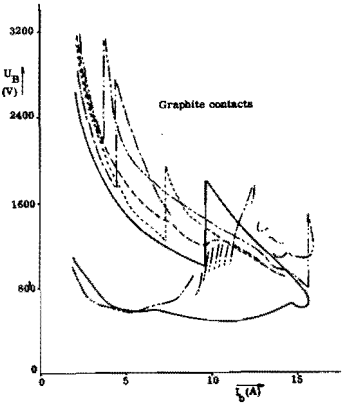

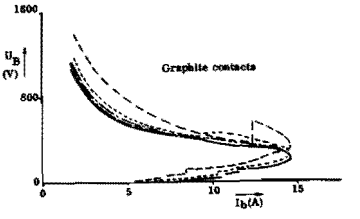

or a glow-discharge is possible depending on whether the current is higher or lower than the critical value respectively. The arc-discharge has a small diameter core of high luminosity. The glow-discharge requires a higher voltage, has a broad diffuse discharge path and shows a number of striations at the cathode. Fig. 4.8.6 reproduced from Edels [25] shows the sudden large jump in current density. The corresponding step in voltage is not as pronounced as may be seen from fig. 4.8.5. The voltage-transition is even continuous when tungsten electrodes are used.

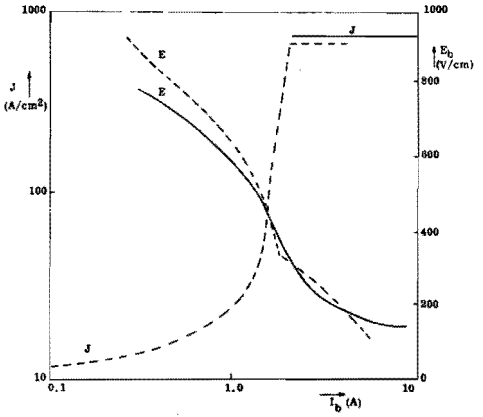

Fig. 4.8.6. Transition from arc- to glow-discharge in hydrogen (1 atm.) according Edels.
J = current density in the discharge
E = voltage gradient
I_b = current through the discharge
solid lines : tungsten electrodes
dashed lines: copper electrodes

However, small contaminations of the cathode produced the same transition as when copper electrodes were used. The curve for the copper electrodes was measured with water cooled electrodes. Comparative measurements carried out in this laboratory with electrodes of graphite and molybdenum in the glow state showed more pronounced voltage jumps but were less reproducible. The latter observation agrees with Edels' [25] opinion. He noticed that the transition is closely linked to the attainement of a critical temperature in the discharge. Besides current, pressure and (for small gaps) the heat extraction of the electrodes are determining factors for this temperature. King [26] found that this critical temperature coincides with the dissociation temperature of hydrogen. The transition occurred in his experiments with cooled electrodes at 1 A and a temperature of appr. 4500°K.

The discharge in the breaker decomposes the oil into a gaseous mixture

consisting mainly of hydrogen, see section 4.1. The discharge in this mixture shows a similar behaviour as in pure hydrogen. Since the parallel capacitance and the series self-inductances of the circuit do not permit a sudden voltage variation for constant current the discharge becomes always unstable and ceases.

The instability-oscillation can be explained with the previously discussed dynamic theory of Rizk. During the transition to a glow-discharge α can assume very high values such that suddenly the condition (4.5.-21) is no longer satisfied.

Since it must be expected that here Θ can also vary considerably [27], a check is not possible. Variations between $f_i \approx 0{,}4$ Mc/s and $f_i \approx 1.4$ Mc/s were measured under identical conditions of experimental set-up and timing. On interruption of resistive currents instability-oscillations of even 2.5 Mc/s were observed. According to Mayr and Rizk, equation (4.5.-22), this frequency $\omega_i = \sqrt{\alpha/\Theta}$ is exclusively determined by α and Θ.

It is not to be expected that the transition from arc- to glow-discharge in air-breakers has any influence. According to Edels [28] this transition takes place at 0.5 A in N_2 at 1 atmosphere (abs). But in still air the time constant is of the order of 100 μs [8, 9, 22], therefore the transition is gradual and hardly leads to instability-oscillation. A monotonic current-chopping of 0.5 A associated with a time-constant of 100 us has nearly the same slope as a nominal 50 cycle current of 7 A (R.M.S.) in its approach to zero. Therefore the transition should be noticed for very small currents only. For an arc length of a few centimeters the jump of the arc voltage is of the order of 500 V. Hence a rate of rise of approximately 5V/μs is sufficient for all transitions to occur without current-chopping. Core formation as a result of dissocation of N_2 occurs for a free burning arc in air at a current of appr. 50 A [26]. According to King*) not a single discontinuity neither in current nor in voltage can be observed in this case.

It is not known at which current the transition arc- to glow-discharge occurs in an air-blast breaker. Neither is a clear indication obtainable from our records. The discharge is very unstable at instantaneous values of appr. 1 A and it is impossible to state whether besides the motion of the discharge and electrical instability also the transition to a glow-discharge plays a role.

*) Private communication, Meeting "Current Zero Club" Baden, 1965.

CHAPTER 5 THE DISCHARGE AFTER CURRENT-CHOPPING

The voltage across the breaker rises with a high rate after current-chopping (see section 6.2). Under the influence of this restriking voltage the discharge can be reignited by two principally different mechanisms namely as a result of thermal or dielectric break-down.

5.1. Dielectric reignition.

The theory of dielectric reignition was developed by Slepian [29, 30] already in 1928-1930. He stated that the dielectric strength between contacts after ceasing of an arc-discharge is a given function of time which increases from the arc voltage to a final value. This final value is determined by the contact-distance and the interrupting medium in cold condition. Once the restriking voltage U_B exceeds at any instant the dielectric strength U_d of the medium break-down and restrike of the arc follows (fig. 5.1.1).

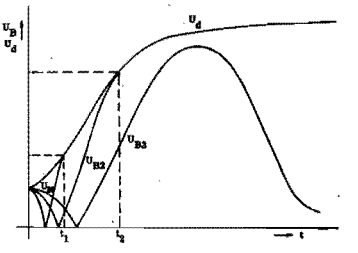

Fig. 5.1.1. Dielectric break-down.
U_d = dielectric strength between the contacts
U_B = restriking voltage across the contacts
U_{B1} and U_{B2} lead to reignition at $t = t_1$ and $t = t_2$ resp.,
U_{B3} gives successful interruption

Dielectric break-down follows Paschen's law and takes place at high values of increasing restriking voltage. In this type of reignition initially a Townsend discharge occurs leading rapidly to a highly ionized narrow discharge channel. As a result the current rises abruptly while the voltage decays at the same time to a very low value, the arc voltage. The losses during this break-down result in a cylindrical shock-wave which Cassie [31] considers the salient mark of a dielectric reignition.

5.2. Thermal reignition, residual current.

Whenever the arc-discharge abruptly ceases the electrical conductivity of the hot gas column does not disappear instantly. The former discharge path is left with a large number of charge carriers which can be accelerated by the restriking voltage. This results in a residual current leading to additional energy input into the discharge path. This input equals the time integral over the product of residual current and restriking voltage. Whenever this energy exceeds the heat extracted the temperature will rise. The degree of ionisation increases in agreement with Saha's equation or in other words the conductivity of the discharge path grows such that the residual current can transfer into a new arc current.

This type of reignition is called thermal or energy break-down. Cassie [31] coined the term "volume break-down" because initially ionisation of the gas takes place in that part of the volume in which the temperature is still sufficiently high. Just after the "breakdown" the discharge contracts into an arc-core of small diameter.

The residual current can flow simultaneously with the appearance of the rising voltage. As a consequence of the influence of the residual current on the circuit the voltage generally is decaying again before "break-down", i.e. transition to an arc-discharge occurs. Reignitions taking place after the voltage maximum are therefore clearly of thermal origin. However, this is not a necessary criterion. For a powerful source and very small parallel capacitance the thermal reignition can no longer be distinguished from a dielectric break-down on voltage oscillograms.

5.3. Discharge and reignition theory.

A first theory of thermal reignition in air-blast breakers was published by Cassie in condensed form in 1939 and later in more detail in 1953 [11, 32]. Cassie assumed a power dissipation process due to convective cooling only resulting in contraction of the arc column. He assumed the energy content (W_c), energy loss per unit time (P_c) and resistance (R_b) (all per unit volume) being constant.

He derived his dynamic-arc-equation

$$\frac{dR_b}{dt} = \frac{R_b}{\Theta_c} \left(1 - \frac{E_b^2}{E_s^2} \right) \qquad (5.3.-1)$$

where

$$\Theta_c = \frac{W_c}{P_c} \text{ (Cassie's time-constant)} \qquad (5.3.-2)$$

E_b = gradient of the dynamic arc

and

$$E_s^2 = P_c R_b = \text{constant} \qquad (5.3.-3)$$

Hence the gradient of the stationary arc ($\frac{dR_b}{dt} = 0$) is given by

$$E_s = \sqrt{\frac{W_c R_b}{\Theta}} = \text{constant} \qquad (5.3.-4)$$

However, a static characteristic presenting the voltage independent of current is not in agreement with the behaviour of a low current arc in the vicinity of current zero.

A second treatment of an energy concept was published by Mayr [12] in 1943. He considered radial thermal conduction to be the only source of energy loss. He assumed a constant diameter of the arc column in which the temperature varies with time and with distance from the axis and obtained the dynamic equation

$$\frac{dR_b}{dt} = \frac{R_b}{\Theta_M}\left(1 - \frac{E_b^2}{R_b P_M}\right) \qquad (5.3.-5)$$

Here $\Theta_M = \frac{W_M}{P_M}$ (Mayr's time-constant)

R_b = dynamic resistance of the arc column per unit length

W_M = characteristic energy content per unit length of the stationary arc

P_M = as constant assumed energy loss per unit length and time of the stationary arc.

This equation yields a static characteristic

$$E_b I_b = P_M = \text{constant} \qquad (5.3.-6)$$

The assumption of energy loss exclusively by conduction is certainly an oversimplification for air-blast breakers. Also the assumption that the thermal time-constant of an arc-discharge should be independent of the current is contradicted by Frind's theoretical studies [27] .
The latter found a considerabe dependence of Θ on I_b. On the other hand the static characteristic is more in agreement with practical results obtained with small currents.

In 1948 Browne [33] compared Cassie's and Mayr's arc models and showed giving due consideration to the characteristic assumption that both can be derived from the basic equation

$$\frac{1}{R} = F(W) = F\left\{\int (P - P_v)\, dt\right\} \qquad (5.3.-8)$$

where

W = energy content of the arc per unit length

$P = E_b I_b$ = energy input per unit length and time

P_v = energy extracted by cooling per unit length and time.

He showed that only Mayr's concept yields an acceptable derivation of the dielectric strength U_d in agreement with Slepian's [30] definition: "The dielectric break-down voltage of a gas column with a residual discharge is the voltage which holds the electrical conductivity constant." Thus he concluded near current zero radial conduction is the predominant mechanism of cooling. He computed from Mayr's theory the redisual current for different shapes of the restriking voltage. The initial steep portion of the dielectric recovery curve of fig. 5.1.1 becomes thus dependent on the history of the discharge and on the characteristic form of the restriking voltage itself (hence also on the circuit). The less steep portion of the curve should be the area of intrinsic dielectric break-down.

Also Cassie [32, 40] agrees with this reasoning. In addition he remarks that dielectric break-down can also occur in the region where still a considerable rest-conductivity is present (fig. 5.3.1) in particular when shortly after current-zero the voltage rises extremely rapidly.

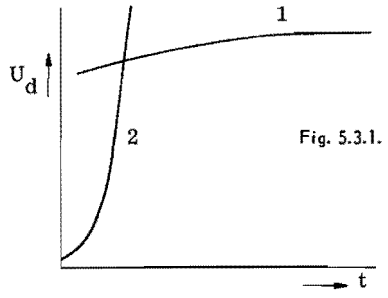

Fig. 5.3.1. Electric strength after current zero according Cassie.
(1) Dielectric break-down.
(2) Energy break-down.

Then the dielectric strength may have been exceeded before the slow thermal arc formation is accomplished. He assumes Paschen's law as criterion for the dielectric break-down.

Later investigations showed that such considerations are inadequately detailed. The reasons are the following.

1. From Mayr's equation (5.3.-5) follows

$$-\frac{d\ln R_b}{dt} = \frac{1}{\Theta_M}\left(\frac{P}{P_M} - 1\right) \qquad (5.3.-9)$$

Plotting $-\frac{d\ln R_b}{dt}$ as a function of arc energy per unit time $P = E_b^2/R_b = E_b I_b$ should result in straight lines as shown in fig. 5.3.2.

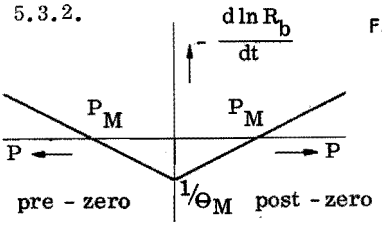

Fig. 5.3.2. Plot of $-\frac{d\ln R_b}{dt}$ versus arc energy per unit time P must give straight lines according Mayr's theory.

The intercepts with the axes are determined from

$$-\frac{d\ln R_b}{dt} = 0 \quad \text{for } P = P_M \qquad (5.3.-10)$$

and

$$P = 0 \quad \text{for } \frac{d\ln R_b}{dt} = \frac{1}{\Theta_M} \qquad (5.3.-11)$$

From voltage and current measurements in the vicinity of current-zero generally straight lines in agreement with theory were found for the pre-zero region,however, infrequently for the post-zero region [34 to 37]. Even negative values of Θ_M are often reported.

2. Experimental research of Sharbaugh et al. [38] and Edels et al. [39] showed that Paschen's law is invalid for temperatures above 2000 to 2500°K.

These results suggested that between the domain of thermal break-down as described by energy considerations (Mayr) and the region of dielectric break-down (thus at temperatures <2500°K) a transition area must exist in which reignitions follow a different mechanism. In the mean time two theories were developed to this end, the first proposed by Rieder and Urbanek [37] , the second by Edels et al. [39]. In case of dielectric break-down a free electron can gather over a mean free path an amount of energy from the electric field which is large compared to its thermal energy kT_e and of equal order of magnitude as the ionization energy of the gas W_i.

Therefore dielectric break-down requires

(1) $e\mathbf{E}.\mathbf{l}_e \gg k\,T_e$

(2) $e\mathbf{E}.\mathbf{l}_e \approx W_i$

e = electronic charge

E = voltage gradient

l_e = mean free path of the electron

k = Boltzmann constant

T_e = electron temperature.

On the other hand thermal break-down can occur when the energy collected from the electric field is insufficient for ionization by collision with a molecule. This energy is completely converted into heat and thus only thermal ionization (according Saha's equation) is possible. Hence the conditions for thermal reignition are

(1) $e \mathbf{E} . l_e \ll k T_e$

(2) $e \mathbf{E} . l_e \ll W_i$

(3) The energy collected from the field must exceed the loss by cooling.

Between these two extreme cases lies the area for which the energy obtained from the field is less than $k T_e$ but of equal order of magnitude, however still not sufficient for ionization. Hence for this area

(1) $e \mathbf{E} . l_e \approx k T_e$

(2) $e \mathbf{E} . l_e \ll W_i$

Now the gas is no longer in thermal equilibrium and the electron temperature rises above the gas temperature. The degree of ionization rises along with the electron temperature, cooling as a result of thermal conduction however corresponds to the lower gas temperature.

From this Rieder and Urbanek [37] derived a modification on the theory of Mayr termed non-equilibrium dynamic arc theory which explains what they call field enhanced thermal reignition.

Their experiments seemingly confirm this theory. It further shows that whenever the resistance of the discharge and/or the restriking voltage decrease after this period the discharge returns to thermal equilibrium and can behave in agreement with Mayr's theory.

The theory of Edels et al. [39] has an entirely different basis.

It states that thermal reignition can occur in agreement with energy considerations until the gas temperature has dropped to 4000 to 3500°K. Dielectric break-down according Paschen's law (hence determined by the density of the gas) is below 2000 to 1500°K possible. In between still a low degree of ionization exists permitting flow of small currents in particular when refractory electrodes are used. This is especially attributed to ther-

mal emission from the electrodes which in this temperature region can still be considerable. The discharge here has more or less the character of a glow-discharge. The transition into an arc-discharge on the other hand is said to have the character of a dielectric break-down. Therefore this break-down is termed ionization disturbed spark break-down.

Also Edels et al. [39] expect that the three regions cannot be clearly differentiated and that in the boundary regions two break-down mechanisms are possible.

The essential difference between both theories outlined above is:
the first considers break-down in the transition region as a special form of thermal reignition, the second as a special case of dielectric reignition. This gives the impression that both processes can occur in succession such that in total four types of reignitions should be distinguishable.
A striking difference between the thoughts of Edels and the other arc theories is the emphasis which the first puts on emission and cooling of the electrodes.

It is generally not possible to conclude from oscillograms whether a reignition is a result of thermal, field enhanced thermal or ionization disturbed spark break-down. Therefore all reignitions after a preceding residual current will be referred hereafter to residual-current reignition.

Finally it should be noted that the theories outlined above were developed mainly to describe the behaviour of the discharge on interruption of high short-circuit currents. Since interruption is accomplished exclusively at current-zero and since the time-constants of the discharge in circuit-breakers are small ($\approx 1\,\mu s$) one cannot expect a fundamental difference when small currents are interrupted.
However, in the latter case the influence of the circuit on interruption can be of an entirely different nature.

5.4. Experimental work on arc time-constants.

Mayr [12] gave the solution for his equation (5.3.-5) for $I = I_s$ = constant (stationary arc),

$$\frac{1}{R_b} = \frac{1}{R_s} + \left(\frac{1}{R_1} - \frac{1}{R_s}\right) e^{-t/\Theta_M} \qquad (5.4.-1)$$

or

$$G_b = G_s + (G_1 - G_s)\, e^{-t/\Theta_M} \qquad (5.4.-2)$$

This indicates that the electrical conductance of the arc G_b, starting from the initial value $G_1 = {}^1/R_1$ at $t = 0$, approaches its steady-state value $G_s = {}^1/R_s$ exponentially with a time-constant Θ_M. This time-constant is a measure for the thermal inertia of the discharge and is therefore of major importance for breaking mechanisms of circuit-breakers.

Several investigators have tried to determine time-constants in arcing-chambers or in circuit-breakers, either in a direct or in an indirect way. One of the most interesting studies in this field was carried out by Yoon and Spindle [8]. They determined Θ_M directly from equation (5.4.-1) by modulating a stationary arc with a small current step and recorded the voltage response. The authors made use of an arcing-chamber which could be filled with various gases and investigated different conditions of current (1 to 6A), contact distance, gas pressure and size of the stabilizing cage. In general the arc time-constant showed to increase with pressure and with current and differed widely in various gases.
The time-constant increased to a smaller extent with the diameter of the hole in the stabilizing cage. The arc-length appeared to have only a moderate effect on the time-constant.
Later Yoon and Browne [22] investigated in a similar way time-constants of low-current arcs under a small air flow. They found that the values of Θ_M increased with increasing current and contact separation and decreased with increasing pressure gradient and flow velocity. Some of their results are given in the figures 5.4.1 and 5.4.2. The decrease of the arc time-constant with increasing flow velocity was said to be due to the decrease of the effective cross-sectional area of the arc column. Extrapolation of the results to sonic air velocities (as used in air-blast circuit-breakers) is not permissible, because rather drastic changes in arc form and character may take place at the higher velocity levels. Yoon and Browne suggested, that the much smaller per unit rates of

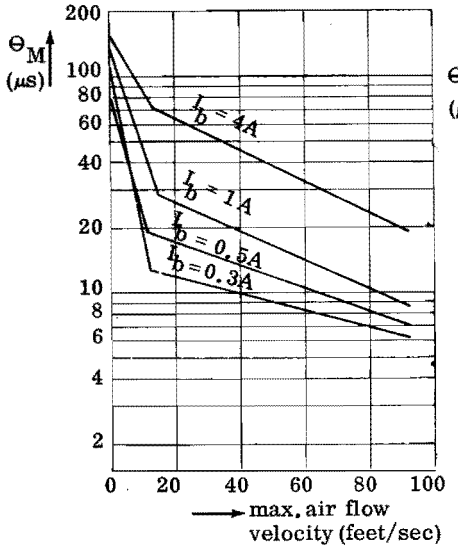

Fig. 5.4.1. Semilog plot of arc time-constant versus maximum air flow velocity, 1-inch long arcs, according Yoon and Browne.

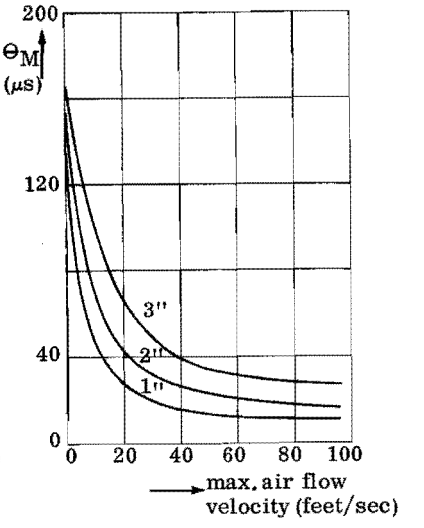

Fig. 5.4.2. Arc time-constant Θ_M versus maximum air flow velocity; 1-, 2- and 3-inch long arcs, according Yoon and Browne.

decrement of W_M and hence of Θ_M at velocities above 5 to 7 m/s, compared with those for lower velocities (see fig. 5.4.2) indicates transition to a "cored", or more concentrated type of arc in the higher velocity range as observed earlier by King [26, 41], (see section 5.5).

Rizk [9] investigated time-constants in a model of an air-blast breaker. He applied just like Yoon and Spindle the method of step modulation but obtained Θ_R directly from the response of the arc voltage (see section 4.5). Since for small disturbances i, (i.e. for $|i/I_b| \ll 1$) this time-constant becomes equal to the time-constant as defined by Mayr *) hereafter $\Theta_R = \Theta_M = \Theta$ will be used.

Rizk too found increasing Θ with increasing current, namely from 0.6 μs at 20 A to 1.1 μs at 90 A. But for pressures from 6.5 to 13 atmospheres in the arcing chamber the time-constants were shown not to vary when the current was kept constant. (The velocity of the airflow is not cited by Rizk.)

*) H.M. Pflanz to be published.

A number of investigators [21, 23, 33 to 35, 42 to 45] determined time-constants in an indirect way. From the theories of Mayr or Cassie they derived Θ from the other quantities of the respective basic relations (see e.g. section 4.6 and section 5.3, fig. 5.3.2). Their results show rather large differences with respect to each other and as compared with the previously discussed references. This may be explained on the one hand with the differences of the applied experimental set-ups (arcing-chambers or circuit-breakers) and on the other hand with occasional over-simplifications, introduced in the derivation of the underlying theories.
As a result only very few reliable data on time-constants for circuit-breakers in the vicinity of current-zero are available.

5.5. Core formation and arc time-constants.

King [26, 41] investigated the transition of low-current arcs into high-current arcs. A low-current arc has a diffuse column, a high current arc has a bright central core within the diffuse column. Based on the early work of ter Horst [46] and Brinkman [47] the transition was explained to be due to molecular dissociation of the arc-gas, leading to an increase of the thermal conductivity. In table 5.5.1 some data are given for the transition in different gases.

Table 5.5.1 Data for high-current to low-current arc transition according King.

Gas	CO_2	O_2	H_2	N_2
Dissociation potential (eV)	4.3	5.084	4.477	9.762
90 % Dissociation temperature (^oK)	3800	5110	4575	8300
Critical current (A)	0.1	0.5	1.0	50

The transition data for air showed to be almost the same as those for N_2. King also found, that the application of an axial gas-blast changes the potential gradient and greatly increases the energy dissipated from the arc column. Therefore an increase in axial temperature is caused at any given current. From this it follows that the effect of the blast is to bring about the transition at lower values of the current.
The effect of increased pressure is in circuit-breakers superimposed on this phenomenon. The result is, that even at very low currents the arc-temperature remains high at a very small cross-section.

These factors contribute to a marked reduction in the arc time-constant.

Maecker [48] calculated the radial temperature distribution in cylindrical arcs in nitrogen, stabilized in a tube of small diameter. Results are given in fig. 5.5.1. From this figure it can be seen that at sufficiently high temperatures a core of high electrical conductivity is formed in the arc. The electrical current is to a large extent concentrated in this core.

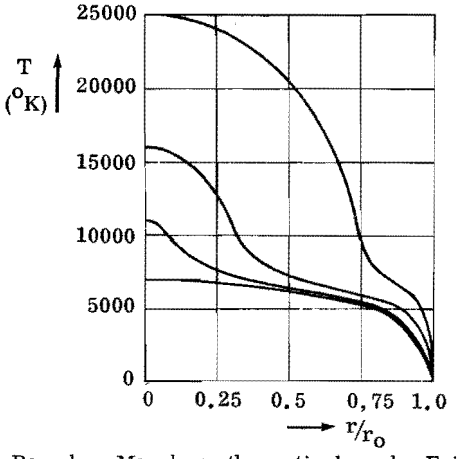

Fig. 5.5.1
Radial temperature distribution in cylindrical arcs in nitrogen, stabilized in a tube of small diameter according Maecker.

Based on Maeckers theoretical work, Frind [27] calculated the time-constant for the electrical conductivity of the arc. He found that the time-constant determined by the unit-step method for a wall stabilized arc is given by

$$\Theta = \frac{r_1^2}{2.4^2 k} \cdot \frac{1}{2} \left(1 - \frac{d \ln U_b}{d \ln I_b} \right) \qquad (5.5.-1)$$

where r_1 = conduction radius of the arc
U_b = stationary arc voltage
I_b = stationary arc current
k = thermal diffusivity, defined as $k = \frac{\kappa \rho}{c_p}$
κ = thermal conductivity
ρ = density
c_p = specific heat at constant pressure (per unit mass)

The time-constant Θ_1 for full decay of the conduction region of the arc column showed to be

$$\Theta_1 = \frac{r_1^2}{2.4^2 k} \qquad (5.5.-2)$$

Here for the first time attention is paid to the time-constant for full recovery. For this case, equation (5.4.-2) changes to

$$G_b = G_1 e^{-t/\Theta_1} \qquad (5.5.-3)$$

The difference between Θ and Θ_1 is small.

For the arc equation $U_b I_b^{\alpha} = K$, it can be seen that

$$\Theta = \frac{1+\alpha}{2} \Theta_1 \qquad (5.5.-4)$$

So for $\alpha = 1$, $\Theta = \Theta_1$

$\alpha = 0,4$, $\Theta = 0.7\, \Theta_1$

Moreover Frind showed that the assumption of one time-constant Θ is a rough approximation only. His derivations are based on the energy-balance equation given in the nomenclature of Finkelnburg and Maecker [49] .

$$\sigma E^2 = -\frac{1}{r} \frac{d}{dr} \left(r \kappa \frac{dT}{dr} \right) + \rho \frac{\partial H}{\partial t} \qquad (5.5.-5)$$

σ = coefficient of electrical conductivity
E = voltage gradient
r = radius
κ = coefficient of thermal conductivity
ρ = density
H = enthalpy = $\int_0^T c_p \, dT$

Radiation and convection are neglected, thermal conduction in radial direction is considered only.
Like Schmitz [50] and Maecker [48], Frind introduced the auxiliary function

$$S = \int_0^T \kappa \, dT \qquad (5.5.-6)$$

and assumed the thermal diffusivity $k = \kappa / \rho c_p$ to be a constant.

Substituting this equation (5.5.-5) changes to

$$\sigma E^2 = -\frac{1}{r} \frac{d}{dr} \left(r \frac{dS}{dr} \right) + \frac{1}{k} \frac{dS}{dt} \qquad (5.5.-7)$$

The general form of the function $\sigma = \sigma(S)$ is given in fig. 5.5.2 [27].
There σ_a is the conductivity in the axis of the arc and $S_a = \int_0^{Ta} \kappa \, dT$ where T_a is the temperature in the axis.

Electrical conductivity σ as a function of $S = \int_0^T \kappa \, dT$ according Frind

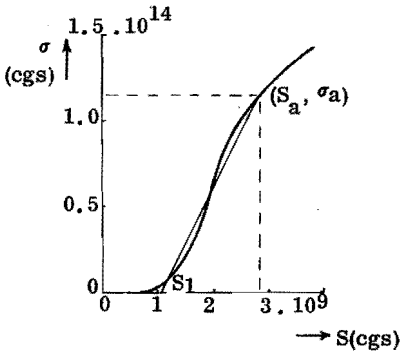

Fig. 5.5.2 Approximation by two straight lines

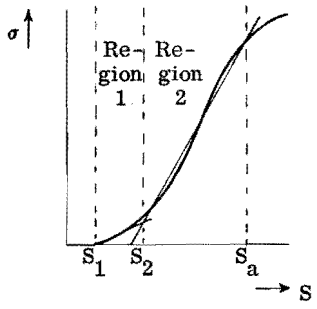

Fig. 5.5.3. Approximation by three straight lines

To find an analytic solution of equation (5.5.-7) this curve was approximated by the two straight lines, OS_1 and S_1S_a. As can be seen $\sigma = 0$ for $0 < S < S_1$ and $\sigma = \sigma^* = B(S-S_1)$ for $S_1 < S < S_a$. With these approximations formula (5.5.-2) was obtained.

However, Frind also shows that the original function $\sigma = \sigma(S)$ must give an infinite range of time-constants and that a much more accurate result will be obtained when $\sigma(S)$ is approached by three intervals as shown in fig. 5.5.3. Then the steep part of region 2 determines the small time-constant Θ_1, a measure for the disappearance of the electrical conductivity of the arc-core. From the flatter portion (region 1), the larger time-constant Θ_2 can be found. The latter describes the decay of the conductivity of the hot gas around the core.

From Frind's equation (5.5.-2) for full recovery it can also be made clear that the use of two time-constants might lead to a better understanding of the interruption phenomena. For the arc-core expressions (5.5.-2) and (5.5.-3) may be used

$$\Theta_1 = \frac{r_1^2}{2.4^2 k_1} \qquad (5.5.-8)$$

and

$$G_{b1} = G_1 e^{-t/\Theta_1} \qquad (5.5.-9)$$

For small r_1 (radius of the arc-core) the temperature of the core decays rapidly to the temperature of the hot gas cylinder surrounding the core.

This latter is the "temperature-hump" for which a second time-constant can be derived in a manner similar to the first

$$\Theta_2 = \frac{r_2^2}{2.4^2 k_1} \qquad (5.5.-10)$$

therefore the rest-conductance becomes

$$G_{b2} = G_2 e^{-t/\Theta_2} \qquad (5.5.-11)$$

It is possible that $r_1 << r_2$ (e.g. in an arc in hydrogen). Then $\Theta_1 << \Theta_2$. Moreover, Frind assumed in his derivation k to be constant. Rizk, however, computed that the thermal diffusivity of air (at 10 atmospheres) is a highly dependent function of temperature, see fig. 5.5.4. Particularly in the temperature range of the "hump" $3000^{\circ} < T < 5000^{\circ}$, k is considerably

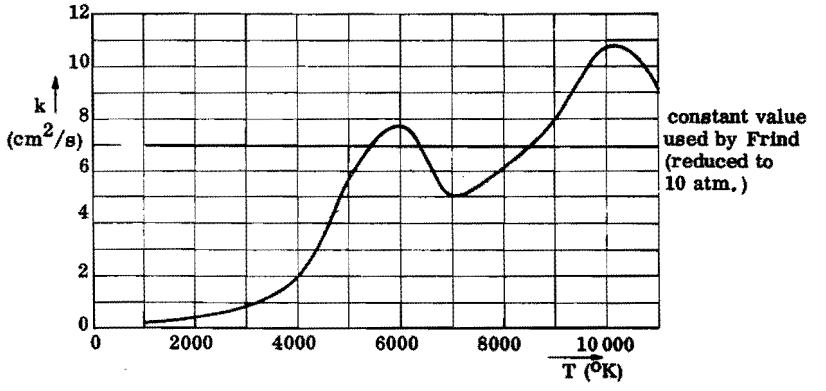

Fig. 5.5.4. Thermal diffusivity k of air (10 atm.) as a function of temperature according Rizk.

Hence if one introduces mean values of k a lower value for Θ_2 than for Θ_1 must be used. But this also means when an intense air-blast is applied such that $r_2 \approx r_1$ one must still work with at least two (mean) time-constants to describe the full decay of conduction

$$\Theta_1 = \frac{r_1^2}{2.4^2 k_1} \qquad (5.5.-12)$$

and

$$\Theta_2 = \frac{r_1^2}{2.4^2 k_2} \qquad (5.5.-13)$$

Therefore in first approximation the full thermal recovery of the gas can

always be expressed by

$$G_b = G_1 e^{-t/\Theta_1} + G_2 e^{-t/\Theta_2} \qquad (5.5.-14)$$

This equation expresses the fact that after the highly conductive arc channel has vanished still a longer lasting rest conductivity exists.
Generally it can be expected that $G_2 << G_1$. Hence a high restriking voltage is necessary to produce a measurable residual current. The time-constant Θ_2 determines how fast the restriking voltage must rise to accomplish this.

CHAPTER 6 THE RESTRIKING VOLTAGE AFTER CURRENT-CHOPPING

THE MEAN-CIRCUIT-CURRENT

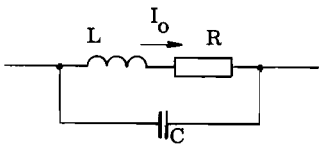

Fig. 6.1. Principle of current-chopping in an inductive circuit.

The current I_o through the self-inductance L of fig. 6.1 produces a magnetic field with energy $W_L = \frac{1}{2}LI_o^2$. When I_o is chopped the electromagnetic energy is converted into electrostatic energy $W_C = \frac{1}{2}CU^2$.
Continued reconversion of energy results in an oscillation of frequency

$$f = \frac{1}{2\pi}\sqrt{\frac{1}{LC} - \frac{R^2}{4L^2}} \qquad (6.-1)$$

Neglecting the damping resistance R and the initial charge on C the maximum voltage across the capacitor is found from

$$\tfrac{1}{2} L I_o^2 = \tfrac{1}{2} C U_{max}^2 \qquad (6.-2)$$

Hence

$$U_{max} = I_o\sqrt{\frac{L}{C}} \qquad (6.-3)$$

The initial rate of rise of the voltage

$$\frac{dU}{dt} = \frac{I_o}{C} \qquad (6.-4)$$

is seen to be independent of L.

6.1. Oscillations of the source- and load-side circuits.

Fig. 6.1.1 is an equivalent circuit representative of single-phase inductive interruption including damping elements. When breaker B interrupts the current through L_s and L_t, the partial circuits L_s, C_s and L_t, C_t oscillate with their natural frequencies f_s and f_t respectively.

The oscillations are damped by the resistances R_s and R_t.
High overvoltages can occur in the interrupted circuit, as will be shown in section 6.3. Here L_t is the (large) self-inductance of an unloaded or inductively loaded transformer. (For a main voltage of 10 kV and an inductive current between 3 and 60A, L_t varies between 10.6 to 0.53 H).

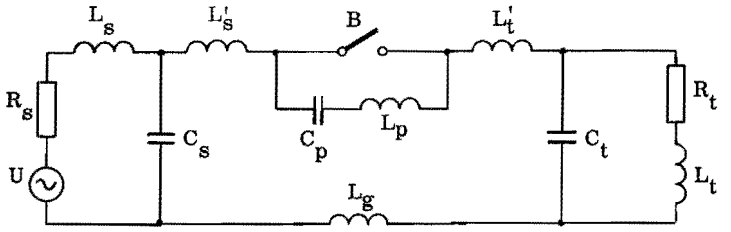

Fig. 6.1.1. Equivalent circuit including damping elements R_s and R_t.

The lumped capacitance C_t represents the distributed capacitances of the transformer (see section 2.2) eventually enlarged by the capacitances of the lines and/or cables between breaker and load. For short connections between breaker and transformer the capacitance of the lines is small and is included in C_p. The order of magnitude of C_t is in this case varying from 2000 to 10 000 pF.

With the above values for L_t, f_t can vary between 5×10^2 and 5×10^3 c/s. The oscillation is damped by R_t. This resistance is mainly determined by the iron losses of the load [23].

The short-circuit impedance of the feeding circuit up to the breaker is generally small. Hence L_s is small. The distributed capacitances of the transformer and of the feeder lines are considered as lumped and included in C_s which can be relatively large. The frequency f_s is generally one order of magnitude higher than f_t. The amplitude of the oscillation of the source-side is not large as follows from equation (6-3).

Moreover this oscillation is highly damped due to the rather large value of the a.c.-resistance R_s for high values of f_s.

6.2. The initial rate of rise of the restriking voltage after current-chopping

When the discharge in breaker B (fig. 6.1.1) suddenly ceases the current continues to flow initially through the parallel capacitance C_p because the self-inductances L'_s, L'_t and L_g do not permit a sudden change of the current. Under normal circumstances C_p is small (some hundred pF), hence the initial rate of rise of the restriking voltage can be very high according equation (6-4). For instance, a current chopped at a level $I_o = 2$ A together with a parallel capacitance C_p of 200 pF can result in an initial rate of rise of $\frac{dU}{dt} = 10\ 000$ V/μs.

Under the influence of such voltages a residual current can flow easily which can lead to reignition (section 5.2). C_p discharges into the new discharge channel with an oscillation of very high frequency (f_{p1} up to 5 to

10 Mc/s) when the reignition occurs sufficiently fast, or with a damped current-step when the reignition proceeds slower. In both cases high current peaks can be found.

Once the energy of C_p is dissipated in the discharge the voltage has decayed to a low value. Therefore the discharge will cease again, the parallel-capacitance is recharged and consequently a new break-down can occur. In this manner the current to be interrupted can be maintained, flowing alternately through the parallel-capacitance and the discharge-path.

Therefore a mean-circuit-current continues to flow through the inductances L_s and L_t. On oscillograms of this current, chopping and reignitions are recognizable, but show an entirely different pattern and smaller amplitudes than in I_b. The difference between the mean-circuit-current (lower trace) and the current through the breaker (upper trace) is clearly shown on fig. 6.2.1. This oscillogram was obtained with the circuit of fig. 6.2.2.

From fig. 6.2.3 it becomes clear that the mean-circuit-current continues through the parallel-capacitance. This oscillogram was obtained using an oil-circuit-breaker in a circuit like fig. 6.2.4.

The upper trace shows the current I'_c through a capacitor C'_p = 174 pF connected parallel to the breaker. The beginning of the oscillogram shows the last four cycles of the instability-oscillation ($f_i \approx 0.7$ Mc/s). Thereafter the current chops at $I_b = I_o \approx 2$A. Subsequently a number of reignitions follow of which only the first three are recorded. (During each break-down the current rises rapidly to a very high value, frequently beyond 100 A, see fig. 6.2.5. These highly transient variations can not be seen on fig. 6.2.3. Just the beginning and the end of each reignition are recorded.)

Between two reignitions an average current of about 0.8 A flows through C'_p. Hence the active parallel-capacitance C_p must be appr. 260 pF in this case.

C_p can also be estimated from the ratio of the peaks of the currents I'_c and I_b (fig. 6.2.5). From a number of such measurements on the same breaker it was found that C_p varied between 180 and 280 pF giving an

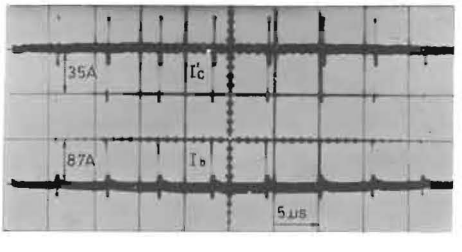

Fig. 6.2.5. Bulk-oil breaker, I =5.2 A (R.M.S.)
Upper line: current through added parallel capacitor 174 pF.
Lower line: current through the breaker.

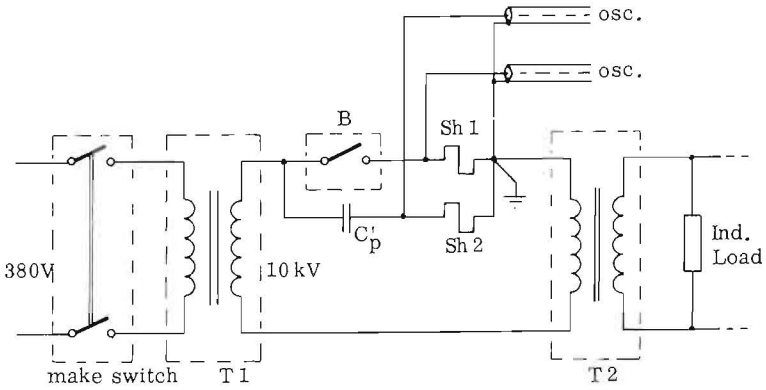

Fig. 6.2.2. Circuit for recording fig. 6.2.1.
Further details on fig. 2.1.5.

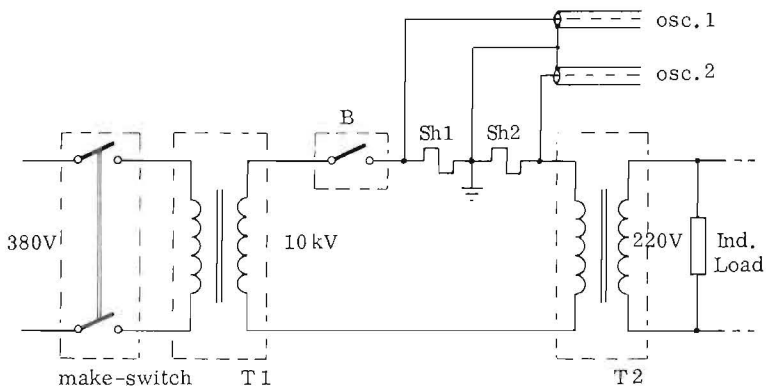

Fig. 6.2.4. Circuit for recording fig. 6.2.3.
Further details on fig. 2.1.5.

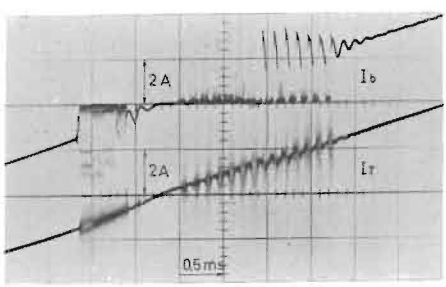

Fig. 6.2.1. Bulk-oil breaker, I = 3.5 A (R.M.S.)
Upper line: current through the breaker
Lower line: meon-circuit-current through load L_1.

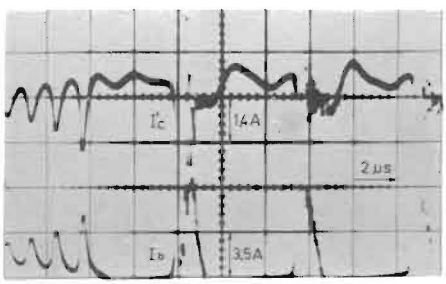

Fig. 6.2.3. Bulk-oil breaker, I = 5.2 A (R.M.S.)
Upper line: current through added parallel capacitor 174 pF
Lower line: current through the breaker.

average value of appr. 230 pF.

The variation of C_p shows that the parallel-capacitance can not be clearly defined for high-frequency phenomena. This shows the influence of the inherent self-inductance (L_p in fig. 6.1.1) of the capacitances. This follows also from the variation of the current I_c' between two reignitions (fig. 6.2.3) and from the fact that the current oscillation of fig. 6.2.5 is not limited to a single frequency. The latter was confirmed by oscillograms with a time-base of 0.2 μs/div.

6.3. Restriking voltages after definite current-zero.

The mean-circuit-current makes it possible that despite instability-oscillation and reignitions simultaneously a definite current zero is reached in the breaker (with its parallel-capacitance) as well as in L_s and L_t. Then the voltage across the breaker will oscillate transiently towards the main voltage which at this instant is near its peak (see fig. 6.3.1). The initial rate of rise of the restriking voltage will be slightly influenced by the feeder circuit. The oscillation of frequency f_s, however, is active just for a short time (see section 6.1) whereafter the restriking voltage is wholly determined by the load according to

$$U_B = U_n - e^{-t/\tau_1} (U_n - U_o) \cos \omega_t t \qquad (6.3.-1)$$

where U_n = peak value of the source voltage of industrial frequency

U_o = absolute value of the voltage across the breaker at current-zero (t = 0)

$\omega_t = \sqrt{\frac{1}{L_t C_t} - \frac{R_t^2}{4L_t^2}}$ = frequency of the load-circuit

L_t, C_t = inductance and equivalent capacitance of the load-circuit

$\tau_1 = \frac{2L_t}{R_t}$ = time-constant of the load-circuit

R_t = equivalent damping resistor.

(In equation (6.3.-1) the polarity of U_n is chosen positive and consequently U_B becomes negative at t = 0).

After about half a cycle the maximum value of the restriking voltage is reached

$$U_{max} = U_n + e^{-t_1/\tau_1} (U_n + U_o) \qquad (6.3.-2)$$

with $t_1 = \frac{\pi}{\omega_t}$

Neglecting damping it is found

$$U_{max} = 2\, U_n + U_o \qquad (6.3.-3)$$

However, when the currents through the breaker and the parallel-capacitance chop simultaneously while the current $I_t = I_o$ still flows through L_t the voltage U_B across the breaker at first will rise further due to the voltage contribution $L_t \frac{dI_t}{d_t}$ from the load-inductance.

Assuming the influence of damping elements is small, such that $\frac{1}{L_t C_t} \gg \left(\frac{R_t}{2L_t}\right)^2$, then the restriking voltage is given by y

$$U_B = U_n - e^{-t/\tau_1} \left\{ (U_n + U_o) \cos \omega_t t + I_o \omega_t L_t \sin \omega_t t \right\} \qquad (6.3.-4)$$

At $t = t_1$ a first maximum appears, called suppression peak. This $U_{max\,1}$ has the same polarity as U_o (see fig. 6.3.2).

It can be approximated by

$$U_{max\,1} = U_n - e^{-t_1/\tau_1} \sqrt{\left\{ (U_n + U_o)^2 + (I_o \omega_t L_t)^2 \right\}} \qquad (6.3.-5)$$

where

$$t_1 = \frac{1}{\omega_t} \left\{ \frac{\pi}{2} - tg^{-1} \frac{U_n + U_o}{I_o \omega_t L_t} \right\} \qquad (6.3.-6)$$

Starting from this suppression peak, U_B approaches zero and rises beyond the voltage of industrial frequency which at this instant is of opposite polarity with respect to $U_{max\,1}$. At $t = t_2$ a second maximum, the recovery peak $U_{max\,2}$ occurs

$$U_{max\,2} = U_n + e^{-t_2/\tau_1} \sqrt{\left\{ (U_n + U_o)^2 + (I_o \omega_t L_t)^2 \right\}} \qquad (6.3.-7)$$

where

$$t_2 = \frac{1}{\omega_t} \left\{ \frac{3\pi}{2} - tg^{-1} \frac{U_n + U_o}{I_o \omega_t L_t} \right\} \qquad (6.3.-8)$$

As a result of the contribution $I_o \omega_t L_t = I_o \sqrt{\frac{L_t}{C_t}}$ this second maximum can reach very high values. In our experiments overvoltages up to

$\frac{U_{max\,2}}{U_n} \approx 4$ were found. Theoretically considerably higher values are possible according equation (6.3.-7). In practical cases these are limited by reignitions. Of course reignitions can occur also during the rise time of U_B to $U_{max\,1}$.

Currents I_s, I_t and I_B and voltages U_s, U_t and U_B before and after current-chopping are shown on fig. 6.3.3. The directions of currents and voltages at the instant of the current chop are indicated on the associated diagrams. Fig. 6.3.4 shows the same currents and voltages for the case that the current is chopped after current zero.

The initial rate of rise of the restriking-voltage is mainly determined by the frequency of the feeder-circuit. In both cases $U_B = U_s - U_t$ rises after the current has ceased. (However, after current-chopping caused by main-circuit-oscillation the restriking voltage decays first and then rises, see section 7.4).

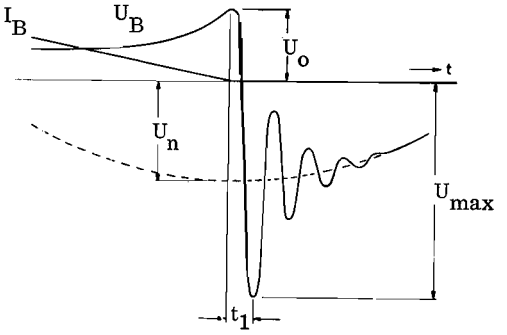

Fig. 6.3.1. Restriking voltage U_B after continuously decaying current I_B

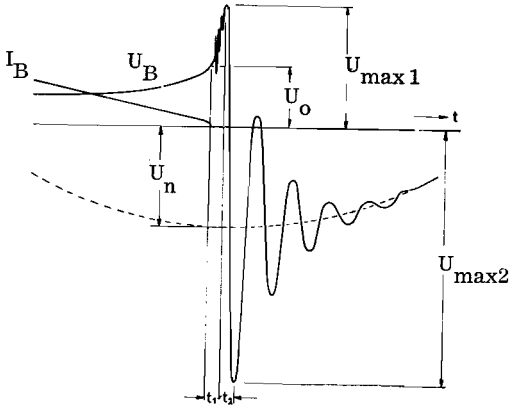

Fig. 6.3.2. Restriking voltage U_B after current-chopping

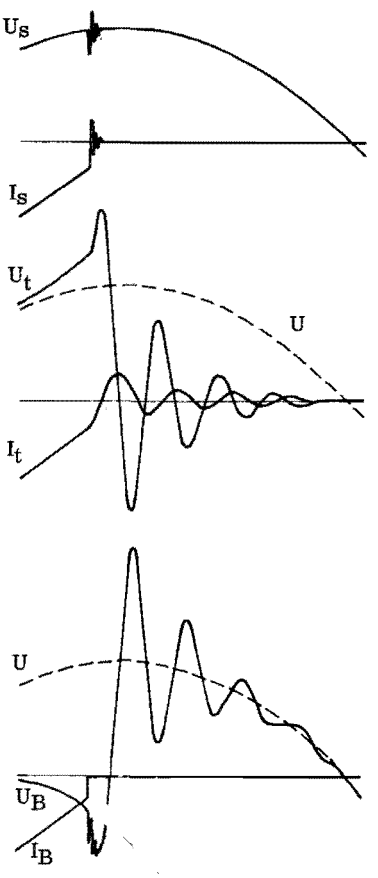

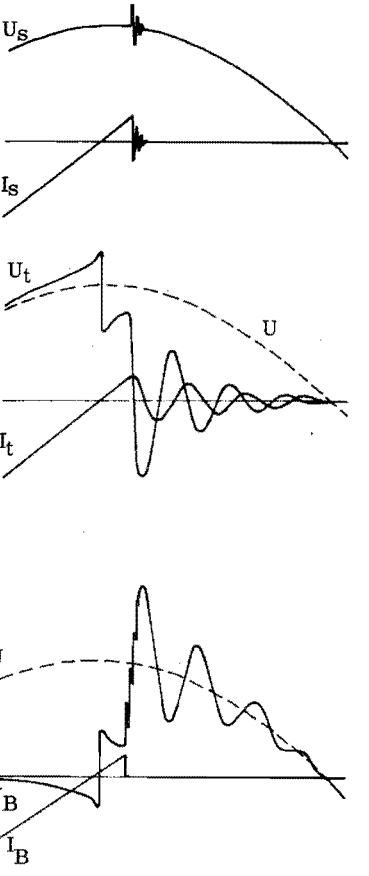

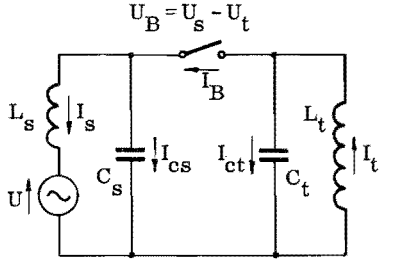

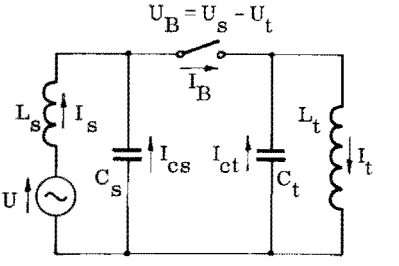

Currents I_s, I_t and I_B and voltages U_s, U_t and U_B before and after current-chopping

Fig. 6.3.3. Chopping before zero passage. Fig.6.3.4. Chopping after zero passage.

CHAPTER 7 THE RESTRIKING CURRENT AFTER REIGNITION. THE MAIN-CIRCUIT-OSCILLATION

After a reignition a current can start to flow again through the circuit. The steady-state part of this current is given by the expression

$$I_{stat} = \frac{U_n}{\omega_n(L_s + L_t)} \sin (\omega_n t + \psi) \qquad (7.-1)$$

with U_n = amplitude of the main voltage U.

$U = U_n \cos \omega_n t$

ω_n = industrial frequency

$\psi = tg^{-1} \frac{R}{\omega_n L}$

Assuming a predominantly inductive circuit ($\psi \approx 0$) and introducing around current-zero for $\sin \omega_n t \approx \omega_n t$ the steady-state current in this region will satisfy

$$I_{stat} = \frac{U_n}{L_s + L_t} t \qquad (7.-2)$$

This implies that the main voltage is supposed to be a constant. In the transition to the steady-state three types of oscillations can generally be distinguished. They will be indicated by

a. first parallel-oscillation, frequency ω_{p1}, f_{p1}
b. second parallel-oscillation, frequency ω_{p2}, f_{p2}
c. main-circuit-oscillation, frequency ω_{st}, f_{st}.

The treatment of these oscillations will be based on the equivalent circuit fig. 7.1, for which the following relations are valid

$$L_p \ll L'_s + L'_t + L_g \ll L_s \ll L_t$$

$$C_p \ll C''$$

and

$$C'' = \frac{C_s C_t}{C_s + C_t}$$

In this circuit resistances are neglected, because mainly the frequency and the order of magnitude of the first amplitude are essential to the

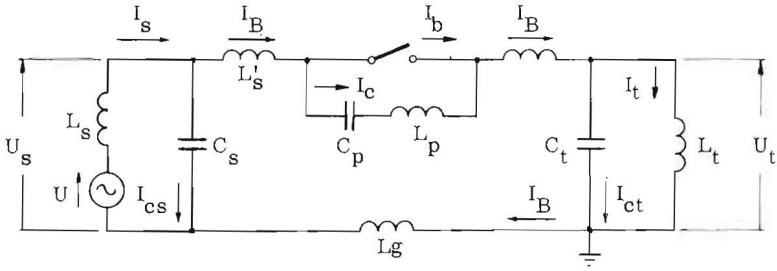

Fig. 7.1. Equivalent circuit for general treatment of restriking currents after reignitions. Diagram 1.

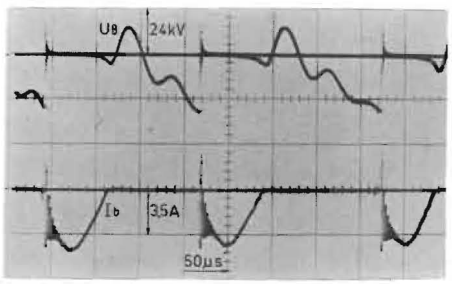

Fig. 7.2. Reignitions in an air-blast breaker. I = 3.5 A (R.M.S.)

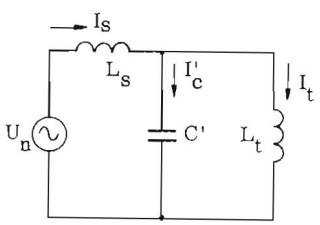

Fig. 7.3.1. Equivalent circuit for main-circuit-oscillation.

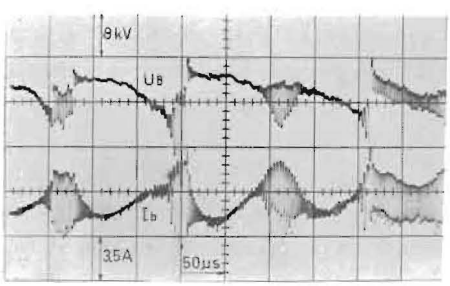

Fig. 7.4.5. Air-blast breaker, I =3.5 A (R.M.S.)

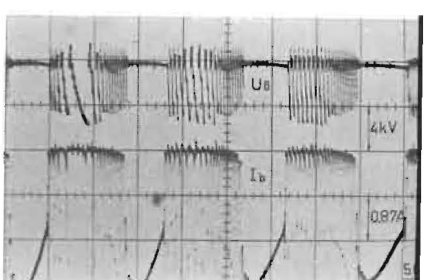

Fig. 7.4.6. Bulk-oil breaker, I = 3.5 A (R.M.S.)

interruption.

A general expression for the restriking current in this circuit would have a complicated form. However, the different oscillations may be considered separately because $\omega_{p1} >> \omega_{p2} >> \omega_{st}$.

Doing so, one gains a clear insight into the character of the oscillations as well as into their influence on interruption.

Fig. 7.2. gives an example of three reignitions, each one followed by oscillations of frequency ω_{p1}, ω_{p2} and ω_{st} in the current-trace.

The amplitudes of the first parallel-oscillation are extremely large and exceed by far the upper and lower boundaries of the oscillogram.

Therefore ω_{p1} can only be noticed in the voltage trace. Only half a cycle of the main-circuit-oscillation can develop, because the discharge ceases again when current-zero is achieved.

7.1. The first parallel-oscillation (circuit C_p - L_p - B).

The first parallel-oscillation is generated by discharging the parallel-capacitance C_p. As stated before (section 6.2) this capacitance is inherent to the direct vicinity of the circuit-breaker.

The frequency is

$$\omega_{p1} = \frac{1}{\sqrt{L_p C_p}} \qquad (7.1.-1)$$

Here L_p is the lumped self-inductance of the discharge circuit. Thus L_p consists of the self-inductances of the breaker (including the electrical discharge path) and that part of the conductors which is related to the first parallel-oscillation.

C_p has a value of some hundred pF, L_p of 2 to 10 μH, dependent on the breaker construction and its location in the circuit. Therefore the frequency f_{p1} is extremely high (2 to 10 Mc/s) and can only develop when the reignition causes sufficiently rapid a low impedance discharge path. This is the case after a dielectric-breakdown and generally also after a thermal-breakdown and generally also after a thermal-breakdown in oil-breakers.

Neglecting the damping the amplitude of this oscillation becomes

$$I_{p1} = U_d \omega_{p1} C_p \qquad (7.1.-2)$$

where U_d represents the voltage across C_p at the instant of reignition. I_{p1} can reach a very high value. When for example U_d = 12000 V, f_{p1} = 6 Mc/s and C_p = 250 pF, then $I_{p1} \approx 110$ A (see also fig. 6.2.5). For measuring the first parallel-oscillation rather extreme requirements must be

fulfilled for the current-recording system.

7.2. The second parallel-oscillation (circuit $C_s - L_s' - B - L_t' - C_t - L_g$).

The second parallel-oscillation can occur when a potential difference between U_s and U_t is produced prior to the reignition. The parallel capacitances C_s and C_t are assumed to be lumped. In reality they are distributed along the windings of the transformers and along the conductors. Therefore the self-inductances L_s' and L_t' are introduced in the equivalent scheme (fig. 7.1), L_g represents the lumped self-inductance of the "neutral" path between source and load.

Then the frequency of the second parallel-oscillation becomes

$$\omega_{p2} = \frac{1}{\sqrt{L'' C''}} \qquad (7.2.-1)$$

where $L'' = L_s' + L_t' + L_g$

$$C'' = \frac{C_s C_t}{C_s + C_t}$$

Assuming the resistance R of the discharge-circuit (mainly the resistance of the gas-discharge) to be constant, then from the differential equation

$$I_{p2} R + L \frac{dI_{p2}}{dt} + \int \frac{I_{p2}}{C_s} dt + \int \frac{I_{p2}}{C_t} dt = 0 \qquad (7.2.-2)$$

the current I_{p2} of the second parallel-oscillation follows

$$I_{p2} = \frac{(U_s)_o - (U_t)_o}{\omega_{p_2} L''} e^{-t/\tau''} \sin \omega_{p2} t \qquad (7.2.-3)$$

Here

$$\omega_{p_2} = \sqrt{\frac{1}{L''C''} - \frac{R^2}{4L''^2}} \approx \frac{1}{\sqrt{L''C''}}$$

$$\tau'' = \frac{2L''}{R}$$

$$(U_s)_o = U_s \quad \text{at} \quad t = 0$$

$$(U_t)_o = U_t \quad \text{at} \quad t = 0$$

When this oscillation is damped out, the voltage across C_s and C_t is given by

$$U_s = (U_s)_o - \int \frac{I_{p2}}{C_s}\, dt \qquad (7.2.-4)$$

(or $$U_t = (U_t)_o - \int \frac{I_{p2}}{C_t}\, dt \;) \qquad (7.2.-5)$$

Hence $$U_s = U_t = \frac{C_s}{C_s + C_t} (U_s)_o + \frac{C_t}{C_s + C_t} (U_t)_o \qquad (7.2.-6)$$

Here the voltage across the breaker is neglected.
At the instant of current-chopping

$$U_s = \frac{L_t}{L_s + L_t} U_n \qquad (7.2.-7)$$

Afterwards U_s rises to U_n, and the oscillation with frequency ω_s is produced. Immediately after current-chopping one may introduce $U_s \approx U_n$ because $L_s \ll L_t$. After a short time ($\approx 200\ \mu s$) the oscillation is damped out and U_s equals U_n. Therefore in equation (7.2.-6), $(U_s)_o = U_n$ may be introduced.
The second parallel-oscillation can develop after the first parallel-oscillation, provided the high conductivity of the discharge lasts sufficiently long. Generally this is not so after thermal reignition in oil-breakers. In this case the energy of C_p is often completely dissipated in the discharge before I_{p2} can rise sufficiently. The small time-constant Θ_1 of the discharge then prevents the generation of the second parallel-oscillation. However, mostly this oscillation is found after a dielectric breakdown in oil-breakers. Also after a thermal breakdown in air-blast breakers and in air-breakers, this oscillation occurs provided the transition to the low impedance discharge is sufficiently fast. The first and second parallel-oscillations may also be excited by sudden variations in the conductivity of the discharge as mentioned in sections 4.1 and 4.2.

In the circuits under investigation the frequency f_{p2} was 0.2 to 0.4 Mc/s. During the first parallel-oscillation the current may pass through zero without causing the discharge to cease. This happens seldom during the second parallel-oscillation. From this an impression of the time-constant of the discharge can be obtained. (See sections 8.2 and 9.2).

7.3. The main-circuit-oscillation (circuit U, L_s, C_s - B - L_t, C_t).

For the main-circuit-oscillation the complete source side circuit (L_s, C_s, U) and load side circuit (L_t, C_t) are implicated. Obviously this oscillation starts simultaneously with the parallel-oscillations mentioned in the preceding sections. As before, here too the oscillation can only develop when the high conductivity of the discharge is maintained sufficiently long. This requirement is generally met after the second parallel-oscillation. For the sake of simplicity it is supposed again that the current of the main-circuit-oscillation I_{st} is still negligible when I_{p2} is already damped out. Then the circuit fig. 7.1 can be simplified to fig. 7.3.1 and equation (7.2.-6) represents the initial voltage $(U_{c'})_o$ on $C' = C_s + C_t$ at the instant $t = 0$.

L_s', L_t' and L_g as well as the voltage across the breaker are neglected. The main voltage U_n is supposed to be constant (at its maximum) and positive. Finally it is assumed that C_s and C_t have the same values as in section 7.2.

From the equations

$$L_s \frac{dI_s}{dt} + L_t \frac{dI_t}{dt} = U_n \qquad (7.3.-1)$$

$$L_t \frac{dI_t}{dt} = (U_{c'})_o + \int \frac{I_{c'}}{C'}\, dt \qquad (7.3.-2)$$

$$I_s = I_t + I_{c'} \qquad (7.3.-3)$$

can be derived

$$I_t = A \sin(\omega_{st} t + \varphi) + \frac{U_n t}{L_s + L_t} + B \qquad (7.3.-4)$$

where

$$\omega_{st} = \frac{1}{\sqrt{L'C'}} = \text{frequency of the main-circuit-oscillation}$$

$$L' = \frac{L_s L_t}{L_s + L_t}$$

$$C' = C_s + C_t$$

A, B and φ are constants, which must be determined from the initial conditions $(I_s)_o$, $(I_t)_o$ and $(U_{c'})_o$. The general expressions for these constants are

$$A = \sqrt{\left[\left\{\frac{1}{\omega_{st}}\left(\frac{(U_{c'})_o}{L_s} - \frac{U_n}{L_s+L_t}\right)\right\}^2 + \left\{(I_t)_o - (I_s)_o\right\}^2\left\{\frac{L_s}{L_s+L_t}\right\}^2\right]} \qquad (7.3.-5)$$

$$B = (I_t)_o \cdot \frac{L_t}{L_s+L_t} + (I_s)_o \cdot \frac{L_s}{L_s+L_t} \qquad (7.3.-6)$$

$$\varphi = tg^{-1}\frac{\omega_{st} L_s \left\{(I_t)_o - (I_s)_o\right\}}{(U_{c'})_o \left\{\frac{L_s+L_t}{L_t}\right\} - U_n} \qquad (7.3.-7)$$

From (7.3.-2) follows

$$I_{c'} = -\omega_{st}^2 L_t C' \quad A \sin(\omega_{st} t + \varphi) \qquad (7.3.-8)$$

The current through the breaker B equals

$$I_B = \frac{C_t}{C'} I_{c'} + I_t \qquad (7.3.-9)$$

Hence

$$I_B = (1 - \omega_{st}^2 L_t C_t) A \sin(\omega_{st} t + \varphi) + \frac{U_n t}{L_s+L_t} + B \qquad (7.3.-10)$$

The first term on the right-hand side represents the current of the oscillation of the main-circuit

$$I_{st} = (1 - \omega_{st}^2 L_t C_t) A \sin(\omega_{st} t + \varphi) \qquad (7.3.-11)$$

This current is superimposed on the beginning of the steady-state current I_{stat}. The steady-state current is expressed by the next two terms of equation (7.3.-10) and thus has (initially) a linear rate of rise starting from the value B.

Equation (7.3.-6) generally may be simplified to $B = (I_t)_o$ since I_s is rapidly damped out after current-chopping and in addition $L_t \gg L_s$.

7.4. The influence of the main-circuit-oscillation on current-chopping

The performance of I_B, I_t, I_s and U_B prior to current-chopping ($t < t_1$) and after current-chopping ($t > t_1$) is presented in fig. 7.4.1 for the case that no reignitions occur. For a reignition arising at the instant $t = t_o = 0$ the following cases may be distinguished:

a. If $t_1 < t_o < t_2$. Then $(I_t)_o < 0$.

The main-circuit-oscillation is superimposed on a steady-state current of the same polarity as before current-chopping. Without this oscillation a natural current-zero could follow. Then no extreme over-voltages would occur (equation (6.3.-1) and fig. 6.3.1). However, the main-circuit-oscillation can force the current through the breaker I_B towards zero again. The current through L_t at that instant follows from the equations (7.3.-9) and (7.3.-8)

$$I_t = \left(\frac{\omega_{st}}{\omega_t}\right)^2 A \sin(\omega_{st} t + \varphi) \qquad (7.4.-1)$$

Since $\omega_{st} \gg \omega_t$ still a rather large current can pass through L_t. Hence main-circuit-oscillation leads to the same effect as current-chopping due to instability-oscillation. Excessive over-voltages may result, according equations (6.3.-5) and (6.3.-7).

b. If $t_2 < t_o < t_3$. Then $(I_t)_o > 0$.

In this case the main-circuit-oscillation is superimposed on a steady-state current of opposite polarity relative to the current before chopping. Without this oscillation reignition might cause failure of interruption. The current-zero as a result of the main-circuit-oscillation may as yet lead to successful interruption. Thus in the region $t_2 < t_o < t_3$ this oscillation may have a favourable effect. From equations (7.4.-1), (6.3.-5) and (6.3.-7) it follows here also that excessive overvoltages may occur.

c. When a reignition is produced shortly after current-chopping then $(I_s)_o \approx (I_t)_o = -I_o$ because of the current through the parallel-capacitance C_p (see section 6.2). Then

$$(U_s)_o = (U_t)_o = U_n \frac{L_t}{L_s + L_t} = (U_c)_o \qquad (7.4.-2)$$

and $A = 0$, $\varphi = 0$ and $B = -I_o$ can be introduced into equation (7.3.-10). In this case no second parallel-oscillation and no main-circuit-oscillation will set in. After C_p has been discharged the current can continue its natural course to zero. Then the reignition is not or hardly noticeable in the current through L_t.

d. When a reignition occurs at the instant $t_o \approx t_2$, then $(I_s)_o = 0$, $(I_t)_o \approx 0$, $(U_s)_o = U_n$ and $(U_b)_o \approx U_{max\,1}$ (see equation (6.3.-5).

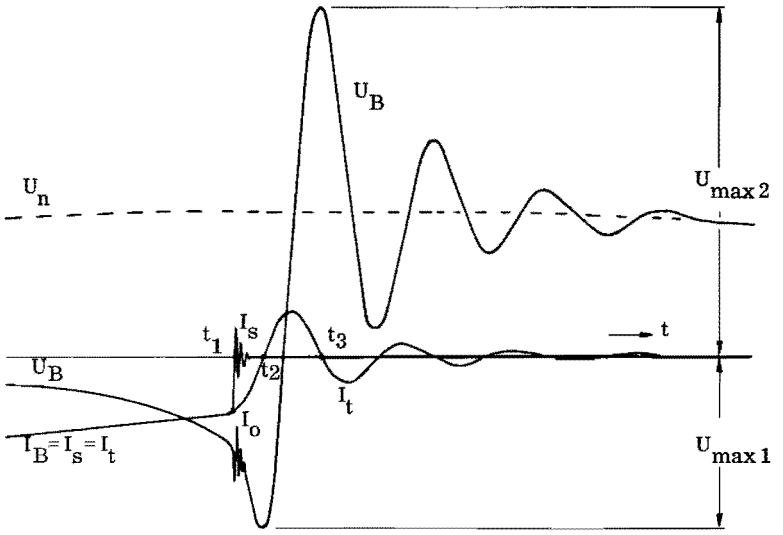

Fig. 7.4.1. Current-chopping not followed by reignitions.

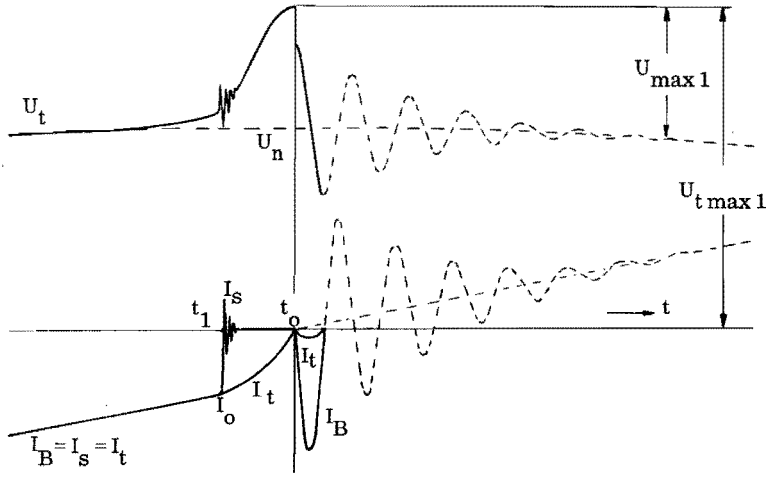

Fig. 7.4.2. Current-chopping followed by reignition near suppression peak U_{max1}.

Always $U_B = U_s - U_t$, such that here $(U_t)_o$ is given by the expression

$$(U_t)_o = U_n - U_{max\,1} = U_{t\,max\,1} \qquad (7.4.-3)$$

From equation (6.3.-5) it follows that always $U_{t\ max\,1} > U_n$ (at L_t the suppression-peak is superimposed on the main voltage).

Equations (7.2.-6), (7.3.-5), (7.3.-6) and (7.3.-7) successively yield

$$(U_{c'})_o = U_n \frac{C_s}{C_s + C_t} + \frac{U_{t\ max\ 1}}{U_n} \cdot \frac{C_t}{C_s + C_t} \qquad (7.4.-4)$$

$$A = \frac{U_n}{\omega_{st} L_t} \left\{ \frac{C_s}{C_s + C_t} - \frac{L_t}{L_s + L_t} + \frac{U_{t\,max\,1}}{U_n} \frac{C_t}{C_s + C_t} \right\} \qquad (7.4.-5)$$

Introducing further $L_t \gg L_s$ and $\omega_{st} \gg \omega_t$ equation (7.3.-10) can be simplified to

$$I_B \approx \omega_{st} C_t \left(1 - \frac{C_s}{C_s + C_t} - \frac{U_{t\,max\,1}}{U_n} \cdot \frac{C_t}{C_s + C_t}\right) U_n \sin \omega_{st} t + \\ + \frac{U_n}{L_s + L_t} t \qquad (7.4.-6)$$

Hence the current through the breaker has always a negative start, in other words still a current zero must follow (see fig. 7.4.2) such that there exists another chance for succesful interruption.
Since $(I_t)_o \approx 0$ and moreover $\omega_{st} L_t \gg \frac{1}{\omega_{st} C_t}$ just a very small portion of I_B flows through L_t. During the passage of I_B through zero the voltage $U_t < U_n$. Because of these two reasons no high overvoltage can result from current-chopping in this case.
Success or failure of interruption depends now highly on the energy-input into the discharge during the first half period of the main-circuit-oscillation and on the rate of decay with which current-zero is approached. Besides the value of the suppression peak (depending on the history of the discharge), ω_{st} and the relationship between C_t and C_s plays an important role according equation (7.4.-6).

e. In case reignition occurs at $t_o \approx t_3$ then $(I_s)_o = 0$, $(I_t)_o \approx 0$, $(U_s)_o = U_n$ and $(U_B)_o \approx U_{max\,2}$, see equation (6.3.-7). Now

$$(U_t)_o = U_{t\,max\,2} = U_n - U_{max\,2} \qquad (7.4.-7)$$

From equation (6.3.-7) follows, that $U_{t\,max\,2} < -U_n$.

The current through the breaker can now be expressed

$$I_B = \omega_{st} C_t \left(1 + \frac{|U_{t\,max\,2}|}{U_n} \cdot \frac{C_t}{C_s + C_t} - \frac{C_s}{C_s + C_t}\right) U_n \sin \omega_{st} t + \frac{U_n}{L_s + L_t} t \qquad (7.4.-8)$$

Here I_B starts with positive polarity. Whether or not a current-zero follows depends on the initial rate of rise of the steady-state current, hence on $\frac{U_n}{L_s + L_t}$ and on the amplitude of the main-current-oscillation (that is on the history as it shows up in $U_{t\,max\,2}$) and on the relation between C_t and C_s.

Fig. 7.4.3 gives an example of a reignition at $t_o \approx t_3$ with large amplitude of I_{st} and a small steady-state current. In this case a new current-zero is certain. Whether or not this interruption is successful depends firstly on the energy input into the discharge during the interval between reignition and the new current-zero, secondly on the rate of decay of I_{st} towards zero and thirdly on the rate of rise of the restriking voltage.
Fig. 7.4.4 a larger steady-state current and a smaller amplitude of the main-circuit-oscillation are assumed. No new current-zero follows. Therefore interruption fails.

Main-circuit-oscillation cannot only occur after a single reignition but also during a number of successive reignitions in oil-breakers. Then I_{st} is superimposed on the mean-circuit-current.
Because a thermal break-down can occur only when there is a sufficient energy input into the residual discharge a series of thermal reignitions can be halted temporarily or permanently when $I_B = I_{stat} + I_{st}$ recedes below the value necessary for break-down (see sections 8.5 and 8.7 and fig. 8.5.2 and 8.7.1). On interruption of currents of a few amperes

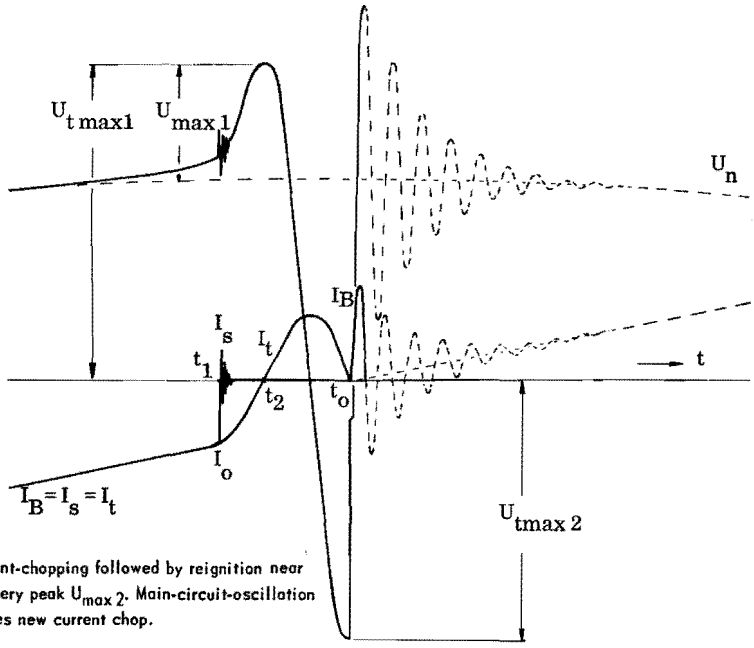

Fig. 7.4.3. Current-chopping followed by reignition near recovery peak $U_{max\,2}$. Main-circuit-oscillation causes new current chop.

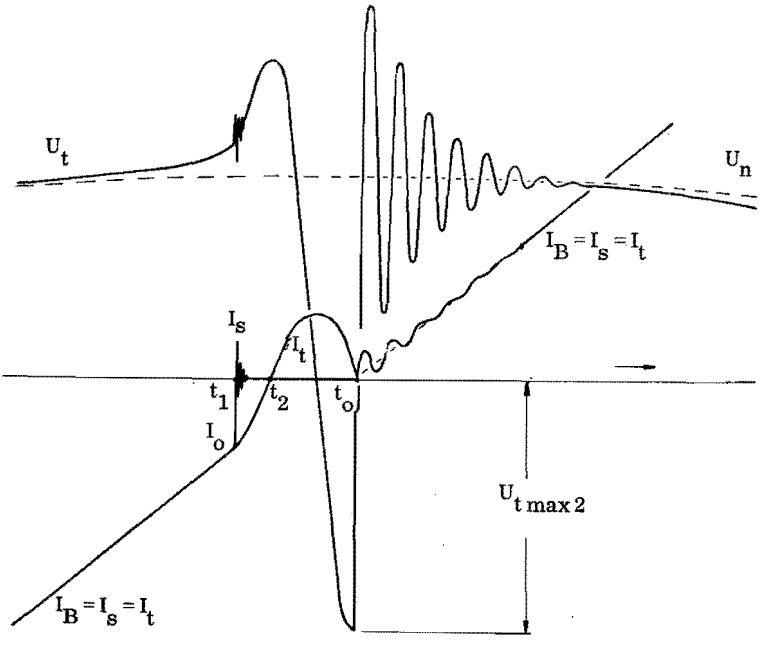

Fig. 7.4.4. Current-chopping followed by reignition near recovery peak $U_{max\,2}$. High rate of rise of steady-state current and small main-circuit-oscillation prevent new current chop.

alternately stable and unstable oscillations in the rhythm of the main-circuit-oscillation can occur (see for example fig. 7.4.5, 7.4.6, page 78 and fig. 8.7.1.

Finally it should be remarked that the restriking voltage across the breaker decreases initially after a forced current-zero due to main-circuit-oscillation.

This is a striking contrast to a "normal" current chop (section 6.3 fig. 6.3.3 and 6.3.4) for which the voltage U_B (in absolute value) always rises immediately after I_B has become zero.

The reason for this is that the direction of I_s at the instant of $I_B = 0$ now has opposite polarity than shown on the diagrams of fig. 6.3.3 and 6.3.4. Hence also the restriking voltage U_s has opposite polarity in the two cases.

Since $\omega_s >> \omega_t$ the start of the restriking voltage across the breaker $U_B = U_s - U_t$ is principally determined by U_s.

The direction of I_s can be derived as follows.

At the instant when $I_B = I_{st} + I_{stat} = 0$, $I_{st} = - I_{stat}$. Now I_{stat} flows mainly through L_t, and I_{st} through C_t, see equations (7.3.-4), (7.3.-8) and (7.3.-10). Hence $I_{st} \approx I_{Ct}$ and $I_{stat} \approx I_t$. The directions of I_t and I_{Ct} are therefore the same as shown on fig. 6.3.3 and 6.3.4. Because prior to chopping C_s and C_t are parallel, the direction of I_{Cs} is equal to that of I_{Ct}. For $I_B = 0$, however, $I_s = I_{Cs}$ and therefore the direction of I_s turns out to be opposite to the notations in fig. 6.3.3 and 6.3.4.

The delay caused thereby in the rise of the restriking voltage, of course, favours interruption.

7.5. The influence of the earthing on the main-circuit-oscillation.

From the preceding it is seen that for successful interruption the main-circuit-oscillation can be of considerable importance. The frequency and the amplitude of I_{st} are highly dependent on the capacitances C_s and C_t. The values of these capacitances, however, depend on the location of earthing. The circuit according fig. 7.1 has the basic configuration of diagram 1 (fig. 2.1.2) and can be considered as part of a three-phase circuit according fig. 7.5.1 (or fig. 2.1.1). The oscillations treated in the previous sections occur therefore also in the three-phase circuit and the investigation carried out with the single-phase circuit (fig. 7.1) is representative of this three-phase situation.

Because of magnetic coupling the interrupting phenomena of one phase can be found back in part in the currents and voltages of the other two phases.

However, there is a 60^{o} phase difference of successive current-zeros and therefore frequently no mutual influence of successive interruptions is noticed.

Earthing between breaker and load (diagram 2, fig. 2.1.3) the equivalent circuit fig. 7.5.2 is obtained. In comparison with fig. 7.1 the frequency of the first parallel-oscillation ω_{p1} will be somewhat lower as C_p represents now the capacitance with respect to earth. The frequency of the second parallel-oscillation is

$$\omega_{p2} = \frac{1}{\sqrt{L'_s C_{s1}}} \qquad (7.5.-1)$$

It too will have a somewhat different value than in the previous case, compare equation (7.2.-1). After the second parallel-oscillation has been damped out there is still no fundamental difference.

The circuit can again be simplified to fig. 7.3.1. Now $C_{s2} = C_s$ because node S has nearly reached earth potential after the breakdown. Equations (7.3.-1) to (7.3.-8) incl. remain valid.

I_B must be expressed as $I_B = I_{C'} + I_t$. Then equation (7.3.-9) becomes

$$I_B = \left\{1 - \omega_{st}^2 L_t (C_s + C_t)\right\} A \sin(\omega_{st} + \varphi) + \frac{U_n t}{L_s + L_t} + B \qquad (7.5.-2)$$

The initial voltages across the capacitance $C' = C_s + C_t$ is in this case $(U_{c'})_0 = (U_t)_0$.

For this situation (7.4.-6) and (7.4.-8) become

$$I_B \approx \omega_{st}(C_s + C_t)\left\{1 - \frac{U_{t\max 1}}{U_n}\right\} U_n \sin \omega_{st} t + \frac{U_n}{L_s + L_t} t \qquad (7.5.-3)$$

and

$$I_B \approx \omega_{st}(C_s + C_t)\left\{1 + \frac{|U_{t\max 2}|}{U_n}\right\} U_n \sin \omega_{st} t + \frac{U_n}{L_s + L_t} t \qquad (7.5.-4)$$

Thus it is shown that earthing in this manner does not change the frequency of the main-circuit-oscillation. The amplitude, however, becomes larger.

Earthing between source and breaker (diagram 3, fig. 2.1.4) has a more pronounced effect. This may be understood from the equivalent circuit fig. 7.5.3. What was said in relation fig. 7.5.2 applies also to the first parallel-oscillation here. The frequency of the second parallel-oscillation is

$$\omega_{p2} = \frac{1}{\sqrt{L'_t C_{t1}}} \qquad (7.5.-5)$$

Also ω_{p2} can deviate somewhat in comparison with the circuit of fig. 7.1. After break-down node T has earth potential and $C_{t2} = C_t$. Again the equations (7.3.-1) to (7.3.-8) remain valid. Equation (7.3.-9) now gives $I_B = I_t$. Therefore expression (7.3.-10) is replaced by

$$I_B = A \sin (\omega_{st} + \varphi) + \frac{U_n t}{L_s + L_t} + B \qquad (7.5.-6)$$

Should A have the same value in both cases then the amplitude of ω_{st} would already be very much smaller than given by equation (7.3.-11), because $\omega_{st}^2 L_t C_t = \left(\frac{\omega_{st}}{\omega_t}\right)^2 >> 1$.

Always $(U_c)_o = (U_s)_o \approx U_n$ and a short time after interruption $(U_c)_o = U_n$.

Substituting this in equation (7.3.-5), moreover A (with $L_s << L_t$) reduces to a very low value in comparison to fig. 7.1.

Hence hardly any main-circuit-oscillation can develop in a circuit according diagram 3.

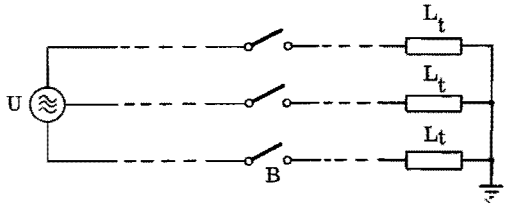

Fig. 7.5.1. Principle of three-phase circuit.

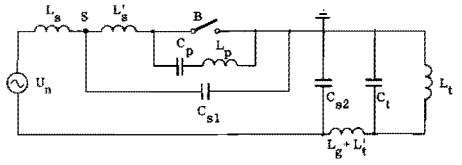

Fig. 7.5.2. Equivalent circuit. Diagram 2.

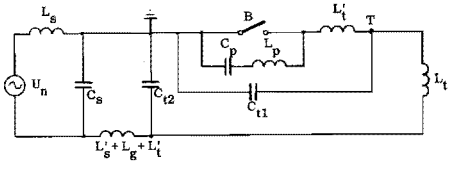

Fig. 7.5.3. Equivalent circuit. Diagram 3.

7.6. Summary of oscillations occurring during interruption.

In table 7.6 all oscillations discussed in chapters 4, 6 and 7 are summarized. For the definition of the letter symbols reference should be made to fig. 7.1. In this table the following assumptions are made

a) as before $L' = \frac{L_s L_t}{L_s + L_t}$ $C' = C_s + C_t$

$L'' = L_s' + L_t' + L_g$ $C'' = \frac{C_s C_t}{C_s + C_t}$

$$L_p \ll L'' \ll L_s \ll L_t$$

b) All damping influences are neglected.

c) The values entered in the last column give the range of the frequencies observed in the circuits investigated.

Name	Frequency	
Instability-oscillation	ω_i (see chapter 4)	f_i = 0.2 to 2.5 Mc/s
First parallel-oscillation	$\omega_{p1} = \frac{1}{\sqrt{L_p C_p}}$	f_{p1} = 2 to 10 Mc/s
Second parallel-oscillation	$\omega_{p2} = \frac{1}{\sqrt{L'' C''}}$	f_{p2} = 0.2 to 0.4 Mc/s
Main-circuit-oscillation	$\omega_{st} = \frac{1}{\sqrt{L' C'}}$	f_{st} = 8 to 20 kc/s
Oscillation of the feeding circuit	$\omega_s = \frac{1}{\sqrt{L_s C_s}}$	f_s = 16 to 20 kc/s
Oscillation of the load circuit	$\omega_t = \frac{1}{\sqrt{L_t C_t}}$	f_t = 0.5 to 5 kc/s
Industrial frequency	ω_n	f_n = 50 c/s

Table 7.6. Summary of the oscillations in the interruption cycle.

CHAPTER 8 INTERRUPTION OF INDUCTIVE CIRCUITS WITH OIL-BREAKERS

8.1. The interruption-cycle

The pattern of current and voltage on interruption with oil-breakers is highly reproducible provided accurate timing of contact separation is obtained. Therefore an idealized picture of an interruption cycle fig. 8.1.1 can be composed. Here voltage variations as a result of motion of the discharge (section 4.1) and main-circuit-oscillations (section 7.3) are neglected. (The influence of the main-circuit-oscillation on interruption will be treated in sections 8.5 and 8.7).

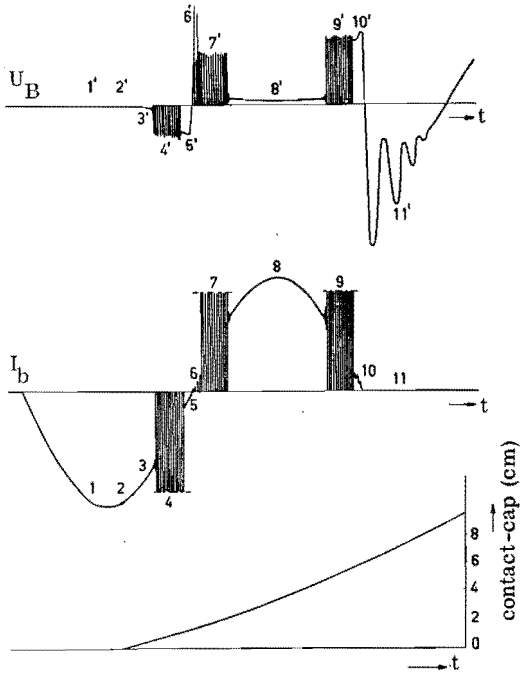

Fig. 8.1.1. Idealized interruption cycle for oil-breakers
U_B = voltage across the breaker
I_b = current through the breaker

In fig. 8.1.1 the following modes can be distinguished.

1,1' Current through the breaker before separating contacts. No voltage is measured across the contacts.

2,2' Contact separation.

3 The current continues to flow undisturbed through the gas-discharge.

3' Across the contacts a small arc voltage is observed.

4 When the current has dropped to a value of $I_b \approx 1.5$ A (see section 4.8) a quickly growing instability-oscillation is generated. Owing to this the current approaches the zero line and the discharge ceases. Then a great number of reignitions follows. During this time as well on the source side as on the load side, a mean-circuit-current flows continuing the current of mode 3 (see section 6.2).

4' After each current interruption the voltage rises with a very high rate, until reignition sets in. The voltage inducing reignitions is rather constant over wide parts of the unstable range.

5 After this unstable range the current stabilizes again, having a value between 0.3 and 0.6 A. Then the current flows apparently uninfluenced to its natural zero.

5' The voltage across the breaker after the unstable interval is 5 to 10 times higher than before. This voltage rises while the current approaches zero. Thus the discharge again obeys a negative current-voltage characteristic.

6,6' After current-zero the restriking voltage (section 6.3) can cause new series of reignitions. The rate of rise of the voltage is considerably lower than in phase 4'. The reignitions develop at differing, much higher, voltages.

7,7' If there is no final interruption (for instance, because the distance between the contacts is still too small) a new unstable range having the same pattern as 4, 4' starts.

8 At about 1.5 A the current becomes stable again, after a damped oscillation (ω_{p2}).

8' The voltage is again of the same order as during period 3'.

9 In the same way as described under 4 a new unstable interval arises. The same kind of reignitions occur.

9' The voltage pattern is the same as in 4'. However, the rather constant value at which reignition develops is higher.

10 Once again the current becomes stable as mentioned under 5.

10' The voltage trace is comparable to mode 5' but has a higher level.

11 The interruption has succeeded.

11' The recovery voltage shows a damped oscillatory transition to the steady-state i.e. the main voltage (section 6.3).

Depending on the current to be interrupted, the moment of contact parting, the mechanical speed of the contacts, the presence of arc control-devices, the values of the circuit elements and the location of earthing, parts of the idealized cycle shown above may not occur. At higher currents for instance the stable parts 5, 5' and 10, 10' are no longer clearly defined. When contacts part immediately after current-zero final interruption can follow after phase 5, 5' or 6, 6'. Capacitors or resistors in parallel to the contacts can initiate the unstable intervals 4, 4' and 9, 9' at higher currents and can lower the repeating frequency and so on. Also the main-circuit-oscillation can seriously disturb this idealized picture.

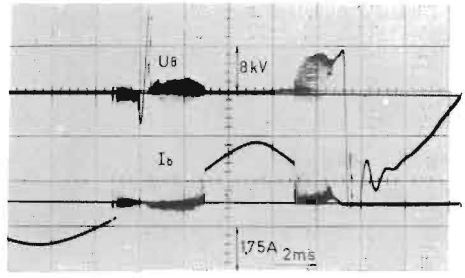

Fig. 8.1.2. Bulk-oil breaker, diagram 3, I ≈ 1.6 A (R.M.S.).
Complete interruption cycle.

Fig. 8.1.2 gives an oscillogram of a complete interruption-cycle which shows close agreement with fig. 8.1.1. (To prevent main-circuit-oscillation this record was made with a circuit according diagram 3.)

8.2. Current-chopping. Time-constant Θ_1.

In the circuits investigated current-chopping always occurred after an instability-oscillation and at a current level of $I_B = I_0 \geq 1.3$ A. The reason for the lower limit of 1.3 A is the transition from an arc- to a glow-discharge, as treated in section 4.8. When the parallel capacitance C_p was enlarged, the current was chopped at higher values (see also fig. 4.6.1). Since current-chopping due to the transition to the glow-discharge is exclusively the result of the discharge itself, the same values for I_o are found when resistive currents are interrupted. Fig. 8.2.1 is an example of this. Here $I_o = 1.5$ A. This oscillogram was obtained with the circuit of fig. 8.2.2. Also fig. 6.2.3 and 8.2.3 show oscillograms of instability-oscillation and current-chopping. Observed frequencies of the

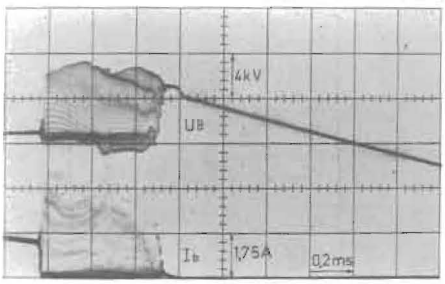

Fig. 8.2.1.
Bulk-oil breaker, I =2.5 A (R.M.S.).
Interruption of resistive current.

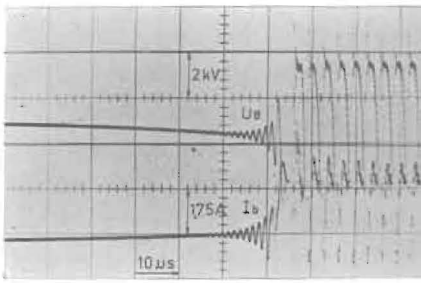

Fig. 8.2.3. Small-oil-volume breaker, I =10.8 A (R.M.S.). Current-chopping due to instability-oscillation, f_i =0.75 Mc/s.

instability oscillation f_i varied between 0.4 and 1.4 Mc/s for inductive single-phase circuits. For the circuit of fig. 8.2.2 the range was $1.7 \leq f_i \leq 2.5$ Mc/s. In the three-phase circuit of fig. 2.1.6 where an 80 m length of ground cable formed the connection between the breaker and the inductive load $f_i \geq 0.2$ Mc/s was measured. These results give the impression that a loose relation exists between ω_i and C_t or between ω_i and ω_{p2}. A definite correlation between ω_i and the other circuit-elements could not be found. Despite identical timing a number of different frequencies between $0.4 \leq f_i \leq 1.4$ Mc/s were found on successive tests with no modification of the circuit.

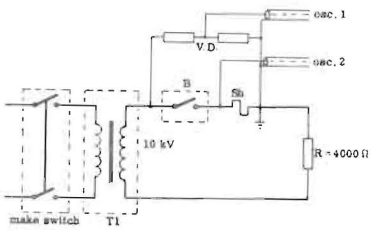

Fig. 8.2.2. Circuit for recording fig. 8.2.1.

Here the time-constant cannot be obtained with high precision from ω_i in accordance with the instability criteria of chapter 4, because the characteristic of the discharge just prior to the current-chop is unknown. Mayr's criterion $\omega_i \Theta_M = 1$ should yield the following results

f_i	2.5	1.4	0.2 Mc/s
Θ_M	0.064	0.11	0.8 µs

However, from the fact that the current chops when $I_b \approx 0$ it can be concluded that the time-constant Θ_1 must be smaller than one quarter of a

cycle of the instability-oscillation. If this should not be the case, then during this oscillation the current would pass the zero line, as it also happens during the first parallel-oscillation after a reignition (see section 6.2. fig. 6.2.5). The lowest frequency observed was in the latter case f_{p1} 5 Mc/s. Therefore an approximate value of Θ_1 lies within the limits.

$$\frac{\pi}{2\,\omega_{p1}} < \Theta_1 < \frac{\pi}{2\,\omega_i} \qquad (8.2.-1)$$

For the frequencies $f_{p1} = 5$ Mc/s and $f_i = 2.5$ Mc/s this inequality gives $0.05 \times 10^{-6} < \Theta_1 < 0.1 \times 10^{-6}$ sec.

In other words:

The first time constant Θ_1 of a discharge in an oil-breaker has an order of magnitude of 0.1 μs for an instantaneous current of appr. 1.5 A.

8.3. Reignitions prior to the definite current-zero.

In section 6.2 a brief discussion is given of the generation of thermal reignitions in the unstable regions 4,4' and 9,9' of fig. 8.1. The behaviour of the discharge and the circuit during these periods as could be derived from a large number of oscillograms will be summarized in the following paragraphs.

8.3.1. On a current-chop as a result of an instability-oscillation the high conductance G_1 decays with a small time-constant Θ_1 (section 5.5). The order of magnitude of Θ_1 is 0.1 μs (section 8.2). However, a residual conductance G_2 remains for a long time. After appr. 200 μs reignitions can still be initiated by a residual current.

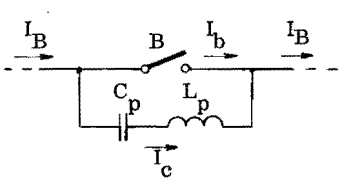

Fig. 8.3.1.
Detail of equivalent circuit showing active parallel circuit.

8.3.2. On a current-chop as a result of an instability-oscillation only the current I_b through the discharge is interrupted. The current I_B is maintained initially through the parallel-capacitance C_p as shown in fig. 8.3.1 which is a detail of the complete circuit fig. 7.1. As a result the voltage across the

breaker rises very rapidly to a high value. The initial rate of this restriking voltage can be up to 10 000 V/μs (e.g. when I_o = 2 A and C_p = 200 pF).

8.3.3. Under influence of this restriking voltage and as a result of the residual conductivity of the discharge path a residual current flows through the breaker. When this residual current exceeds a certain value I_d the conductivity increases again to a higher value resulting in reignition. At this instant the voltage U_B has reached the maximum U_d and decays hereafter.

8.3.4. During the reignition the electric charge of C_p transfers into the discharge path. In this way the first parallel-oscillation of frequency ω_{p1} is excited (section 7.1). The first peak of this oscillation is of the order of 100 A (section 6.2). The energy stored in C_p is almost entirely dissipated in the discharge path and the first parallel-oscillation is damped out after a few cycles. Then $U_B \approx 0$ and the gas-discharge ceases again as a consequence of the very low value of Θ_1. The second parallel-oscillation can not develop.

8.3.5. Now C_p is charged again by I_B. As before a new reignition results in a new first parallel-oscillation when again $I_b = I_d$ and $U_B = U_d$ are reached. In this manner a large number of consecutive reignitions can occur.

8.3.6. The values I_d and U_d are generally fairly constant during the entire unstable region. The time interval between two consecutive reignitions has only little influence on I_d and U_d. However, the rate of increase of the conductivity decreases considerably for longer time intervals after the voltage U_d and the current I_d have been reached.

For I_d values ranging from 0.3 to 0.6 A and for U_d between 6 and 16 kV were measured. The higher values of U_d were essentially found with small-oil-volume breakers. U_d increases (somewhat) with contact-distance.

8.3.7. The circuit-current I_B can flow alternately either through C_p or the gas-discharge during the entire unstable period. Hence a mean-circuit-current flows during this period through L_t. It does not deviate much from a current which would flow through a continuous discharge (fig. 6.2.1).

8.3.8. Whenever $I_B < I_d$ the transition to the high conductivity discharge is no longer possible. Therefore reignitions can only occur in the region

$I_o \geq I_B \geq I_d$ where $I_o \geq 1.3$ A and I_d is 0.3 to 0.6 A.

To illustrate the above described behaviour figures 6.2.1, 8.2.1, 8.2.3 and 8.5.1 may serve.

Paragraphs 8.3.1 to 8.3.8 permit the following conclusions.
Since up to 200 μs after a reignition a new break-down can be initiated by the residual current the time-constant Θ_2 must be of the order of 100 μs. Because U_d and I_d often hardly vary within the same unstable region (irrespective of the time between two reignitions) rough dynamic discharge characteristics of the form of fig. 8.3.2 can be deducted for this period. Curve 1 is valid for an extremely fast restriking voltage. Curves 2 and 3 apply for restriking voltages of decreasing steepness. The second time-constant Θ_2 is responsible for the shift in these dynamic characteristics.

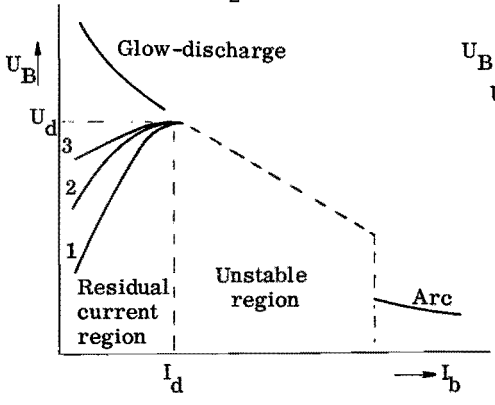

Fig. 8.3.2.
Dynamic discharge characteristics for oil-breakers.

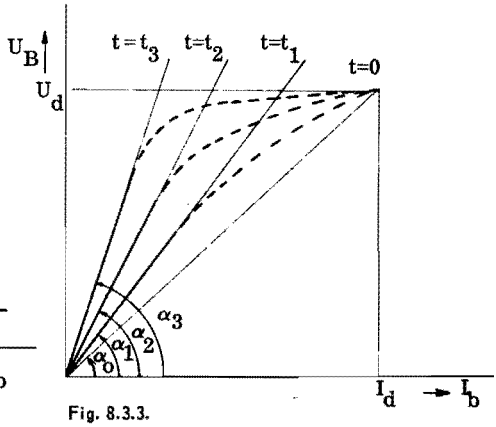

Fig. 8.3.3.
Residual-discharge characteristics for various time-intervals before the restriking voltage starts.

Starting from a given time-constant Θ_2 a number of quasi-static characteristics with time as parameter can be constructed for the residual discharge, see fig. 8.3.3. These characteristics would be followed if a step-voltage would be applied at time t_i. In equation (5.5.-11):

$G_{b2} = G_2 e^{-t_i/\Theta_2}$, the residual conductance G_2 is then a constant. The derivatives of these lines are given by

$$\operatorname{tg} \alpha_i = \left(\frac{1}{G_{b2}}\right)_{t=t_i} = \frac{1}{G_2 e^{-t_i/\Theta_2}} \qquad (8.3.-1)$$

In fact the voltage does not rise with an infinite rate. The actual course of

voltage and current is shown in fig. 8.3.4. For higher values of I_b the energy input into the discharge is no longer negligible. The total energy input into the residual discharge is

$$W_r = \int_0^{t_r} U_B I_d \, dt \qquad (8.3.-2)$$

As a result the residual conductance G_2 rises and the dynamic characteristics bend towards the point U_d, I_d following the dashed lines. After reignition the energy stored in C_p is added to the gas column such that in total the energy

$$W_d = \int_0^{t_r} U_B I_d \, dt + \tfrac{1}{2} C_p U_d^2 \qquad (8.3.-3)$$

is dissipated in the discharge during the time t_d between two reignitions.

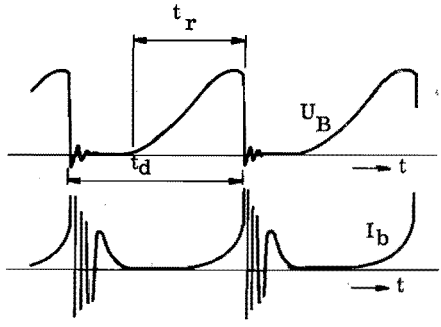

Fig. 8.3.4. Traces of voltage and current in the region of consecutive reignitions.

Letting $U_b = U_o$ and $I_b = I_o$ at the instant of the current chop (due to the transition from arc- to glow-discharge) and assuming constant cooling during the time interval of the reignition region then the criterion for a new energy break-down is in first approximation

$$\int_0^{t_r} U_B I_b \, dt + \tfrac{1}{2} C_p U_d^2 = U_o I_o t_d \qquad (8.3.-4)$$

Measurements show indeed that this criterion is acceptable.
(For example, when $U_o = 1500$ V, $I_o = 1.6$ A, $C_p = 200$ pF, $U_d = 10\,000$ V and $I_d = 0.3$ A, then

$$\tfrac{1}{2} C_p U_d^2 = 10^{-2} \text{ (J)}$$

$$U_o I_o t_d = 2400\, t_d \text{ (J)}$$

Letting further $t_r = \frac{2}{3} t_d$

$$U_B = \frac{t}{t_r} U_d$$

and $$I_b = \left(\frac{t}{t_r}\right)^2 I_d \quad \text{(see fig. 8.3.4)}$$

one obtains $$\int_0^{t_r} U_B I_b \, dt = 500\, t_d \quad (J)$$

From (8.3.-4) follows the time between two reignitions $t_d \approx 5.3\ \mu s$. This is a good average of the observed times.
An accurate check would bring about serious problems as regards measuring technique because U_o, I_o, U_d and I_d must be determined simultaneously, while also the active capacitance C_p must be known.)

If condition (8.3.-4) is fulfilled the mean temperature of the discharge path will remain constant during the unstable period. This might explain the regular behaviour of the discharge in this region. The repetition times of reignitions are usually from 2 to 10 μs. Generally t_d will decrease with decreasing current I_B because the steepness of the restriking voltage decreases.

The main-circuit-oscillation can disturb the regularity of the pattern (see section 8.5). As a result the time between two reignitions can increase to tens of microseconds. But the new break-down still occurs for nearly the same values of U_d and I_d (see for example fig. 8.5.1) and also the dynamic characteristic of fig. 8.3.2 is followed again. The transition into the discharge of high conductivity, however, is much slower. Therefore this is certainly not an "ionization disturbed spark break-down" in the sense of Edels' definition (see section 5.3), although the high voltage and the relatively low current reminds one of a glow-discharge.

The number of reignitions which successively occur can be estimated roughly as follows.
Assume the unstable region lasts from $I_B = 1.5$ A to $I_B = 0.5$ A. Then with $I_B = I_n \sin \omega_n t$ the corresponding time interval is given by

$$\Delta t = \frac{1}{\omega_n}\left(\sin^{-1}\frac{1.5}{I_n} - \sin^{-1}\frac{0.5}{I_n}\right) \qquad (8.3.-5)$$

For $I_n > 1.5$ A this expression can be approximated by

$$\Delta t \approx \frac{1}{\omega_n} \sin^{-1}\frac{1}{I_n} \qquad (8.3.-6)$$

For the total number of reignitions N one finds then

$$N \approx \frac{\Delta t}{t_d} = \frac{\sin^{-1} \frac{1}{I_n}}{\omega_n t_d} \qquad (8.3.-7)$$

With a mean repetition time $t_d = 5\ \mu s$ and an industrial frequency $f_n = 50$ c/s one obtains

I_n	3 A	10 A	20 A
N	210	70	35

These values give an idea of the large number of reignitions which can occur after a current chop.

8.4. Stable passage through zero due to glow-discharge

For $I_B < I_d$ the maximum U_d, I_d of the dynamic U_b-I_b-characteristic (fig. 8.3.2) cannot be reached any more. Apparently the condition (8.3.-4) can then no longer be fulfilled, in other words the gas cools. For sufficiently high voltage U_B the discharge now transfers to a glow-discharge (5.5' and 10.10' in fig. 8.1.1). The subsequent behaviour is then mainly determined by the elements of the main circuit (U_n, L_s and L_t). In effect the high resistance of the glow-discharge is now incorporated in the circuit and the equivalent circuit assumes the simple form of fig. 8.4.1. Here the transition into a glow-discharge is simulated by opening of breaker B at the instant when $I_B = I_d$. All capacitances and the smaller self-inductances are neglected, because the high series resistance ($R_g \approx 20\,000\ \Omega$) prevents high-frequency oscillations.
Before B is opened

$$U = U_n \cos \omega_n t \qquad (8.4.-1)$$

$$I_B = I_n \sin \omega_n t \qquad (8.4.-2)$$

$$I_n = \frac{U_n}{\omega_n (L_s + L_t)} \qquad (8.4.-3)$$

When B is opened at the time $t = t_1$ the circuit equation becomes

$$(L_s + L_t) \frac{dI_B}{dt} + R_g I_B = U_n \cos \omega_n t \qquad (8.4.-4)$$

With the initial condition

$$I_B = I_n \sin \omega_n t_1 = I_d \quad \text{at} \quad t = t_1$$

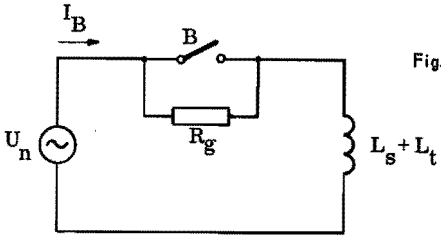

Fig. 8.4.1. Equivalent circuit for the glow-discharge period.

it is found that

$$I_B = e^{-(t-t_1)/\vartheta} \left\{ I_d - \frac{U_n}{Z} \cos(\omega_n t_1 - \psi) \right\} + \frac{U_n}{Z} \cos(\omega_n t - \psi) \qquad (8.4.-5)$$

where

$$Z = \sqrt{\{ R_g^2 + \omega_n^2 (L_s + L_g)^2 \}} \qquad (8.4.-6)$$

$$\psi = \operatorname{tg}^{-1} \omega_n (L_s + L_t)/R_g \qquad (8.4.-7)$$

$$\vartheta = \frac{L_s + L_t}{R_g} \qquad (8.4.-8)$$

The last term of solution (8.4.-5) gives a new steady-state with lower amplitude and less phase shift than before. The transition to this state follows a damped exponential function with time-constant . When the current during or after this transition passes through zero the discharge ceases and this can bring about final interruption of the current.
The slope with which the current decays to zero follows from

$$\left(\frac{dI_B}{dt} \right)_{t=t_1} = -\frac{U_n}{Z} \omega_n \sin(\omega_n t_1 - \psi) - \frac{1}{\vartheta} \left\{ I_d - \frac{U_n}{Z} \cos(\omega_n t_1 - \psi) \right\} \qquad (8.4.-9)$$

or more simply when $\cos \omega_n t_1 \approx -1$.

$$\left(\frac{dI_B}{dt} \right)_{t=t_1} = -\omega_n I_n \left(1 + \frac{R_g}{U_n} I_d\right) \qquad (8.4.-10)$$

Hence the transition to the new state of the discharge is coupled with a

higher rate of current-decay which without transition would have been equal to $-\omega_n I_n$. The difference is not great. For instance, when R_g = 20 000 Ω, U_n = 10 000 √2 Volts, I_d = 0.35 A the rate is

$$\left(\frac{dI_B}{dt}\right)_{t=t_1} = -1.5\ \omega_n I_n \qquad (8.4.-11)$$

(With the bulk-oil-breaker somewhat lower, with the small-volume oil-breaker somewhat higher values were found.)

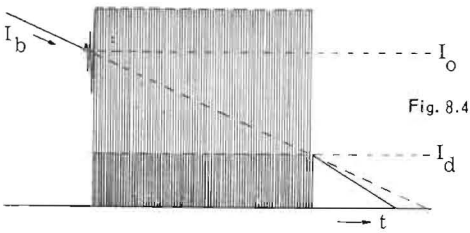

Fig. 8.4.2. Steadily decaying current of glow-discharge after reignition-region.

When the dynamic residual discharge transfers to a quasi-stable glow-discharge the current continues its natural course towards zero with a higher rate of decay, fig. 8.4.2. The character of a glow-discharge is evident from the high discharge-voltage, which increases with the steadily decaying current, see for example fig. 8.1.2 and 8.4.3. (In fig. 8.4.3 the higher rate of decay of the current in the glow-discharge region is neutralized by an inrush effect.)

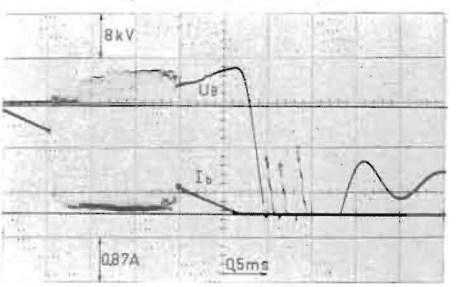

Fig. 8.4.3.
Bulk-oil breaker, diagram 3, I ≈ 1.6 A (R.M.S.)
Reignition region and glow-dischorge.

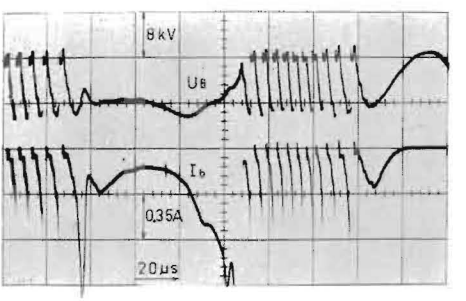

Fig. 8.5.1.
Bulk-oil breaker, I =3.6 A (R.M.S.).
Influence of main-circuit-oscillation on residual-current reignitions.

8.5. The influence of the main-circuit-oscillation prior to current-zero

The regular pattern described in the previous sections is in general found with a circuit according diagram 3 only. With circuits according diagrams 1 and 2 main-circuit-oscillation is produced by repetitive reignitions (sections 7.3 to 7.5). As a result a component of current I_{st} and frequency ω_{st} is superimposed on the circuit-current. Because the initial rate of

rise of the restriking voltage is directly proportional to I_B the repetition frequency of the reignitions is modulated by the main-circuit-oscillation, see fig. 8.5.1.

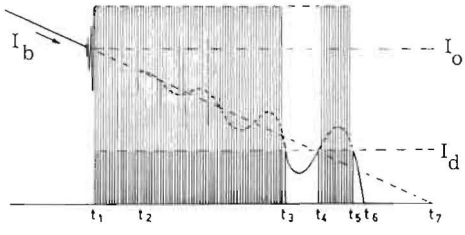

Fig. 8.5.2. Stable part in the reignition region and definite current-chop due to main-circuit-oscillation.

t_1 : current-chopping due to instability-oscillation
t_2 : start af main-circuit-oscillation
t_3 : $I_b < I_d$; start of stable part
t_4 : $I_b > I_d$; end of stable part
t_5 : $I_b < I_d$; start of stable part
t_6 : definite current-zero
t_7 : natural current-zero
I_b : current through the discharge
I_o : critical current for arc- to glow-discharge transition
I_d : level for residual-current-reignition.

Due to this oscillation it may happen temporarily that $I_B < I_d$, i.e.during about half a cycle of I_{st}. Then within the unstable region a quasi-stable portion lasting for appr. $\frac{\pi}{\omega_{st}}$ sec. occurs (fig. 8.5.2, t_3 to t_4). Such stable portions can be found in the oscillograms of fig. 8.5.1 and 6.2.1. If the current to be interrupted is very small (a few amps) a number of quasi-stable regions can occur in succession.

Finally, the current I_B can be abruptly forced to zero by the main-circuit-oscillation (fig. 8.5.2, t_5 to t_6). In section 7.4 (paragraph a) it is shown that this can result in high overvoltages. Sometimes a small component I_{st} is found continuing in the region of the glow-discharge without much influence on the interruption (fig. 8.5.3).

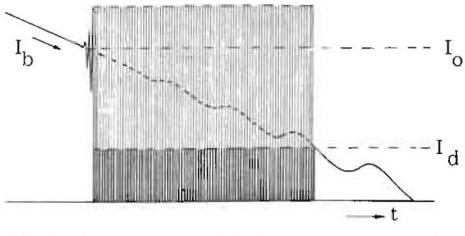

Fig. 8.5.3. Main-circuit-oscillation continuing in the glow-discharge current.

8.6. Reignitions after the definite current-zero.

When I_B steadily approaches zero the current interrupts simultaneously in B, L_s and L_t. At that instant U_B changes its direction, passes zero and oscillates to and about the main voltage U_n (see section 6.3, equation (6.3.-1) and fig. 6.3.1). Prior to the voltage-zero no new reignition can occur. This is region 5.5' of fig. 8.1.1.
However, if I_B is forced to zero by the main-circuit-oscillation, U_B will rise further towards the suppression peak $U_{max\,1}$ (section 6.3, equation (6.3.-4) and fig. 6.3.2). Before U_B changes direction reignitions can occur. They arise from a residual current when $U_{max\,1}$ is reached within 100 to 200 μs. These reignitions not necessarily lead to interruption failure because the direction of the restriking current is the same as before the chop (section 7.4, paragraph d). Hence a new zero of the current must follow.

A favourable effect of these reignitions is that they limit the voltages $U_{max\,1}$ and hence also $U_{max\,2}$. A disadvantage is that they increase again the temperature of the discharge path. Since at the instant of the breakdown, $U_B = (U_t)_o - (U_s)_o = U_{max\,1} - U_n$, the effective voltage can be relatively high, hence the energy of the first parallel-oscillation is large. Therefore it is impossible to state definitely and in a general way whether current-chopping due to main-circuit-oscillation has a favourable or unfavourable influence on interruption.

After the voltage has passed through zero a reignition can only occur after $|U_B|$ has become larger than $|U_{max\,1}|$. The behaviour of the discharge is now less regular than before because during the relatively long pause of current flow the gas column between the contacts has become less homogeneous with respect to temperature and composition. On successive tests under identical conditions of circuit and timing the first reignition after the voltage zero can therefore be sometimes either of a dielectric nature (fig. 8.6.1) or arise from a residual current (fig. 8.6.2).
In case of a dielectric break-down the first parallel-oscillation induces rapid heating of the discharge-channel. The energy $\frac{1}{2} C_p U_d^2$ is large because the dielectric break-down voltage is much higher than the voltage at which thermal break-down is initiated (fig. 8.6.1: $U_d = 25$ kV, fig. 8.6.2: $U_d = 10.8$ kV).

After the first parallel-oscillation the core of the discharge ceases again.

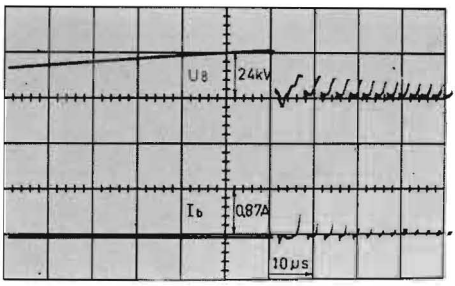

Fig. 8.6.1.
Small-oil-volume breaker, I = 10.8 A (R.M.S.).
Dielectric break-down after zero of the current.

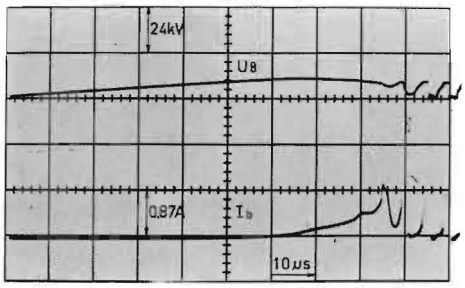

Fig. 8.6.2. Small-oil-volume breaker, I = 10.8 A (R.M.S.).
Residual-current break-down after zero of the current.

The mechanism follows the same sequence as described in par. 8.3.4. A small residual conductivity remains here too. As a result of the voltage difference between U_s and U_t, C_p is being charged again. Therefore the voltage rises rather fast. Hence rapidly new reignitions can follow, but now generally after a residual current and thus at a lower voltage than was necessary for the first reignition. The second parallel-oscillation is not observed because the discharge channel ceases too quickly.

If the first reignition occurs after a residual current the break-down is much slower. Hence no first parallel-oscillation can develop, but the beginning of the second is observed (fig. 8.6.2). Again the current is forced towards a low value. Subsequent reignitions arise in the same manner as after a dieelectric break-down.

In both cases the pattern of the reignitions is somewhat more irregular than prior to zero.

Due to repetitive reignitions a mean-circuit-current in agreement with paragraph 8.3.7 can flow again. If this current exceeds the value of I_o a stable discharge is possible again. Then interruption at the current-zero under consideration has failed (end of 7.7', fig. 8.1.1).

If the current to be interrupted is very small (a few amps) the mean-circuit-current cannot rise sufficiently fast to cause a long series of repetitive reignitions. After the difference between U_s and U_t has been reduced to a low value the reignitions cease until this voltage difference is again sufficiently large for a new break-down. Fig. 8.4.3 is a typical example. It shows three bursts of reignitions which do not lead to interruption failure.

8.7. The influence of the main-circuit-oscillation after current-zero.

As before the main-circuit-oscillation disturbs the regular pattern of

reignitions after current-zero (unless diagram 3 is applied). This results sometimes in the excitation of series of reignitions in the rhythm of these oscillations (fig. 8.7.1 and 7.4.6). During a positive amplitude of I_{st} a stable arc can occur temporarily ($I_b > I_o$) which ceases again when the current decays ($I_b < I_o$).

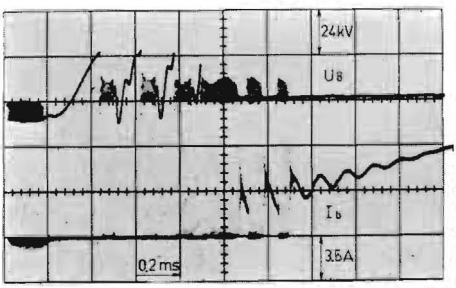

Fig. 8.7.1.
Small-oil-volume breaker, I =10.8 A (R.M.S.).
Reignitions and main-circuit-oscillation after current-zero.

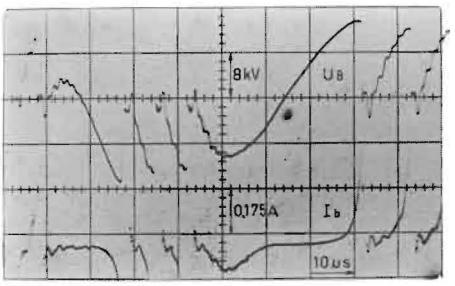

Fig. 8.7.2.
Small-oil-volume breaker, I = 10.8 A (R.M.S.).
Alternately changing polarity of reignitions.

This occurs twice at I_o = 1.8 A in fig. 8.7.1. Thereafter I_b remains larger than I_o. Subsequently the main-circuit-oscillation is damped out and the steady-state circuit current remains only. At this current-zero interruption failed. The transition into a stable arc is each time via a second parallel-oscillation.

Here too the main-circuit-oscillation can have favourable as well as unfavourable influence. Favourable in the sense that again and again pauses of zero current are forced and the restriking voltage across the breaker decays at the beginning of each pause (see section 7.4). Unfavourable in the sense that the steepness of the restriking current is very much higher than that of the steady-state current by itself. Therefore a considerable amount of energy is pumped again into the discharge path during a series of reignitions. When the restriking voltage rises during a current pause a new series of reignitions is easily initiated by the residual current. It is even possible that a series of reignitions of negative polarity occurs temporarily because the decaying restriking voltage has passed sufficiently far beyond the zero line. Fig. 8.7.2 shows a typical example of this phenomenon.

At last the restriking voltage during the current pause becomes steeper, depending on the increase of the amplitude of I_{st}, see section 7.4, paragraphs a, b en d. This is clearly shown on fig. 8.7.1.

CHAPTER 9 INTERRUPTION OF INDUCTIVE CIRCUITS WITH AIR-BLAST BREAKERS

9.1. The interruption-cycle.

In fig. 9.1.1, 9.1.2 and 9.1.3 complete interruption-cycles are given for currents of 3.6 A, 18 A and 60 A (R.M.S.) respectively. These oscillograms show an entirely different pattern than those obtained with oil-breakers. This is due to the following differences in the behaviour of the discharge.

a. The movement of the discharge is more pronounced especially for small currents.
b. The discharge voltage is much higher.
c. The main time-constant Θ_1 is much larger ($\approx 1\ \mu s$).
d. The second time constant Θ_2 is much smaller.
e. The residual conductivity is much larger.
f. The pronounced influence of the transition arc- to glow-discharge is missing.

These facts result for the lower currents to be interrupted in less reproducible oscillograms. On the other hand successive tests showed remarkable reproducibility when currents of 60 A (R.M.S.) were interrupted. (Compare for example fig. 9.1.4 and 9.1.5 which were recorded in succession.) On a number of repetitive tests the pressure in the air tank varies considerably. As a result the contact speed as well as the cooling of the discharge vary leading to a considerable modification of the pattern of the interruption-cycle.
(All records of 60A-tests were obtained with a circuit according to fig. 2.2.2 excepting a short-circuit on the secondary terminals of the transformer on the loadside. Then $L_t \ll L_s$ and therefore no main-circuit-oscillation can be excited.)

9.2. Current-chopping and reignitions.

With air-blast breakers current-chopping occurs for small instantaneous values of current I_b in the same manner as with oil-breakers. As before current-chopping is initiated by an instability-oscillation of frequency ω_i

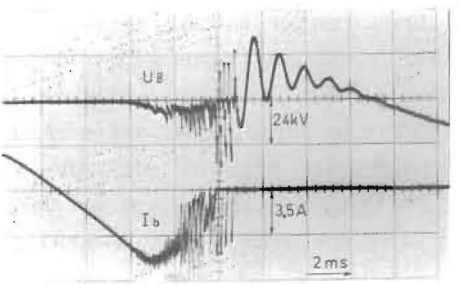

Fig. 9.1.1. Air-blast breaker, I = 3.6 A (R.M.S.). Complete interruption-cycle.

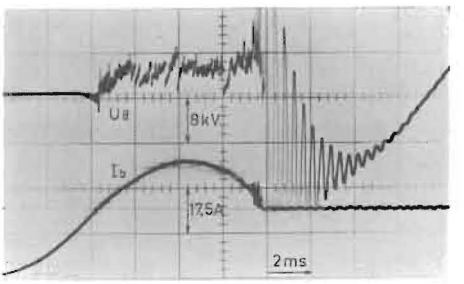

Fig. 9.1.2. Air-blast breaker, I = 18 A (R.M.S.). Complete interruption-cycle.

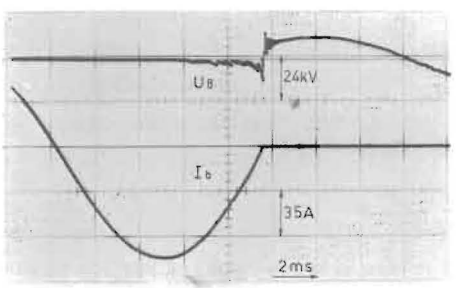

Fig. 9.1.3. Air-blast breaker, I = 60 A (R.M.S.). Complete interruption-cycle.

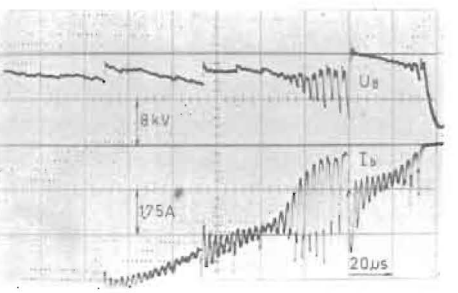

Fig. 9.1.4. Air-blast breaker I = 60 A (R.M.S.). Instability-oscillation, reignitions and final current-zero.

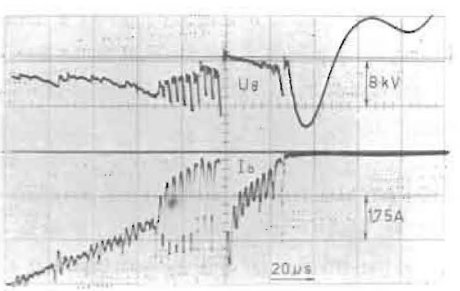

Fig. 9.1.5 Identical conditions as fig. 9.1.4. These two figures were recorded in succession.

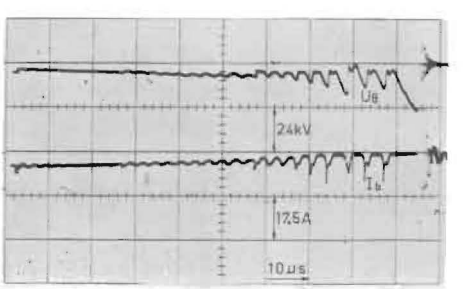

Fig. 9.2.1. Air-blast breaker, I = 60 A (R.M.S.). Instability oscillation and reignitions.

and increasing amplitude.

In contradistinction to the oil-breaker sudden current chops are seldom, although the amplitude of the current increases it does not quite reach the zero value. The instability-oscillation flows more or less steadily over into a pattern of thermal reignitions. These thermal reignitions occur so slowly that the first parallel-oscillation can not or hardly occur. After a series of thermal reignitions the zero line is frequently approached closely. Then the residual conductivity has nearly vanished and the restriking voltage rises quickly to a high value (section 6.3). If then a new break-down occurs it is always of a dielectric nature. In this case a highly conductive discharge channel is formed rapidly and consequently the first as well as the second parallel-oscillation can be excited. This is always followed by main-circuit-oscillation provided the circuit permits it. Fig. 9.2.1 is an example of these phenomena while fig. 9.1.4 and 9.1.5 show also the instability-oscillation, thermal reignitions, dielectric break-down and the second parallel-oscillation. The first parallel-oscillation can be faintly seen in the voltage trace. (The main-circuit-oscillation cannot develop in this circuit.)

In section 4.2 it is stated that the discharge in the air-blast breaker is in continued motion. The irregular pattern of the voltage and (for low instantaneous values of I_b) also of the current is caused particularly by frequent alternating elongations and break-downs over a smaller distance. These break-downs are independent of the value of I_b and are clearly of a dielectric nature. Rapidly a new highly conductive discharge-path is formed. Because prior to the break-down the voltage has risen to a high value break-down is followed always by a first parallel-oscillation (ω_{p1}), a second parallel-oscillation (ω_{p2}) and, if circuitry permits also by a main-circuit-oscillation (ω_{st}). Often the second parallel-oscillation lasts for a long time. It is conceivable that the oscillation-circuit concerned is excited by aerodynamic disturbances.

All these variations together are the reason that neither α or K (in equation 4.3.-1) nor the time constants Θ_1 and Θ_2 remain constant. It is to be expected that for a short length of the discharge α is larger than for a longer discharge column, because the influence of elongation is relatively much more pronounced in the first case. On the other hand it is obvious that a shorter arc is more difficult to interrupt, hence the time constant

Θ_1 can be larger in this case.

A rough indication of the order of magnitude of Θ_1 is obtained as before from the fact that the current of the second parallel-oscillation after a dielectric break-down (i.e. at a short arc length) can pass the zero line without chopping (see e.g. fig. 9.2.1, 9.1.4, 9.1.5 and 7.2). On the other hand instability-oscillation always leads to current-chopping.

In the circuits considered $f_{p2} \approx 0.4$ Mc/s while $f_i \geq 0.2$ Mc/s. In agreement with equation (8.2.-1) the order of magnitude of Θ_1 is estimated from

$$\frac{\pi}{2\,\omega_{p2}} < \Theta_1 < \frac{\pi}{2\,\omega_i} \qquad (9.2.-1)$$

or

$$0.63 < \Theta_1 < 1.25 \quad \mu s$$

These simplified considerations permit the conclusion:
The first time-constant Θ_1 of the discharge in the air-blast breaker is of the order of 1 μs for instantaneous currents of 3 to 4 A.
This result is in good agreement with Rizk's direct measurements of time-constants in a model of an air-blast breaker. He found a variation from 0.6 to 1.1 μs at 20 to 90 A (see section 5.4).

It was found impossible to obtain from our records a clear indication of the magnitude of Θ_2, because never a voltage zero was followed by a residual-current reignition. Also with the air-blast breaker (see e.g. fig. 7.4.5) lasting series of residual-current reignitions can occur. Here every time new energy is added to the discharge path such that the residual conductivity is maintained as was described for the oil-breaker (section 8.3). The impression is gained that Θ_2 is highly variable and is perhaps of the order of 5 to 10 μs.

9.3. The influence of the main-circuit-oscillation.

In suitable circuits main-circuit-oscillation is continually initiated by the motion of the discharge. It amplifies the irregular pattern of the current trace at small instantaneous values of the current. Due to the main-circuit-oscillation the steepness of the current varies continually and the instability criteria can be satisfied frequently. But for the same reason instability-

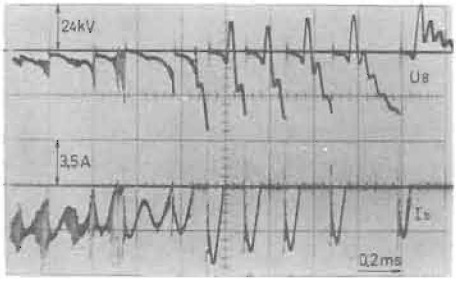

Fig. 9.3.1. Air-blast breaker, I =3.6 A.
Influence of main-circuit-oscillation before and after current-chopping.

oscillations do not always lead to current-chopping, as they occur in the rhythm of the main-circuit-oscillation (fig. 9.3.1, first 600 μs and fig. 7.4.5). Like in the oil-breaker these oscillations can force a current-zero, followed by high overvoltages (paragraph 7.4.a). The restriking voltage has again a rather low initial rate of rise determined mainly by I_s and ω_s, because now I_B reaches zero simultaneously in the breaker and the parallel capacitance. Since in the air-blast breaker the second time-constant Θ_2 is small an eventual reignition must be of dielectric nature. However, (for the larger contact-distances) the dielectric break-down voltage can be high. The restriking voltages after current-chopping are therefore also much higher in air-blast breakers than in oil-breakers. However, the reason is not due to current-chopping as a result of instability, but due to main-circuit-oscillation . On current-chopping after instability-oscillation the rate of rise of the restriking voltage of the circuits investigated was always very much higher. The reignitions were therefore initiated at lower voltages. Each dielectric break-down is followed again by a first and a second parallel-oscillation and half a cycle of the main-circuit-oscillation (fig. 9.3.1 and 7.2).

Reignitions after the zero value of the load current I_t (see paragraph 7.4.6) were observed in the air-blast breaker only when the contact separation was timed shortly before the zero, i.e. for small contact gaps. In this case the main-circuit-oscillation forces the current to zero again, and moreover results in high overvoltages which lead to break-down for short contact-distances.

CHAPTER 10 INTERRUPTION OF INDUCTIVE CIRCUITS WITH LOAD-BREAK SWITCHES

10.1. The interruption-cycle.

The contacts of the load-break switch under test are located within a narrow interrupting chamber with walls made from plastic material (nylon or teflon based). During the interruption process the discharge develops gas from the plastic which in turn increases the pressure and favours interruption. On interruption of small currents, however, this mechanism is of little effect. Hence a number of cycles is passed before interruption succeeds. Fig. 10.1.1 shows a portion of an interruption-cycle at a current of 10 A (R.M.S.). Characteristic of the behaviour of the load-break switch is:

a. Initially the arc voltage is low, but rises to a high value for large contact gaps.
b. The time-constants Θ_1 and Θ_2 are very large.
c. The transition residual- to arc-discharge is often very slow.

10.2. Current-chopping and reignitions.

Since Θ_1 is very large no instability-oscillation with resulting current-chop can occur. However, at very low instantaneous values the current can be chopped by arc motion. This motion becomes important when the moving contact has left already the arcing chamber. The high discharge voltage at large contact gaps can also advance the current-zero somewhat.

Because here current-chopping is not dominant the current-zero is not followed by a high overvoltage. Therefore reignitions prior to the zero of the restriking voltage have never been observed. The restriking voltage is determined by equation (6.3.-2) and can at most reach $2U_n + U_o$ (equation 6.3.-3).

With the switch tested residual-current reignitions were found exclusively. These were observed as late as 1000 to 2500 μs after current-zero (fig. 10.2.1). Detailed records of the region around current-zero show that this is not a normal glow-discharge, because the residual discharge

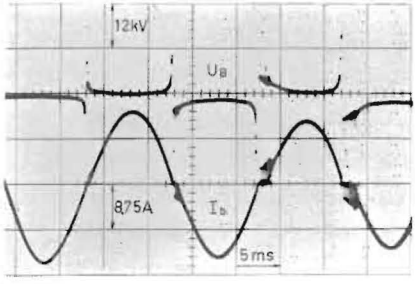

Fig.10.1.1. Load-break switch, I = 10 A (R.M.S.). Portion of an interruption-cycle.

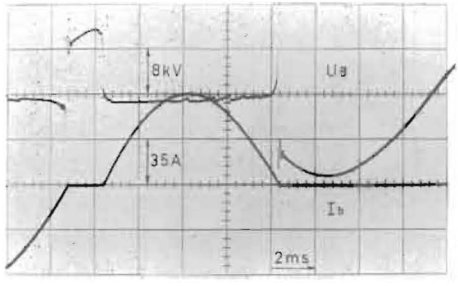

Fig.10.2.1. Load-break switch, I = 60 A (R.M.S.). Residual-current-reignition 1600 μs after current-zero.

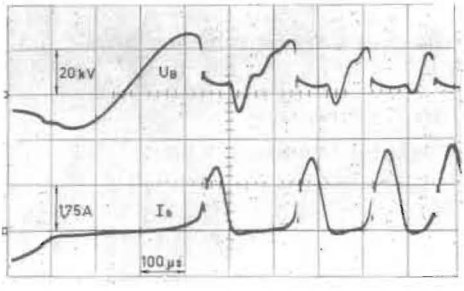

Fig.10.2.2. Load-break switch, I = 10 A (R.M.S.). Residual-current reignitions and new current-zeros due to main-circuit-oscillation.

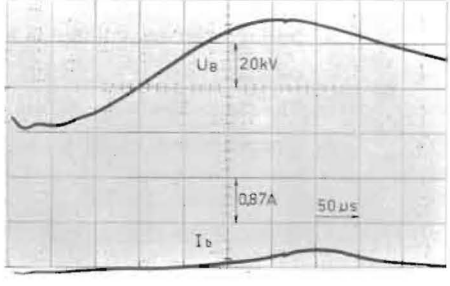

Fig.10.2.3. Load-break switch, I = 10 A (R.M.S.). Residual-current without transition into an arc.

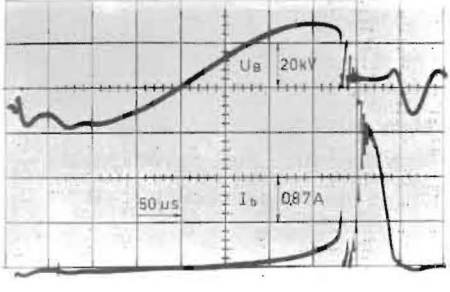

Fig.10.2.4. Load-break switch, I = 10 A (R.M.S.). Residual-current-reignition, followed by second parallel-oscillation and main-circuit-oscillation.

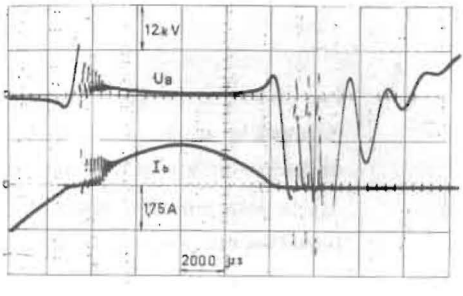

Fig.10.3.1 Load-break switch, I = 1.5 A (R.M.S.). Successful interruption due to main-circuit-oscillation.

has a positive characteristic. This can be concluded from the oscillograms fig. 10.2.2, 10.2.3 and 10.2.4, which were recorded under identical conditions. Fig. 10.2.2 shows that the current at an instantaneous value of appr. 0.5 A has a somewhat accelerated decay (begin of the oscillogram), but does not completely reach zero. As a result of the increased rate of decay of the current the voltage rises still somewhat before it changes direction.
In all three records the residual current lags the voltage till the instant of reignition (increasing current at decreasing voltage). Fig. 10.2.3 shows the critical situation where the residual current increases initially despite decreasing voltage but nevertheless no break-down occurs.

The break-downs are so slow that no first parallel-oscillations can arise (just as with the air-blast breaker). However, a second parallel-oscillation is found. Frequently it is highly damped as shown in fig. 10.2.2, but sometimes the oscillation is violent, e.g. in fig.10.2.4.

10.3. The influence of the main-circuit-oscillation.

Circuitry permitting the main-circuit-oscillation arises again after the second parallel-oscillation. As a result the current through the switch decays to zero and can chop. The residual discharge lasts for a long time (large value of the second time-constant Θ_2) similar as with the oil-breaker. As a consequence a number of successive residual-current-reignitions are easily excited, which produce repeatedly arc-discharges well over half cycles of the main-circuit-oscillation (fig.10.2.2). When the steady-state current I_{stat}, equation (7.3.10), has risen sufficiently so that always $I_B > 0$, then interruption fails and the main-circuit-oscillation is damped out. This situation is found after each current-zero on fig. 10.1.1. Especially for small currents to be interrupted, i.e. slowly rising I_{stat}, repetitive current-zeros due to main-circuit-oscillation can still result in successful interruption. Fig. 10.3.1 shows a typical example of this.
From this figure it can also be seen that the current after a reignition can pass the zero line. This situation is critical: under apparently identical conditions I_B can pass the zero line or can be chopped as well. Here the observed frequency of the main-circuit-oscillation was appr. 7.2 kc/s. From this a rough indication of the order of magnitude of Θ_1 can be obtained.

Equation (8.2.-1) becomes now

$$\Theta_1 \approx \frac{\pi}{2\ \omega_{st}} \qquad (10.3.-1)$$

and with $\omega_{st} = 2\pi \times 7200$ is found: $\Theta_1 \approx 35\ \mu s$.

CHAPTER 11 SUMMARY AND CONCLUSIONS

In this thesis a survey and explanation is given of the many cooperative phenomena which can occur during interruption of small inductive currents (1.5 A - 60 A, R.M.S.) with high voltage circuit-breakers. The study is based on the manner in which these phenomena are shown in the current through and the voltage across the breaker.

11.1. Current-chopping.

Current-chopping can be produced in a variety of ways as there are: motion of the discharge, electrical instabilities, main-circuit-oscillation and transition from arc to glow-discharge. Electrical instability is determined by the discharge-characteristic $U_b = f(I_b)$, the first time-constant Θ_1 of the discharge and the circuit in the direct vicinity of the breaker.

The discharge-characteristic and the time-constant Θ_1 are dependent on length and heat-extraction of the discharge and thus likewise on motion of the discharge.

The inherent capacitances and inductances of the breaker and its direct vicinity can have great influence on the chopping level. Stability theories are based on mathematical models of the discharge in which the characteristic and the time-constant are considered to be constant. Therefore these theories can only be checked experimentally when it can be shown at the same time that these conditions are fulfilled. In general this will be not so in high voltage circuit-breakers.

The transition from arc to glow-discharge can lead to instability and current-chopping in oil-breakers at a critical current: $1.3 \leq I_o \leq 2A$. This current-limit depends on the temperature in the axis of the discharge and therefore is a function of pressure in the discharge and to a certain degree also of contact-distance.

11.2. Restriking voltage after current-chopping.

On current-chopping as a result of main-circuit-oscillation the currents through the discharge and through its parallel-capacitance chop at the same time. Then the initial rate of rise of the restriking voltage is determined by the feeder-circuit. Moreover, the possible amplitude is

given by the interrupted circuit. After the current chop the voltage initially decays and afterwards rises to reach a high value, called suppression peak.

On current-chopping due to any of the other reasons mentioned only the current through the discharge is chopped. The circuit-current can initially continue through the parallel-capacitance. This capacitance is usually very small and therefore very high rates of rise of the restriking voltage can be produced. At the instant of current-chopping the voltage across the breaker is already high and hereafter rises further to the suppresion peak.

After a current-zero without chopping the voltage decays, changes polarity and oscillates to the recovery voltage (main voltage). In this case no excessive steepness or amplitude of the restriking voltage occur.

11.3. The discharge.

For a complete description of the behaviour of the breaker near current-zero the following properties of the discharge have to be considered:

a. The discharge characteristic $U_b = f(I_b)$.
b. The first time-constant Θ_1 with which the high conductivity in the axis of the discharge disappears.
c. The second time-constant Θ_2 with which the lower conductivity of the residual hot gas-column decreases.
d. The speed with which a residual discharge can transfer into a new low-impedance discharge under the influence of a rising restriking voltage.

For short time-intervals (some tens of micro-seconds) the discharge characteristic can be approximated by the expression $U_b I_b^{\alpha} = K$. The constants K and α are strongly dependent on the length and the motion of the discharge. In a relatively still discharge in oil $\alpha \approx 1$. During violent motion of the arc α rises to a high value. In the air-blast breaker α varied between $0.5 \leq \alpha \leq 6$.

From the various oscillations occurring during interruption an impression is obtained of the order of magnitude of Θ_1 and Θ_2:

oil-breakers	$\Theta_1 \approx 0.1$ μs	$\Theta_2 \approx 100$ μs
air-blast breaker	1 μs	5 μs
load-break switch	30 μs	1000 μs

The time-constant Θ_2 is a measure for the time-interval in which reignitions after a residual current are still possible. The speed of reignition not only depends on the restriking voltage but also on the time elapsed since the preceding low-impedance discharge has extinguished. In the oil-breaker residual-current reignitions of dielectric break-down type are still possible after appr. 10 μs. After a longer time the transition proceeds more slowly and can require up to some tens of microseconds. In the air-blast breaker and load-break switch residual-current reignitions arise slower than in the oil-breakers. The minimum time lag was of the order of 1 μs in both cases.
During a dielectric break-down a highly conductive discharge is induced within a very short time. In this case the rate of rise of restriking current is determined by the parallel circuit (C_p, L_p) of the breaker. Then rates of rise of 10 000 A/μs are possible.
When a number of reignitions rapidly succeed each other a "mean-circuit-current" is maintained through source and load. This current flows alternately either through the discharge or the parallel-capacitance C_p.

11.4. The restriking current.

In the circuits investigated the following oscillations in the restriking current could be distinguished: first parallel-oscillation, second parallel-oscillation and main-circuit-oscillation. Amplitude and frequency of both parallel-oscillations are governed firstly by stray capacitances and selfinductances in the immediate vicinity of the breaker, secondly by the way they are located in the circuit due to earthing. The main-circuit-oscillation depends on the selfinductances and capacitances of feeder side and load side and also on the location of earthing. These oscillations together determine the energy-input into the discharge-path immediately after reignition. Moreover they cause new current-zeros which can result in new current chops. It is impossible to state generally whether their influence on interruption is predominantly favourable or unfavourable.

11.5. The circuits.

Dependent on the location of earthing three single-phase circuits were investigated and compared with three-phase circuits. Earthing between source and load is most representative for the three-phase condition.

However, this circuit involves measuring difficulties because both terminals of the breaker are alive during interruption. It was shown that earthing between breaker and load gives no essential differences in comparison with three-phase circuits. The same oscillations may occur. Earthing between source and breaker prevent main-circuit-oscillation. Therefore this single-phase circuit has entirely different properties than the three-phase circuit.

11.6. Conclusions with respect to circuit-breaker testing.

In this thesis the great influence of the circuit on the mechanism of interruption of small inductive currents is shown. In general too little attention is paid to this aspect. The literature dealing with this subject gives little detailed information about circuitry and earthing.
In short-circuit testing stations, among other things, the ability of a breaker to interrupt small inductive currents should be checked. But here the composition of the circuit is as shown of essential importance. Apparently small modifications may have great consequences. Therefore one may wonder what value can be attached to the results of such tests, taking into account that it is usually not known in what circuit the breaker finally will be erected.
In order to be able to execute adequate and comparable tests further investigations particularly of circuits occurring in service is necessary. This should lead to determination of standarized test-circuits for which not only the main elements (source, load and connections), but also the data of additional quantities (active capacitances and inductances) and the location and way of earthing should be prescribed. Then the only justified criterion should be that one and the same breaker must show the same interruption-cycle in each laboratory provided the circumstances of timing and measuring techniques are identical. It goes without saying, that such a standardization on an international level would bring about serious difficulties.

(Also in the investigation of short-circuit interruption there is great need for comparable circuits. Upon suggestion of the "Current-Zero Club" Cassie and Rieder [51] made up a list of all circuit data to be reported in publications on this subject. This list is so extensive, that determination of the listed data often will require much more time than the performance of the short-circuit tests in itself. In this field standardization

of the test-circuits would also bring about essential advantages. The difficulties, however, are here still more serious because the sources and loads are much more voluminous and expensive.)

Also the measuring techniques used during investigations in the field of interruption of small inductive currents require great attention. Because of the importance of the active parallel-capacitance of the breaker voltage-dividers with small self-capacitance (≤ 25 à 50 pF) must be applied. The primary resistors of the divider should have a high total value ($\geq 10^5\ \Omega$/kV). For basic research the current through the breaker can only be accurately measured directly at the location of the breaker-terminal. Measuring devices which are added to the circuit on this spot should have a low impedance ($R \leq 1$ à 2 Ω, $L \leq 0{,}1\ \mu H$).

LIST OF REFERENCES

1	AEG. Mitt. Bull. Oerlikon	No. 5/6, (1941). No. 231 and no. 232, (1941).
2	L.V. Bewley	"Travelling waves on transmission systems", Book, Dover Publ., New York 1963.
3	P. Hammarlund	"Transient recovery voltage subsequent to short-circuit interruption", Book, Stockholm 1946.
4	T.H. Lee,	Trans. A.I.E.E. 79 (1960) 535.
5	A. Greenwood	Trans. A.I.E.E. 79 (1960) 545.
6	E.B. Wedmore W.B. Whitney C.E.R. Bruce	I.E.E. Journal 67 (1929) 557.
7	C.G. Suits,	Phys. Rev. 55 (1939) 561.
8	K.H. Yoon H.E. Spindle,	Trans. A.I.E.E. 77 (1958) 1632.
9	F.A.-M. Rizk	"Interruption of small inductive currents with air-blast circuit breakers" Thesis Göteborg 1963 An abstract is given in Cigré-report 107 (1964).
10	H.Th. Simon	Phys. Z. 6 (1905) 297.
11	A.M. Cassie	Cigré Report 102 (1939).
12	O. Mayr	Arch. f. El. 37 (1943) 588. ETZ-A 75 (1954) 447.
13	W. Kaufman	Ann. d. Ph. 2 (1900) 158.
14	H. Nöske	"Zum Stabilitätsproblem beim Abschalten kleiner induktiver Ströme mittels Hochspannungsschaltern", Thesis, Berlin (1955). An excerpt is given in Arch. f. El. 43 (1957) 114.
15	A.C. van Sickle	Trans. A.I.E.E. 54 (1935) 178.
16	H. Puppikofer	Bull. S.E.V. 30 (1939) 334.
17	A.F.B. Young	Proc. I.E.E. 100 (1953) 337.
18	P. Baltensperger	Cigré Report 116 (1950).
19	P. Baltensperger P. Schmid	S.E.V. Bulletin 46 (1955) 1.
20	H. Kopplin	"Untersuchung des Löschverhaltens eines 110 KV - Expansionsschalters mit Hilfe einer Nachstrom - Messapparatur", Thesis, Berlin (1959).
21	O. Mayr	Int. Conf. on Ion. Ph. in Gases, Delft (1955).
22	K.H. Yoon T.E. Browne	Trans. A.I.E.E. 82 (1963) 1002.
23	G.C. Damstra	Cigré Report 120 (1964).
24	C.G. Suits	J. Appl. Phys. 10 (1939) 648.
25	H. Edels,	Int. Conf.on Ion. Ph. in Gases, Venetia (1957).
26	L.A. King	Journ. E.R.A. 16 (1962) 8.

27	G. Frind	Z. f. Ang. Phys. 12 (1960) 231. Z. f. Ang. Phys. 12 (1960) 515.
28	H. Edels W.A. Gambling	Br. J. of App. Phys. 5 (1954) 36.
29	J. Slepian	Trans. A.I.E.E. 47 (1928) 1398.
30	J. Slepian	Trans. A.I.E.E. 49 (1930) 421.
31	A.M. Cassie	Discussion to [38] .
32	A.M. Cassie	E.R.A. Report G/XT 314 (1953).
33	T.E. Browne	Trans. A.I.E.E. 67 (1948) 141.
34	T.E. Browne A.P. Strom	Trans. A.I.E.E. 70 (1951) 1.
35	A.M. Cassie F.O. Mason	Cigré Report 103 (1956).
36	W. Rieder J. Pratl	Scientia El. 11 (1965) 33.
37	W. Rieder J. Urbanek	Int. Conf. on Ph. in Ion. Gases, Belgrade (1965).
38	A.H. Sharbaugh P.K. Watson D.R. White T.H. Lee A. Greenwood	Trans. A.I.E.E. 80 (1961) 333.
39	H. Edels D. Whittaker K.G. Evans A.B. Shaw	Proc. I.E.E. 112 (1965) 2343.
40	A.M. Cassie	El. Journ. 162 (1959) 991.
41	L.A. King	Int. Conf. on Ion. Ph. in Gases, Munich (1961).
42	H. Kopplin E. Schmidt	E.T.Z.-A. 80 (1959) 805.
43	G.A.W. Rutgers V.K. Bisht	Electrotechniek 39 (1961) 265.
44	T. Ushio T. Ito	Mitsubishi Denki Lab. Rep. 2 (1961) 121.
45	T. Ushio T. Ito	Mitsubishi Denki Lab. Rep. 2 (1961) 241.
46	D.Th.J. ter Horst	"Boogontladingen met wisselstroom", Thesis, Utrecht 1934.
47	H. Brinkman	"Optische studie van de electrische lichtboog" Thesis, Utrecht 1937.
48	H. Maecker	Z.f. Phys. 157 (1959) 1.
49	W. Finkelnburg H. Maecker	Handb. d. Phys. XXII, Book, Springer, Berlin (1959).
50	G. Schmitz	Z.f. Naturforsch. 5a (1950) 571.
51	A.M. Cassie W. Rieder	E.T.Z.-A. 85 (1964) 312.

SAMENVATTING

In deze dissertatie wordt een overzicht en een verklaring gegeven van de fenomenen die optreden tijdens het onderbreken van kleine induktieve stromen (1,5 A - 60 A eff) door hoogspanningsschakelaars. Hierbij wordt uitgegaan van de wijze waarop deze verschijnselen tot uiting komen in de stroom door de schakelaar en de spanning over de schakelaar.

1. Stroombreking.

Stroombreking kan een gevolg zijn van de boogbewegingen, van elektrische instabiliteit, van de hoofdcircuit-oscillatie en van de overgang van boogontlading in glimontlading.
De elektrische instabiliteit wordt bepaald door de U_b - I_b - karakteristiek, de eerste tijdconstante Θ_1 van de ontlading en door het circuit in de omgeving van de schakelaar.
De krrakteristiek en de tijdconstante Θ_1 zijn afhankelijk van de lengte en de koeling van de ontlading en dus tevens van de boogbeweging.
In de circuits kunnen de inherente capaciteiten en zelfindukties van de schakelaar en zijn direkte omgeving van belangrijke invloed zijn op de stroombreking.

Stabiliteitstheorieën gaan uit van mathematische modellen van de ontlading waarbij de karakteristiek en de tijdconstante als constanten worden beschouwd. Ze kunnen daarom slechts experimenteel getoetst worden, wanneer tegelijk wordt aangetoond, dat deze onderstelling juist is. Dat zal in het algemeen in hoogspanningsschakelaars niet het geval zijn.

In de olieschakelaars leidt de overgang van de boogontlading naar de glimontlading tot instabiliteit en stroombreking bij een kritische stroomsterkte: $1,3 \leq I_o \leq 2$ A. Deze grensstroom hangt samen met de temperatuur in de as van de ontlading en is daarom afhankelijk van de druk in de ontlading en tot zekere hoogte ook van de contact-afstand.

2. Terugkerende spanning na stroombreking.

Bij stroombreking ten gevolge van hoofdcircuit-oscillatie onderbreekt de stroom door ontlading en parallel-capaciteit gelijktijdig. De aanvangssteilheid van de wederkerende spanning wordt dan bepaald door het voedende circuit, de mogelijke amplitude door het onderbroken circuit. Na de stroom-

breking daalt de spanning aanvankelijk, om vervolgens toe te nemen eventueel tot een zeer hoge waarde, de bluspiek.
Bij stroombreking door één van de overige onder 1. genoemde oorzaken onderbreekt alleen de stroom door de gasontlading. De circuitstroom handhaaft zich in eerste instantie door de parallelcapaciteit. Deze capaciteit is doorgaans zeer klein zodat hieruit zeer steile wederkerende spanningen kunnen ontstaan. De spanning over de schakelaar is al hoog op het ogenblik van stroombreking en stijgt hierna verder tot de bluspiek.
Na een stroomnuldoorgang zonder breking daalt de spanning, keert van polariteit om en slingert in naar de netspanning. In dit geval ontstaan geen extreme steilheden of amplituden.

3. De ontladingen.

Voor een volledige beschrijving van het gedrag van de schakelaar in de omgeving van de nuldoorgang dienen de volgende eigenschappen mede te worden overwogen:

a. De ontladingskarakteristiek $U_b = f(I_b)$.
b. De eerste tijdconstante θ_1, waarmede de hoge geleidbaarheid in de as van de ontlading verdwijnt.
c. De tweede tijdconstante θ_2, waarmede de lagere geleidbaarheid van de resterende hete gaskolom afneemt.
d. De snelheid waarmede een restontlading onder invloed van een wederkerende spanning weer kan overgaan in een nieuwe ontlading met kleine impedantie.

Voor korte tijden (enkele tientallen microseconden) kan de ontladingskarakteristiek als kwasi-statisch worden beschouwd en worden benaderd door de uitdrukking $U_b I_b^{\alpha} = K$.
Hierin zijn K en α sterk afhankelijk van de lengte en de beweging van de ontlading. Bij een rustige ontlading in olie is $\alpha \approx 1$. Bij intensieve boogbeweging neemt α sterk toe. In de luchtdrukschakelaar varieerde α tussen $0.5 \leq \alpha \leq 6$.

Uit de optredende oscillaties werd een indruk verkregen van de grootte orde van θ_1 en θ_2:

olieschakelaars	$\theta_1 \approx 0.1\ \mu s$	$\theta_2 \approx 100\ \mu s$
luchtdrukschakelaar	$1\ \mu s$	$5\ \mu s$
lastscheider	$30\ \mu s$	$1000\ \mu s$

De tijdconstante Θ_2 is een maat voor de tijd waarin nog herontstekingen uit een reststroom mogelijk zijn. De snelheid waarmede deze herontstekingen verlopen hangt niet alleen af van de wederkerende spanning, maar ook van de tijd die sedert de voorafgaande ontlading met kleine impedantie is verstreken. In de olieschakelaar kunnen nog na ca 10 μs reststroom-herontstekingen ontstaan die het karakter van een diëlektrische doorslag hebben. Na langere tijd komt de overgang trager tot stand en kan meerdere tientallen microseconden vergen. In de luchtdrukschakelaar en in de lastscheider ontstaan de reststroom-herontstekingen langzamer dan in de olieschakelaar. Voor beide gevallen is de minimale opbouwtijd van de orde van 1 μs.
Bij een diëlektrische doorslag wordt een ontlading met hoge geleidbaarheid zeer snel opgebouwd. Na de herontsteking wordt de steilheid van de wederkerende stroom bepaald door het parallelcircuit C_p,L_p. Hierbij komen steilheden voor tot 10.000 A/μs.

Wanneer een aantal herontstekingen snel achtereen optreedt, handhaaft zich een "gemiddelde circuitstroom" door de voedingsbron en de belasting. Deze vloeit om beurten door de ontlading en de parallelcapaciteit.

4. De wederkerende stroom.

In de onderzochte circuits konden de oscillaties in de wederkerende stroom worden onderscheiden in de eerste parallel-oscillatie, de tweede parallel-oscillatie en de hoofdcircuit-oscillatie.
De amplitude en frequentie van de beide parallel-oscillaties zijn bepaald door toevallige capaciteiten en zelfindukties in de omgeving van de schakelaar en de wijze waarop deze door de aarding in het circuit zijn opgenomen.
De hoofdcircuit-oscillatie is afhankelijk van de zelfindukties en capaciteiten van de voedingszijde en de belasting en van de wijze van aarding.
Deze oscillaties bepalen de energie die direkt na een heronsteking in de ontladingsbaan kan worden gebracht. Ze kunnen bovendien nieuwe stroomnuldoorgangen en daardoor stroombreking veroorzaken. Men kan niet algemeen vaststellen of hun invloed op de onderbreking overwegend gunstig of ongunstig is.

5. De circuits.

Afhankelijk van de plaats van aarding werden drie enkelfasige beproevingscircuits onderzocht en met driefasen-schakelingen vergeleken. Aarding tussen voeding en belasting geeft een circuit dat het meest representatief is

voor de situatie in driefasen-netten. Dit circuit geeft echter grote meettechnische moeilijkheden, omdat beide zijden van de schakelaar op hoogspanningsniveau blijven. Het kan worden aangetoond, dat aarding tussen schakelaar en belasting geen principiële verschillen met de driefasen situatie oplevert. Bij aarding tussen voeding en schakelaar ontstaat praktisch geen hoofdcircuit-oscillatie. Dit laatste circuit heeft daarom geheel andere eigenschappen dan de driefasen-schakelingen.

6. Conclusies ten aanzien van de beproeving van schakelaars.

Uit dit proefschrift blijkt de grote invloed die het circuit heeft op het mechanisme van de onderbreking van kleine induktieve stromen. In beproevingslaboratoria waar een beslissende uitspraak wordt gedaan over de geschiktheid van een schakelaar voor het onderbreken van kleine induktieve stromen is de samenstelling van het circuit daarom van eminente betekenis. Ogenschijnlijk kleine wijzigingen kunnen grote gevolgen hebben. Men kan zich dan ook terecht afvragen, welke waarde gehecht moet worden aan de resultaten van dergelijke beproevingen, waarbij doorgaans niet bekend is in welke schakeling de schakelaar uiteindelijk zal worden opgesteld.

Om toch adequate en vergelijkbare beproevingen te kunnen uitvoeren is nadere bestudering van de praktisch voorkomende circuits noodzakelijk. Dit zou moeten leiden tot het vaststellen van genormaliseerde beproevings-circuits waarvan niet alleen de hoofdelementen (voedingsbron, belasting en verbindingen), maar ook de secundaire grootheden (werkzame capaciteiten en zelfinduktie) en de plaats en wijze van aarding moeten worden beschreven. Het enig juiste criterium zou hierbij zijn, dat één en dezelfde schakelaar in elk laboratorium onder dezelfde omstandigheden van programmering en meetmethoden eenzelfde uitschakelcyclus zou moeten vertonen.

Ook de meetmethoden vereisen grote aandacht. Omdat de werkzame parallelcapaciteit van de schakelaar van belang is, dienen spanningsdelers met een geringe eigen-capaciteit (≤ 25 à 50 pF) te worden toegepast. De primaire deler-weerstanden moeten tezamen een hoge waarde hebben ($\geq 10^5\ \Omega$/kV). Voor fundamenteel onderzoek kan de stroom door de schakelaar alleen direkt aan de schakelaar nauwkeurig worden bepaald. Meetapparaten die op deze plaats in het circuit worden gebracht dienen een zeer lage impedantie ($R \leq 1$ à $2\ \Omega$, $L \leq 0{,}1\ \mu$H) te bezitten.

STELLINGEN

1. Na het onderbreken van magnetiseringsstromen van spanningstransformatoren in hoogspanningsnetten kunnen extreem grote transiënte stromen ontstaan. Men zou dit verschijnsel "spanningsbreking" kunnen noemen.

2. Bij het uitschakelen van hoogspannings-railsystemen door vermogens-schakelaars met capacitieve spanningssturing ontstaat gevaar voor thermische vernieling van de spanningstransformatoren ten gevolge van subharmonische ferroresonantie, tenzij ook de stroom door de stuurcapaciteiten wordt onderbroken.

3. In tegenstelling tot de gangbare mening kunnen in railsystemen waarbij de beide buitengeleiders in één vlak met en op gelijke afstand van de binnengeleider zijn opgesteld, tijdens driefasensluitingen grotere elektro-dynamische krachten optreden dan tijdens tweefasensluitingen.

4. Bij het berekenen van de elektro-dynamische krachten in railsystemen waarbij de beide buitengeleiders in één vlak met en op gelijke afstand van de binnengeleiders zijn opgesteld komt Babikow tot de onjuiste conclusie dat de buitengeleiders tijdens stationaire driefasen-belastingen het zwaarst belast worden.
   (M.A.Babikow "Wichtige Bauteile Elektrischer Apparate",
   V.E.B. Verlag Technik, Berlijn 1954, blz. 196 e.v.)

5. In het experimentele deel van zijn werk tracht Nöske zijn stabiliteits-theorieën van gasontladingen te verifiëren aan de hand van oscillogrammen van stroomonderbrekingen door een expansieschakelaar. Hij gebruikt hiertoe echter hoofdcircuit-oscillaties in plaats van instabiliteits-oscillaties.
   De door Nöske afgeleide tijdconstanten zijn daarom veel te hoog.
   (H. Nöske "Zum Stabilitätsproblem beim Abschalten kleiner induktiver Ströme mittels Hochspannungsschaltern",
   Diss. Berlijn 1955, Arch. f. El. 43 (1957) 114.)

6. Tijdens metingen met spanningsdelers voor hoge frequenties en hoge spanningen moet door centrale aarding verzekerd zijn, dat de retourstroom door de geaarde mantel van de verbindingskabel gelijk is aan de stroom door de binnenader.

7. Het ijken van spanningsdelers voor hoge frequenties en hoge spanningen heeft slechts zin, wanneer dezelfde verbindingskabel en oscillograaf en hetzelfde principe van aarding wordt gebruikt als tijdens de uiteindelijke metingen.

8. Ten onrechte wordt de dynamische energie-vergelijking van de elektrische boogontlading aan Heller en Elenbaas toegeschreven. Deze vergelijking werd voor het eerst door ter Horst gepubliceerd.
(D. Th. J. ter Horst "Boogontladingen met wisselstroom", Diss. Utrecht, 1934.)

9. Als kunst een scheppende activiteit is en esthetica de normatieve leer daarvan, kunnen nieuwe normen in de kunst uitsluitend achteraf door de esthetica geevalueerd worden.

10. Het uitschrijven van fotowedstrijden waarbij het recht van gratis publicatie van ingezonden werken wordt bedongen, is in het algemeen niet correct ten opzichte van beroepsfotografen.

Eindhoven, 14 juni 1966

W. M. C. van den Heuvel